

Analysis of the Gut Microbiota of
Japanese Alzheimer's Disease Patients and
Characterization of Their Butyrate-Producing Bacteria

2018, July

NGUYEN THI THUY TIEN

Graduate School of Environmental and Life Science
(Doctor's Course)

OKAYAMA UNIVERSITY

I. GENERAL INTRODUCTION

1. Overview of Alzheimer's disease

a. Description/Definition

Alzheimer's disease (AD) is the most common type of age-related disease (aged over 65 years old), accounting for about 55 – 70% of dementia (Bertram, 2007; Bu *et al.*, 2015; Mandell and Green, 2011). AD is characterized by progressive loss of memory and neurodegeneration of the central nervous system, leading to disorder in cognition and behavior of AD patients (Bertram, 2007; Mandell and Green, 2011). The life span of AD patients from onset may last about 10 years but can be as long as 20 years.

b. Stages and symptoms of Alzheimer's disease

Stages of AD vary among individual and determination of stages that patients are suffering from is the most importance of AD treatment. The standard approach to classify AD stages relies on a mental status examination, the Mini-Mental State Examination (MMSE) (Folstein *et al.*, 1975; Knopman). AD manifestations can be categorized into three stages with symptoms (López and DeKosky, 2008) presented in Table 1.

Table 1. MMSE scores and symptoms of each stage of AD (López and DeKosky, 2008)

Stage by MMSE scores	Cognitive	Behavioral	Neurological
Mild (score \geq 20)	Cognitive function is still in fairly good condition. In this stage, IADL of patients may be affected, but not ADL	Apathy and heavy stresses may occur. However, their mood is still stable.	The neurological exam cannot detect the changes. However, mild parkinsonism may have in some patients.
Moderate (score 10 – 19)	All cognitive domains are affected. All IADL and some ADLs are disabled.	Apathy is prominent. A depressive disorder is less frequent than in early stages. Their mood is more aggressive; psychosis is more frequent.	The neurological exam can be normal. More parkinsonism in some patients.
Severe (score \leq 9)	Severe deterioration of all cognitive domains. All IADL and ADLs were affected.	Apathy is prominent. Major depression is less frequent than in other stages. Psychosis, aggression, and agitation are more frequent.	The neurological exam is nonfocal but mild to moderate. Parkinsonism can be present in the majority of the patients. Myoclonic movements can be observed during the day.

Note: IADL, instrumental activities of daily living (e.g., job performance, managing finances); ADL, activities of daily living (e.g., getting dressed, control of sphincters).

Furthermore, according to Alzheimer’s Association (<https://www.alz.org/>), symptoms of AD’s stages can be described as following:

- Mild stage (early-stage):

They can work most of the activities by themselves. However, they may have difficulties in:

- Remembering of words or names

- Performing plans or tasks
- Forgetting or misplacing important things
- Moderate stage (middle-stage):

This is the longest stage during the AD progress, with typical symptoms:

- Forgetting most of events or information of someone's, such as phone numbers or schools from which they graduated
- Confusing of places, direction and time
- Changing in sleeping, sleep at daytime and restless at night
- Feeling moody and decreasing suspiciousness
- Late stage (severe stage)

At this stage, AD patients need much assistance with all activities, with symptoms such as:

- Losing awareness of their surrounding activities
- Getting difficulties with daily physical abilities, walking, sitting, swallowing or communicating.
- Being sensitive to infectious factors, especially pneumonia (https://www.alz.org/-alzheimers_disease_stages_of_alzheimers.asp)

c. *Prevalence of Alzheimer's disease*: mainly depends on age, geography and gender.

- Age: Prevalence of AD increases with age and depends on the ethnicity.
- + In Europe, the prevalence of AD was described in Table 2.

Table 2. Prevalence of AD in Europe (Niu *et al.*, 2017)

Age	65 – 74	75 – 84	> 85	< 79	> 80
Prevalence, %	0.97	7.66	22.35	3.18	14.04

+ In America: the prevalence of AD was described in Fig 1.

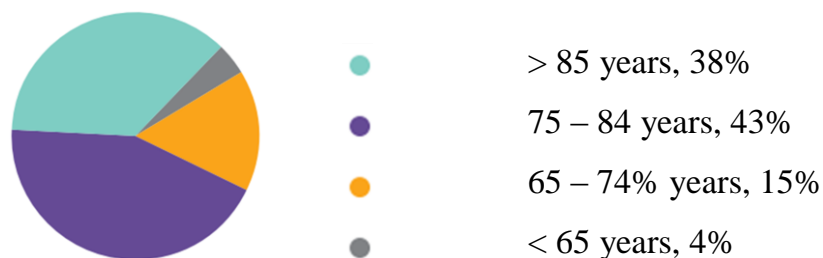


Fig 1. Ages of people with AD in the United States, 2018 (Alzheimer's Association, 2018)

The highest risk of AD incidence belonged to a group of older than 85 years old, up to 22.35%. The lowest prevalence was people in the age of 65 – 74. In America, the people with AD accounted for up to 43% at the age of 75 – 84.

- Geography:

- + Europe: 6.88% and 4.31% in Southern European countries (Spain, Italy, and Greece) and in northern European countries (France, the Netherlands), respectively (Niu *et al.*, 2017).

- + America: 10% of people aged over 65 has AD. Approximate 5.7 million Americans of all ages are suffering from AD in 2018, with 5.5 million people age over 65 and the remaining age under 65 (Alzheimer's Association, 2018).

- Gender: Women have a higher risk at AD than men, with two-thirds of Americans with AD are women. With aged more than 71 years old, 16% of women suffer from AD or other dementia compared with 11% of men in America in 2018 (Alzheimer's Association, 2018).

d. Risk factors for Alzheimer's disease

The etiology of AD is consequences of multiple factors, including some typical factors such as:

- Age: AD is an age-specific disease. Age is the highest risk of AD with most of AD patients are over 65 years old (Alzheimer's Association, 2018; Mandell and Green, 2011).

- Family history: This factor is unclear to lead to the onset of AD but people who have a parent, brother or sister have three- to four-fold higher risk than other individuals (Mandell and Green, 2011). This may come from a shared environmental and/or lifestyle factors in the same families (Alzheimer's Association, 2018).

- Apolipoprotein E (APOE)- ϵ 4 gene: APOE is an important protein that takes part in many physiological functions inside the bodies. There is three form of the APOE gene, ϵ 2, ϵ 3, and ϵ 4 and each individual inherits one form from their parents encoding for APOE. People who carry ϵ 4 form have a higher risk at AD than others who carry other forms. People do not contain ϵ 4 form have threefold and eight to twelve-fold lower risk of generating AD than those who inherit one copy and two copies of the ϵ 4 form, respectively (Alzheimer's Association, 2018; Mandell and Green, 2011).

- Education: The higher education people obtain; the lower AD risk they may have. This may be explained by their career since those who have higher education need more mentally stimulating to perform their cognition tasks (Alzheimer's Association, 2018).

e. Pathophysiology

There are two hypotheses have been used to explain for AD pathology, amyloid β ($A\beta$) and tau hypotheses. These hypotheses were given based on the deposition of two kinds of abnormal structures in the brain of AD patients: senile plaques and neurofibrillary tangles, respectively (Kametani and Hasegawa, 2018). Senile plaque deposition consists of amyloid fibrils composed of the amyloid β ($A\beta$) peptide, a product of cleavages of amyloid β precursor protein (APP) by β -secretase and γ -secretase, which is densely accumulated outside neurons. Neurofibrillary tangles aggregation of hyperphosphorylated tau protein, a microtubule-associated protein which helps microtubule polymerization and stabilization, deposited inside nerve cell bodies (Karran *et al.*, 2011; Selkoe and Hardy, 2016).

According to the amyloid hypothesis, an imbalance of formation and clearance of $A\beta$ causes the accumulation of $A\beta$ in the brain of aged subjects or pathological conditions. $A\beta$ contains $A\beta$ 40 and $A\beta$ 42 (more hydrophobic than $A\beta$ 40) which consists of 40 and 42 amino acid residues, respectively. A higher level of $A\beta$ 42 or the ratio of $A\beta$ 42 induces $A\beta$ amyloid fibril formation. This leads to the deposition of $A\beta$ into senile plaque, stimulating tau pathology and causing neuronal cell death and neurodegeneration (Kametani and Hasegawa, 2018).

Amyloid hypothesis has been used as a mainstream theory to explain for AD pathogenesis (Hardy and Selkoe, 2002). However, evidence from mouse models experiments indicated that mice with $A\beta$ accumulation did not have nerve cell death as well as tau protein formation (Kametani and Hasegawa, 2018). This means $A\beta$ is not a cytotoxic factor cause the degeneration of the nerve cell. The deposition of $A\beta$ is a common phenomenon of aging because amyloid deposits of elderly non-demented patients are as much as dementia patients (Kametani and Hasegawa, 2018). Meanwhile, other evidence demonstrated that AD onset is associated with tau protein accumulation, unrelated to amyloid (Kametani and Hasegawa, 2018).

f. Changes in the brain of AD patients

Alzheimer's brain may be distinguished with the healthy brain by the expression of some typical hallmarks:

- Whole brain: AD patients' brain is smaller than healthy people because of the dramatically shrinking of brain tissue losses (Fig. 3) (https://www.alz.org/alzheimers-dementia/what-is-alzheimers/brain_tour_part_2).

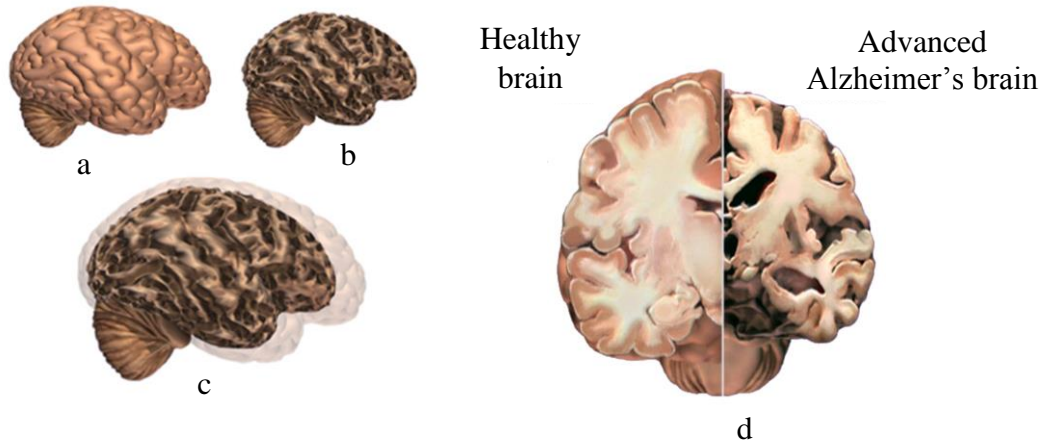


Fig 2. Changes in brains of AD patients. a) A healthy brain; b) A brain with severe AD; c) Comparison of the two whole brains, and d) Comparison of a crosswise "slice" through the middle of the brain between the ears of healthy brain and AD brain (https://www.alz.org/alzheimers_disease_4719.asp).

- Brain tissues: Brain tissue of healthy people has more nerve cells and synapses than that of AD patients. Tangles which made by dead and dying nerve cells in healthy people are also less than in AD patient's brain. Furthermore, the transport system of nutrients and other materials to the cells is destructed by tangles. When protein tau, which assists strands for delivering essential material to cells in parallel straightness, is collapsed into twisted strands, tangles are forming. This formation leads to the disorder of strands, they become disintegrated. Consequently, nutrients and other essential compounds cannot move through the cells, causing cell's death (Fig. 3) (https://www.alz.org/alzheimers-dementia/what-is-alzheimers/brain_tour_part_2).

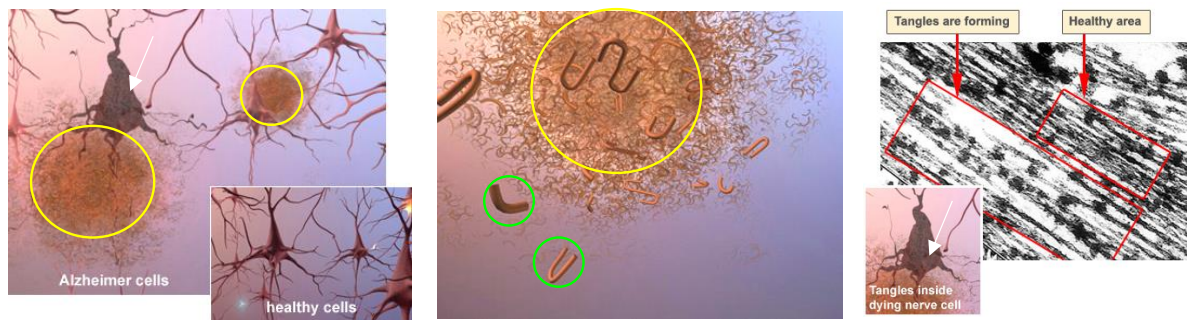


Fig 3. Brain tissue of AD patient and healthy people under the microscope. Plaques were shown in yellow circles, beta-amyloid was shown in green circles, tangles inside dying death and dying cell were indicated by arrows. Areas where tangles are forming were shown in red arrows with straight parallel strands of protein tau in healthy people (small red rectangle) and dying cell were indicated by arrows.

At the early step, the changes may start about 20 years before diagnosis by the formation of plaques and tangles in learning and memory, and thinking and planning areas of the brain. The middle stage generally lasts from 2 – 10 years and develop with more plaques and tangles in mentioned areas. Moreover, speaking and understanding speech and positions where make sense in relation to objects are also affected. At the late stage, most of the cortex is covered by plaques and tangles, caused dying of brain cell (Fig. 4.) (https://www.alz.org/alzheimers-dementia/what-is-alzheimers/brain_tour_part_2).

- The progress of plaques and tangles deposition at different stages of Alzheimer's brain was showed in Fig. 4.

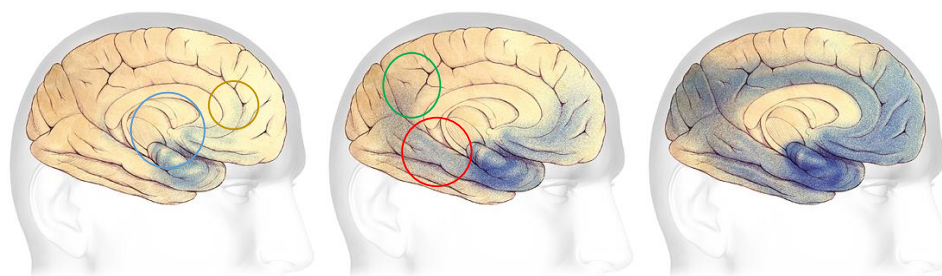


Fig 4. Changes in brain at different stages of AD patient's. Early stage (left), mild stage (middle) and severe stage (right). Areas where plaques and tangles formed (the blue-shaded areas) are in learning and memory (blue circle) and thinking and planning (brown circle) areas at early stage, in speaking and understanding speech (red circle) and sense of place in

relation to objects areas (green circle) at middle stage, and in most of the cortex at late stage. (https://www.alz.org/alzheimers-dementia/what-is-alzheimers/brain_tour_part_2)

2. Overview of human gut microbiota

a. Definition

The human gut microbiota is a microorganism community that lives in the human gastrointestinal tract, estimating 1×10^{13} to 1×10^{14} individuals. A number of these organisms is believed to be 10 times higher than the number of human cells (Cryan and Dinan, 2012). The density of gut microbiota in the gastrointestinal tract is shown in Fig. 6. Colon is a known ecosystem contains the highest cell densities (O'Hara and Shanahan, 2006) (Fig. 5).

The human gut microbiome is the collective genomes of all gut microbiota. It is estimated containing 150 times as many genes as the human genome and is referred to as a forgotten organ (Cryan and Dinan, 2012).

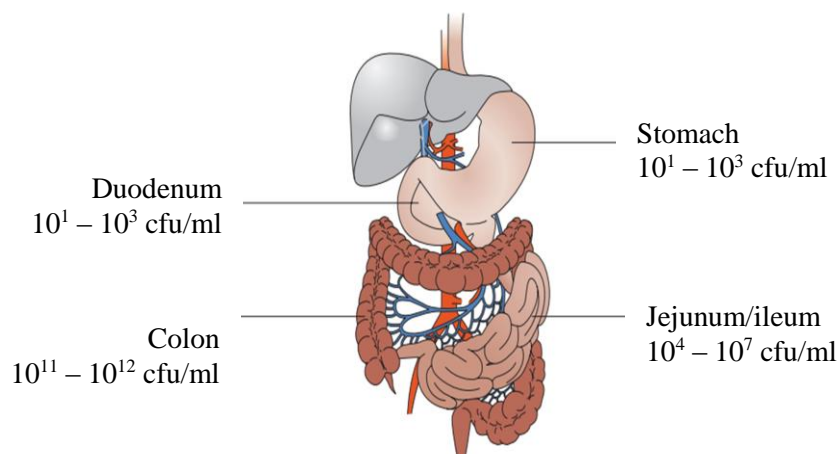


Fig 5. Bacteria density in the human gastrointestinal tract (increasing from stomach, duodenum, jejunum, to colon (O'Hara and Shanahan, 2006)).

b. Roles of gut microbiota in human health and disease

Along with our growth and maturation from baby to senescence, the human gut microbiota gradually develops and changes. Their composition and nature are influenced by a number of factors including ethnicity, age, sex, and diet intake of the individual (Hollister *et al.*, 2014; Wang *et al.*, 2017). The gradual development of the gut microbiota is essential for channelizing the process of immune system priming which includes development of immunological memory by pattern recognition property of the immune cells. This process is also important to define reaction towards infection, inflammatory diseases and autoimmunity in the host system (Nieuwdorp *et al.*, 2014). The commensal gut microbiota establishes a

symbiotic relationship with the human host and plays essential roles like energy regulation, metabolism and priming immune system in order to improve the quality of life of the host (Clemente *et al.*, 2012; Wang *et al.*, 2017). The gut microbiota colonization in newborn is affected by the nature of delivery which can be noted as abundance of skin-like microbial communities in the caesarean section and vaginal-like microbial communities in the vaginal delivery. The nature of the gut immune system also varies between a newborn and an adult. This signifies the importance of relationship between physiological state of the body and gut microbiota composition. As a newborn move onto further developmental stages the initial gut microbial community gives way to a diverse gut microbial community. At these stages, the gut microbiota helps in priming the immune system of the body by utilizing the characteristic ‘memory’ feature of the immune cells (Clemente *et al.*, 2012) (Fig 6).

Furthermore, considered as a “forgotten organ”, gut microbiota takes part in processes of vitamin synthesis, bile salt metabolism, and xenobiotic degeneration. All of their final biochemical output is called as “metabolome” (O'Hara and Shanahan, 2006). It has been reported widely that the gut microbiota contains more versatile metabolic genes as compared to human genome. Therefore, they play a key role in energy and metabolism of the host by providing specific enzymes and biochemical pathways which in turn increases the rate of energy extraction, nutrient harvest as well as alters the appetite signaling (Wang *et al.*, 2017). In addition to this, various metabolic processes that are carried out by the microbiota in the human gut are either associated with nutrient acquisition or xenobiotic processing such as the metabolism of undigested carbohydrate and biosynthesis of vitamins.

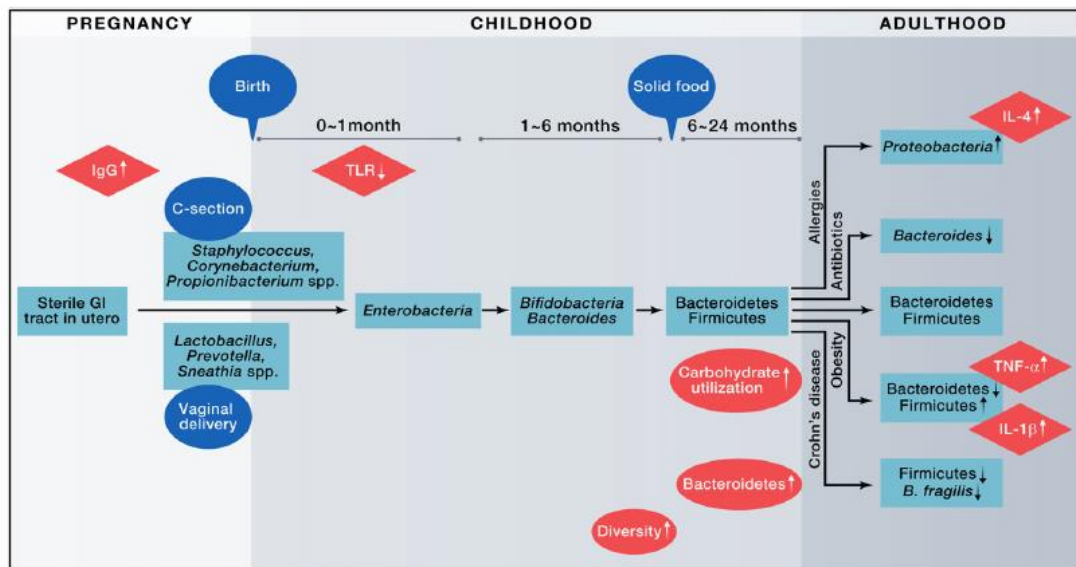


Fig 6. Developmental stages of the gut microbiota in the human life.

As the food is treated by various salivary amylases in the mouth of the host and is further acted upon by the gastric and bile juices, indigestible carbohydrates are amongst the substrates which are available to the gut microbiota for further energy generation. Depending on the bacterial communities colonized in the gut, these substrates are reduced to various simpler hydrocarbons like short chain fatty acids (SCFAs), carbon dioxide, ammonia, choline, amines, phenols, indoles, mercaptanes, hydrogen sulfide and hydrogen gas. These products are essential for both the host as well as the commensal gut microbiota (Nieuwdorp *et al.*, 2014). The human gut microbiome is responsible for producing about 50-100 mmol/l per day of SCFAs. These SCFAs, which can be instantly absorbed by the gut, are starting material for various metabolic pathways which produce energy for the host intestinal epithelium (Duncan *et al.*, 2009). In addition to energy production, the SCFAs has various other health promoting benefits such as regulation of gut motility, anti-inflammation, and glucose homeostasis (Flint *et al.*, 2012). Altered SCFA production by intestinal microbiota leads to perturbations in bile acid, lipid, and glucose metabolism as well as increased intestinal permeability, resulting in aggravated metabolic endotoxemia and subsequent low-grade inflammation (Fig 7). Furthermore, glycine, taurine or sulfate conjugates constitute the bile acid, which accompanies the indigested food as it enters the intestine of the host. These conjugates are broken down into simpler components that can be absorbed and recycled to bile, by the intestinal microbial community (Jones *et al.*, 2008).

In addition, the commensal gut microbiota plays an indispensable role in maintaining the immunological homeostasis by creating a bridge between the pathogen recognition and development of immune system. The bacterial cell wall has components like lipopolysaccharides, gangliosides, pili or flagella which act as microbe-associated molecular patterns which can be recognized by Toll-like receptors (TLRs) on the host cell as antigens (O'Hara and Shanahan, 2006; Round *et al.*, 2011). The microbe-associated molecular patterns (MAMPs) of commensal bacteria in the gut interact with TLRs and thus aid in immunological tolerance, reduction of inflammatory reactions and maintain the immunological homeostasis of the host. The gut microbiota also influences the adaptive immune system of the host by initiating self-/non-self-discrimination in the T-cell differentiation process as well as by priming the adaptive immunological cells (Lathrop *et al.*, 2011; Lee and Mazmanian, 2010).

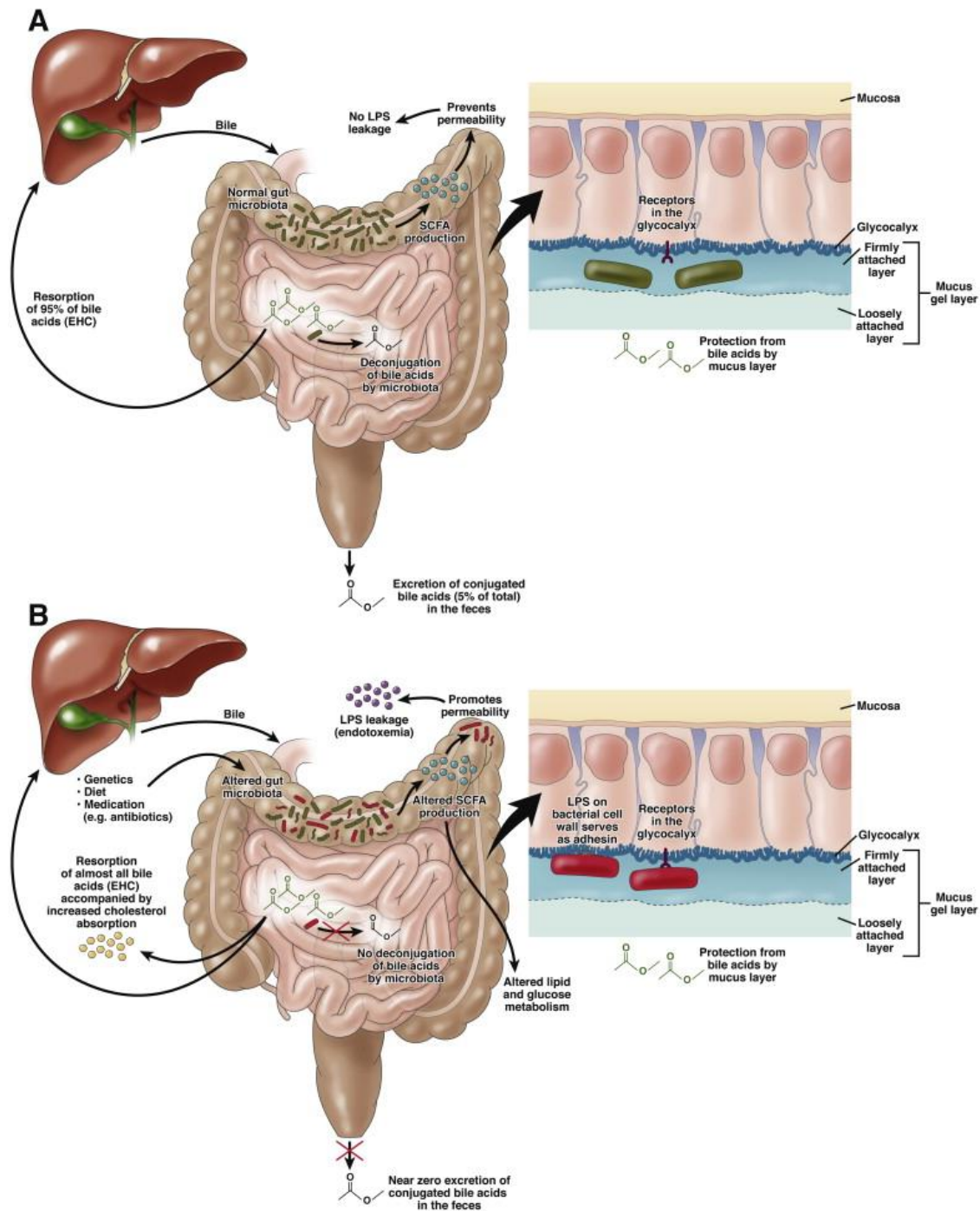


Fig 7. Metabolism of bile acid and SCFA in the (A) healthy physiological and (B) pathophysiological state (Nieuwdorp *et al.*, 2014).

3. The bidirectional communication between the gut microbiota and the central nervous system

The human central nervous system (CNS) and intestinal microbiota together constitute microbiota-gut-brain-axis, with emphasis on the multi-factorial relationship (Forsythe *et al.*, 2012; Thakur *et al.*, 2014). Multiple potential direct and indirect pathways exist through

which the gut microbiota can modulate the gut–brain axis. They include endocrine (cortisol), immune (cytokines) and neural (vagus and enteric nervous system) pathways (Cryan and Dinan, 2012). The vagus nerve is a significant bridge that establishes the gut-brain axis (Bravo et al., 2011). Some metabolites that are produced as a result of various microbial metabolic pathways in the gut, such as tryptophan, butyrate, serotonin and SCFAs, act as neurotransmitters (Gruninger et al., 2007). Prior studies have reported that SCFAs produced by gut commensals when paired with enteroendocrine receptors lead to parallel increase of a circulating peptide YY which is associated with appetite stimulation. Thus higher production of SCFAs are often associated with binge eating habits of the host (Samuel et al., 2008). An example of the gut-brain communication under stress conditions is represented in Fig 8.

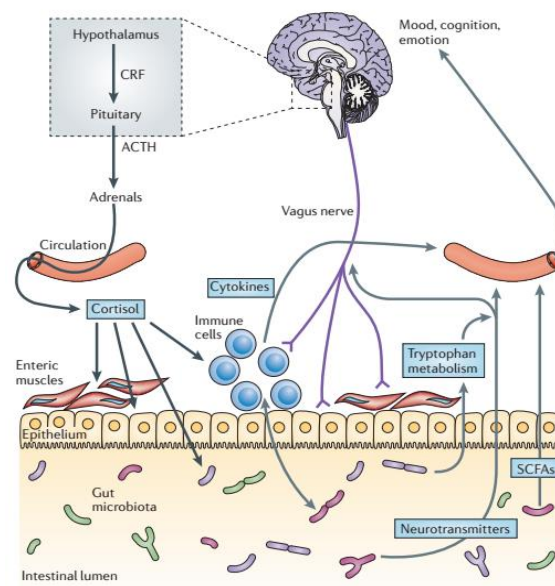


Fig 8. Gut-brain-microbiota axis: a multi-factorial relationship. ACTH, adrenocorticotropic hormone; CRF, corticotropin-releasing factor.

The hypothalamus–pituitary–adrenal axis regulates cortisol secretion, and cortisol can affect immune cells (including cytokine secretion) both locally in the gut and systemically. Furthermore, cortisol can alter gut permeability and barrier function, and change gut microbiota composition. On the other hand, the gut microbiota and probiotic agents can alter the levels of circulating cytokines, and this can have a marked effect on brain function. Both the vagus nerve and modulation of systemic tryptophan levels are strongly implicated in relaying the influence of the gut microbiota to the brain. In addition, SCFAs can also

modulate brain and behavior. The abnormal gut microbiota may lead to the abnormal CNS function and vice versa (Fig 9).

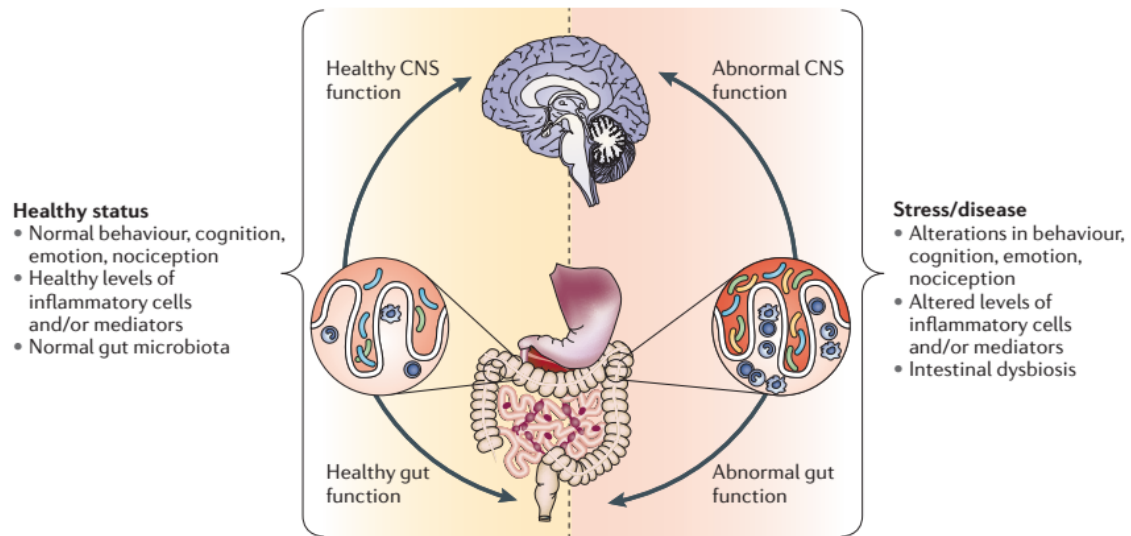


Fig 9. Impact of the gut microbiota on the gut–brain axis in health and disease (Cryan and Dinan, 2012).

A stable gut microbiota contributes to maintain a normal behavior or cognitions with its appropriate regulation along the gut-brain axis while an abnormal gut microbiota can adversely influence gut physiology, leading to inappropriate gut–brain axis signaling and associated consequences for CNS functions and resulting in disease states. Conversely, stress at the level of the CNS can affect gut function and lead to perturbations of the microbiota (Cryan and Dinan, 2012).

4. Motivation, objectives and hypotheses

a. Motivation

Ageing population has become a big social-economic burden of each country because of high pressure in healthcare service associated with old age diseases, especially dementia. Japan is home to the world’s most aged population with 33 per cent were aged 60 years or over in 2015. (http://www.un.org/en/development/desa/population/publications/pdf/ageing/WPA2015_Report.pdf). In 2018, Japan has more than 4.6 million people are living with dementia, causing the most concerned issue in terms of diseases which associate with elderly in this country (<https://www.alz.org/jp>).

As aforementioned, the human gut microbiota has bidirectional communication with the central nervous system. Various studies have reported the interaction between the gut

microbiota and neurodegenerative diseases (AD, Parkinson's disease (PD), Huntington's disease...) as well as other mental dysfunction disease (autism) (De Angelis *et al.*, 2015; Hu *et al.*, 2016; Mancuso and Santangelo, 2018; Sharon *et al.*, 2016). Scheperjans *et al.* reported a strong reduction of *Prevotellaceae* abundance in feces of PD patients compared with that of control volunteers (Scheperjans *et al.*, 2015). Reduced *Prevotella*, *Coprococcus* and unclassified *Veillonellaceae* were found in autism (Kang *et al.*, 2013) and *Clostridium tetani* may stimulate this disease (Bolte, 1998). In multiple sclerosis disease, clostridial species considered as main candidates were responsible for the differences in gut microbiota between patients and controls (Miyake *et al.*, 2015). Especially, a study which compared the gut microbiota of American who diagnosed with AD and the gut microbiota of healthy controls indicated a decline in *Firmicutes* and an increase in *Bacteroidetes* in AD participants (Vogt *et al.*, 2017). These findings confirmed a theory claims gut microbiota may implicate in a wide range of brain diseases.

However, the human gut microbiota depends on ethnicity, referring citizens of each country over the world may have their own gut microbiota (Hollister *et al.*, 2014). Japanese has their unique gut microbiota thanks to the specific dietary culture and habits. Their gut microbiomes have more genes for aquatic plant-derived polysaccharide-degrading enzymes than those of Americans (Nishijima *et al.*, 2016). Thus, although the study which reported the alteration of the gut microbiota in AD patients in comparison with healthy persons were carried out in American, we still wanted to know whether the similar changed direction happens to the gut microbiota composition of AD patients and healthy persons in Japan or not. Furthermore, we also wanted to compare the gut microbiota structure of Japanese and American who were both diagnosed with AD to understand the different in their gut microbiota.

Besides, within the community of human gut microbiota, the group of butyrate-producing bacteria attracts particular attention because of the specific health-promoting effects they provide to their hosts (Vital *et al.*, 2014). Their major metabolic end-product, butyrate, is not only a preferred energy source for colonocytes but also a major contributor to the preservation of intestinal epithelial permeability and the protection of the host from carcinogenic, inflammatory, and oxidative factors (Hamer *et al.*, 2008). Butyrate or butyrate-producing bacteria may have positive effects on memory improvement in mouse models of dementia-related diseases, including AD (Govindarajan *et al.*, 2011; Liu *et al.*, 2015). Thus, here we wanted to determine if butyrate-producing bacteria are at all present or completely

absent in the gut microbiota of AD patients by investigating their phylogenetic diversity and butyrate-producing ability. The application of single or mixtures of butyrate producers in studies associated with dementia-related disease emphasizes the importance of identifying butyrate-producing bacteria and to assess their rate of butyrate production.

b. Objectives and hypotheses

With the described motivations, in the study presented here, we aimed to:

- Compare the gut microbiota composition of Japanese AD patients (AD group) and Japanese healthy controls (HC group).
- Compare the gut microbiota composition of Japanese AD patients (Japanese group) and American AD patients (American group).
- Characterization of butyrate-producing bacteria isolated from feces of Japanese Alzheimer's disease patients.

Based on these objectives, firstly, we hypothesized that there are changes in gut microbiota of AD group in comparison with HC group in terms of their composition, diversity, and predicted metabolic pathways. Secondly, differences in microbial population of Japanese AD patients and American AD patients was speculated based on the same criteria. And thirdly, we hypothesized the AD gut microbiota is characterized by low phylogenetic diversity of butyrate-producing bacteria.

II. CHARACTERIZATION OF GUT MICROBIOTA OF JAPANESE ALZHEIMER'S DISEASE PATIENTS

Abstract

AD is the most common type of age-related disease, characterized by progressive loss of memory and neurodegeneration of the central nervous system. This degenerative disorder disease is thought to be associated with their gut microbiota. In this study, the comparison of the gut microbiota of 17 Japanese AD group with that of 17 Japanese HC were carried out. The hypervariable regions V3–V4 of 16S rRNA gene of bacterial genome which were purified from all fecal samples of Japanese were sequenced with primers Tru357F and Tru806R using MiSeq platform (Illumina). The resulting sequences were analyzed with QIIME 1.9.1 and the outputs were used to assess the bacterial compositions, diversities, and metabolic pathways. Total sequences of 181,580 reads were assigned to 2,583 OTUs (operational taxonomic units), consisted of 12 phyla, 22 classes, 33 orders, 70 families and 147 genera. The phyla of *Actinobacteria*, *Verrucomicrobia*, *Cyanobacteria*, and *TM7*

contributed to the differences in phylum level between the two groups with $p < 0.05\%$. Notably, a higher abundance of *Cyanobacteria* in AD group was an interesting result since this group of bacteria is believed to be correlated with AD due to their production of (Banack et al., 2010) neurotoxins, such as β -N-methylamino-L-alanine, anatoxin-a and saxitoxin. These compounds may contribute to the onset and development of cognitive dysfunctions, a signal of AD invasion. The Faith's phylogenetic diversity was significantly reduced in the HC group, reached 12.66 ± 2.1 in the HC group and 15.99 ± 2.29 in AD group ($p < 0.05$). The weighted and unweighted UniFrac distances between AD and HC groups were significant differences at $p < 0.001$. Predicted metabolic pathways of these gut microbiota indicated that the AD group was enriched in 10 pathways as compared to the HC group, especially AD pathway of the neurodegenerative disease pathway. The gut microbiota of 17 Japanese AD and 25 American AD group was also evaluated. The hypervariable regions V4 of 16S rRNA gene of the purified DNA of AD group were sequenced. The total reads were 4,000,035 reads which were grouped into 14,593 OTUs, comprised 12 phyla, 26 classes, 30 orders, 79 families, and 180 genera. The phylum *Proteobacteria* was specifically enriched in Japanese group than the American group. Hence, this is the most important finding and may explain the alteration of this community in the human gut microbiota according to the variation in geographical location and health status. The microbial richness, characterized by observed OTU and Chao1 index, of American group was higher than those of Japanese group. The beta diversity of the gut microbiota of AD group in American differed from that in Japanese AD group. These findings may help to clarify the differences in the gut microbiota between the Japanese AD patients and Japanese healthy people as well as the differences in the gut microbiota of American AD patients and Japanese Ad patients.

1. Introduction

AD is the most popular type, accounting for 60 – 80% of all dementia type (Alzheimer's Association, 2017). AD is characterized by a gradual loss of memory and cognition, a progressive neuron-degenerative disorder of a central nervous system. The original cause leads to AD has been unknown but age and history family were blamed for two main risk factors. According to the amyloid cascade hypothesis of AD pathogenesis, deposition in the brain of extracellular protein fragments called beta-amyloid plaques and an intracellular abnormal form of protein tau were considered as two hallmarks of the AD. Up to now, there is no treatment or effective and appropriate therapy for the AD (Alzheimer's Association, 2017).

Recently, there has been increasing evidence indicating that etiology of diseases associated with the central nervous system (CNS) has relationship with gut microbiota, creating a complex gut-brain-axis (Thakur *et al.*, 2014; Wang *et al.*, 2017). The bidirectional communication between gut flora and CNS plays a key role in physiological as well as mental health, influencing the immune system, the gastrointestinal tract and the CNS function. In AD, many studies have carried out to discover the correlation between AD and microorganism. By using next-generation sequencing (NGS), a method allows to identify almost bacteria in samples, a bacterial community in the extracted postmortem brain tissue of AD patients was shown a higher abundance of *Propionibacteriaceae* and *Corynebacteriaceae* in AD brain tissues than that of controls (Emery *et al.*, 2017). *Helicobacter pylori*, *Clamydophila pneumoniae* and spirochetes or Herpes simplex virus were found to be related to AD (Miklossy, 2011). Oral microbiota was richer density in AD postmortem brain, indicating the correlation between AD and oral hygiene situation (Miklossy and McGeer, 2016). The risk of the AD or other neurodegenerative diseases might be enhanced by the elevated proportion of *Cyanobacteria* in the intestinal flora (Banack *et al.*, 2010). A study which compared the gut microbiota of American with AD and the gut microbiota of American healthy controls indicated a decline in *Firmicutes* and an increase in *Bacteroidetes* in AD participants (Vogt *et al.*, 2017). These findings confirmed a theory claims gut microbiota may implicate in a wide range of brain diseases.

Japan is home to the world's most aged population with 33 per cent were aged 60 years or over in 2015. In 2018, Japan has more than 4.6 million people are living with dementia, causing the most concerned issue in term of diseases which associate with elderly in this country (<https://www.alz.org/jp>). Although the relationship between the gut microbiota and AD was investigated in American participants (Vogt *et al.*, 2017), this interaction is still necessary to study in Japan since Japanese has their own gut microbiota. The findings may help to clarify the modification in the gut microbiota of Japanese when they are diagnosed with AD. Furthermore, the gut microbiota of Japanese and American AD patients were also compared to have an insight of the gut microbiota of AD patients in different geographical locations.

2. Materials and Methods

a. Materials

Fresh fecal samples from 17 Japanese Alzheimer's disease patients (86.29 ± 6.48 years old) were collected. Samples were immediately sealed in a plastic bag containing an AnaeroPack-Anaero (Mitsubishi, Japan) and then transported to the laboratory at 4°C within two days. In the laboratory, 1 g of feces was treated with 1 ml of phosphate buffer saline (PBS, Life Technologies, Japan) and 2 ml of 40% glycerol (Nacalai Tesque, Japan) in an anaerobic chamber (Bactron, Shel Lab, USA) to generate a fecal stock sample. Subsequently, the fecal stock samples were quickly frozen in liquid nitrogen and stored at -80°C until use (Nishijima *et al.*, 2016). The study was approved by the Ethics Committee of Okayama University, Japan (Approval number 1610-025). Written informed consents were obtained from all participants or their relatives.

b. Methods

- Bacterial DNA extraction

Bacteria from fecal samples were collected following the previous study with a minor modification (Morita *et al.*, 2007). 0.5 g of wet fecal samples was mixed with 45 ml of PBS and then the mixture was divided into three equal parts. Each 15 ml suspension was filtered through a 100- μ m-mesh nylon filter using agitation with a plastic bar. The debris on the filter was washed twice with 10 ml PBS. Repeated with the two remaining aliquots with the same method by using new filters and new tubes. The three filtrates were centrifuged at 5000 \times g for 10 min at 4°C, and each precipitate was washed with 35 ml of PBS. All precipitates were combined and washed again with 35 ml of TE buffer (pH 8.0) and centrifuged again. The precipitate was re-suspended in 800 μ l of TE 10 and used for DNA extraction (Morita *et al.*, 2007).

The suspension was incubated at 37°C for 1 h with 15 mg/ml lysozyme (Sigma-Aldrich). Next, purified achromopeptidase (Wako, Japan) was added to the suspension to obtain 2000 units/ml and incubated at 37°C for 30 min. The enzymatic treatment was continued by adding 1 mg/ml proteinase K (Merck, Germany) and 100 μ l of 10% sodium dodecyl sulfate (Nacalai Tesque, Japan) and kept at 55°C for 1 h. The bacterial DNA was separated with phenol:chloroform:isoamyl alcohol (25:24:1) (Nacalai Tesque, Japan) and precipitated with 99.5% isopropanol (Wako, Japan) and sodium acetate 3 M. The DNA pellet was obtained by washing twice with 75% ethanol, dried and dissolved in TE buffer overnight. RNA was removed by incubating the solution with 1 μ l RNase A (Novagen, USA) at 37°C for 1 h. The genomic DNA was recovered by precipitation with 26% PEG (Polyethylene

glycol, Nacalai Tesque, Japan) in 1.6 M NaCl (Nacalai Tesque, Japan) on ice for 30 min and followed by centrifugation at 15,000 *g* for 15 min at 4°C. The pellet was rinsed with 75% ethanol, dried and dissolved in 10 mM Tris-HCl buffer (pH 8) (Invitrogen), and stored at –20°C until subjected to identification of genes involved in butyrate formation in bacteria (Morita *et al.*, 2007)

- 16S rRNA library preparation and pair-end sequencing

The fecal DNA was sequenced by using Illumina Miseq platform. First, 16S rRNA amplicon libraries were prepared by subjecting the purified DNA to two-steps polymerase chain reaction (PCR). At the first step, there are two primer sets were used to amplify different region of 16S rRNA gene of the genomic DNA of AD group.

- Primer set 1: Tru357F (5'-CGCTCTTCCGATCTCTGTACGGRAGGCAGCAG-3') and Tru806R (5'-CGCTCTTCCGATCTGACGGACTACHVGGGTWTCTAAT-3') (Odamaki *et al.*, 2016) aimed to amplify the V3 – V4 region of 16S rRNA gene of AD group's DNA.

- Primer set 2: (forward: 5'-ACACTCTTTCCTACACGACGCTCTTCCGATCTG-TGCCAGCMGCCGCGGTAA-3'; reverse: 5'-GTGACTGGAGTTCAGACGTGTGCTCT-TCCGATCTGGACTACHVGGGTWTCTAAT-3') aimed to amplify the V4 region of 16S rRNA gene of AD group's DNA (Kozich, 2013; Vogt *et al.*, 2017).

The PCR protocol was started at 95°C for 3 minutes for initial denaturation, followed by 25 cycles of denaturation at 95°C for 30 seconds, annealing at 55°C for 30 seconds, elongation at 72°C for 30 seconds and a final elongation at 72°C for 5 minutes and then hold at 4°C. The PCR product's size was measured by Agilent 2100 Bioanalyzer (Agilent Technologies). Next, AMPure XP beads (Beckman Coulter, Inc., USA) were used to purify the amplicon of the 16S rRNA gene away from free primers and primer dimer species. The purified amplicons were moved to an index PCR to attach dual indices and sequencing adapters using the Nextera XT Index Kit (Illumina, Inc., San Diego, CA, USA). The PCR running program was performed as above protocol but the cycles were 8 cycles. Again, AMPure XP beads (Beckman Coulter, Inc., USA) were used to clean up the final library before quantification. Finally, the resulting library was checked the length on Agilent 2100 Bioanalyzer (approximately 630 bp) (Illumina, 2013; Klindworth *et al.*, 2013).

DNA concentration of each purified library was diluted with 10 mM Tris pH 8.5 and adjusted to 4 nM using Qubit 3.0 Fluorometer (Life technologies, USA) with Qubit dsDNA

HS Assay Kit (Life technologies, USA). Aliquot 5 μ l of each diluted library was mixed to make unique indices. The pooling library was pair-ends sequenced using Illumina Miseq platform with MiSeq v3 reagent kits (Illumina, USA) at BioBank, Okayama University, Japan.

- Study design

With primer set 1, the gut microbiota of 17 Japanese AD participants (AD group, mean \pm SD, 86.29 \pm 6.48 years old, Female/Male: 14/3) was compared with that of 17 Japanese healthy participants (HC group, mean \pm SD, 85.47 \pm 2.72 years old, Female/Male: 12/5) ($p = 0.64$). DNA sequences of these controls were downloaded from a public data (accession number DRA004160). They were also amplified with primers, Tru357F and Tru806R, and sequenced by using Illumina Miseq sequencer (Odamaki *et al.*, 2016).

For V4-specific primers: DNA sequences of Japanese gut microbiota in AD group (Japan group) were compared with those of American Alzheimer's patients (American group, mean \pm SD, 71.26 \pm 7.13 years old; Female/Male: 17/8) ($p < 0.001$). These reference sequences, which were provided by Dr. Volt (Vogt *et al.*, 2017), were DNA sequences of the gut microbiota of American who were diagnosed with AD. The V4-specific primer was used to amplify the V4 region of the 16S rRNA gene. The resulting product was sequenced with the Illumina Miseq sequencer.

- 16S rRNA gene-sequencing analysis

Raw sequences of all samples were analyzed using QIIME software package version 1.9.1 (<http://qiime.org/>) (Caporaso *et al.*, 2010). Pair-end sequences assembled with 50 bp overlapping were used for subsequence analysis. Chimeras were identified and eliminated from joined sequences by using USEARCH 6.1 (<http://www.metagenomics.wiki/tools-qiime/install/usearch61>) (Edgar, 2010). After quality filtering, sequences were assigned into Operational Taxonomic Units (OTUs) using the Greengenes reference database (ftp://greengenes.microbio.me/greengenes_release-/gg_13_5/gg_13_8_otus.tar.gz, May 2013) with 97% similarity threshold. OTUs $< 0.001\%$ of the total sequence reads were filtered out from the dataset to account for sequencing errors.

Relative abundance of OTUs existing in each group was evaluated at different levels. The linear discriminate analysis (LDA) effect size (LEfSe) (<http://huttenhower.sph.harvard.edu/galaxy/>) was used to analyze the differences in taxonomies of the two groups. Alpha value for the factorial Kruskal-Wallis test among each group was 0.05. The threshold

on the logarithmic LDA score for discriminative features was 2.0. LDA scores (log 10) of significantly different pathways and taxonomies were plotted as bars (Segata *et al.*, 2011). Chao1, observed species, phylogenetic diversity and Shannon diversity index were calculated to estimate alpha diversity. Beta diversity metrics, weighted and unweighted UniFrac, were generated using normalized OTUs-level data in QIIME. Weighted and unweighted UniFrac distances were evaluated to compare the microbial diversity between AD group and HC group by using t-test ($\alpha = 0.05$).

PICRUst (Phylogenetic Investigation of Communities by Reconstruction of Unobserved States) (Langille *et al.*, 2013) was used to analyze metagenome predicted functions in microbial communities. OTUs which were picked using the open reference database (gg_13_8) were re-picked up using a close reference database (gg_13_5) for PICRUst analysis. The OTU table was normalized by the 16S rRNA copy number. The resulting normalized OTUs table was used to create the final metagenome functional predictions of KEGG (Kyoto Encyclopedia of Genes and Genomes) (Kanehisa and Goto, 2000) based on bacterial composition. Predicted metabolic pathways were collapsed into hierarchical KEGG pathways using the categorized by function command in PICRUst. The LEfSe was used to analyze the differences at level 1, 2 and 3 of these pathways. Primer 7 (<http://www.primer-e.com/>) was used to create box plots which presented to compare relative abundances of different taxonomies in this study. The datasets used and/or analyzed during our study are available from the author of this dissertation.

3. Results

a. Comparison of the gut microbiota of Japanese AD patients and Japanese healthy controls

- Taxonomic analysis

There were 181,580 ($5,340.59 \pm 3,018.08$) reads were assigned to 2,583 OTUs, consisted of 10 phyla, 22 classes, 33 orders, 70 families and 147 genera. At the phylum level, in both groups, the most abundant phylum was *Firmicutes* with $71.94 \pm 11.70\%$ and $77.06 \pm 12.71\%$, in HC and AD groups, respectively. The second abundant phylum was *Bacteroidetes* with $19.32 \pm 9.96\%$ and $13.06 \pm 7.31\%$ in HC and AD groups, respectively. The less abundant phyla included *Proteobacteria* ($7.77 \pm 5.60\%$, $6.18 \pm 8.19\%$), *Actinobacteria* ($0.63 \pm 1.23\%$, $1.81 \pm 2.38\%$), *Fusobacteria* ($0.14 \pm 0.45\%$, $0.74 \pm 2.60\%$), *Verrucomicrobia* ($0.03 \pm 0.07\%$, $0.17 \pm 0.28\%$), and *Cyanobacteria* ($0.002 \pm 0.009\%$, 0.095

$\pm 0.134\%$), corresponding to HC and AD group, respectively. The box plots showed in figure 10 displayed compared relative abundances between the two group.

The phyla of *Actinobacteria*, *Verrucomicrobia*, *Cyanobacteria*, and *TM7* made the differences at phylum level between the two groups with $p < 0.05\%$. Two phyla of *Cyanobacteria* and *TM7* seemed to disappear in HC group, reached 0.095% and 0.02% relative abundance in HC group, respectively. There were no significant differences in major phyla of *Firmicutes*, *Bacteroidetes*, and *Proteobacteria*.

The dissimilarity in different taxonomic levels between the two groups based on statistical and biological significance, ranking them according to the effect size was shown in the bar plot (Fig. 11.). A cladogram was also created to show the differences in the known hierarchical structure of their phylogeny (Fig. 12). On the two figures, the red color indicated for AD group and the green color presented for HC group. On the bar plot, the length of the bar represented a log 10 transformed LDA score of the relative abundance of the nearest taxonomies which made the differences between the two groups. The green bars on the right side indicated the order *Turicibacterales*, families *Bacteroidaceae*, *Lacnospiraceae*, and *Turicibactericeae*, and genera *Bacteroides*, *Faecalibacterium*, *Coprococcus*, *Turicibacter*, and *Christensenella* were more abundant in HC group than in AD group. Others with red bars indicated they were more abundant in AD group than those in HC group, included 14 genera, 12 families, 2 classes, 4 orders, and 3 phyla. The cladogram showed the differences according to phylogeny so that it was easy to understand which phylotypes contributed to the differences between the two groups. As indicated on the cladogram, at the phylum level, the phyla *Actinobacteria*, *Verrucomicrobia*, *Cyanobacteria*, and *TM7* abundances were higher in AD group than that in HC group.

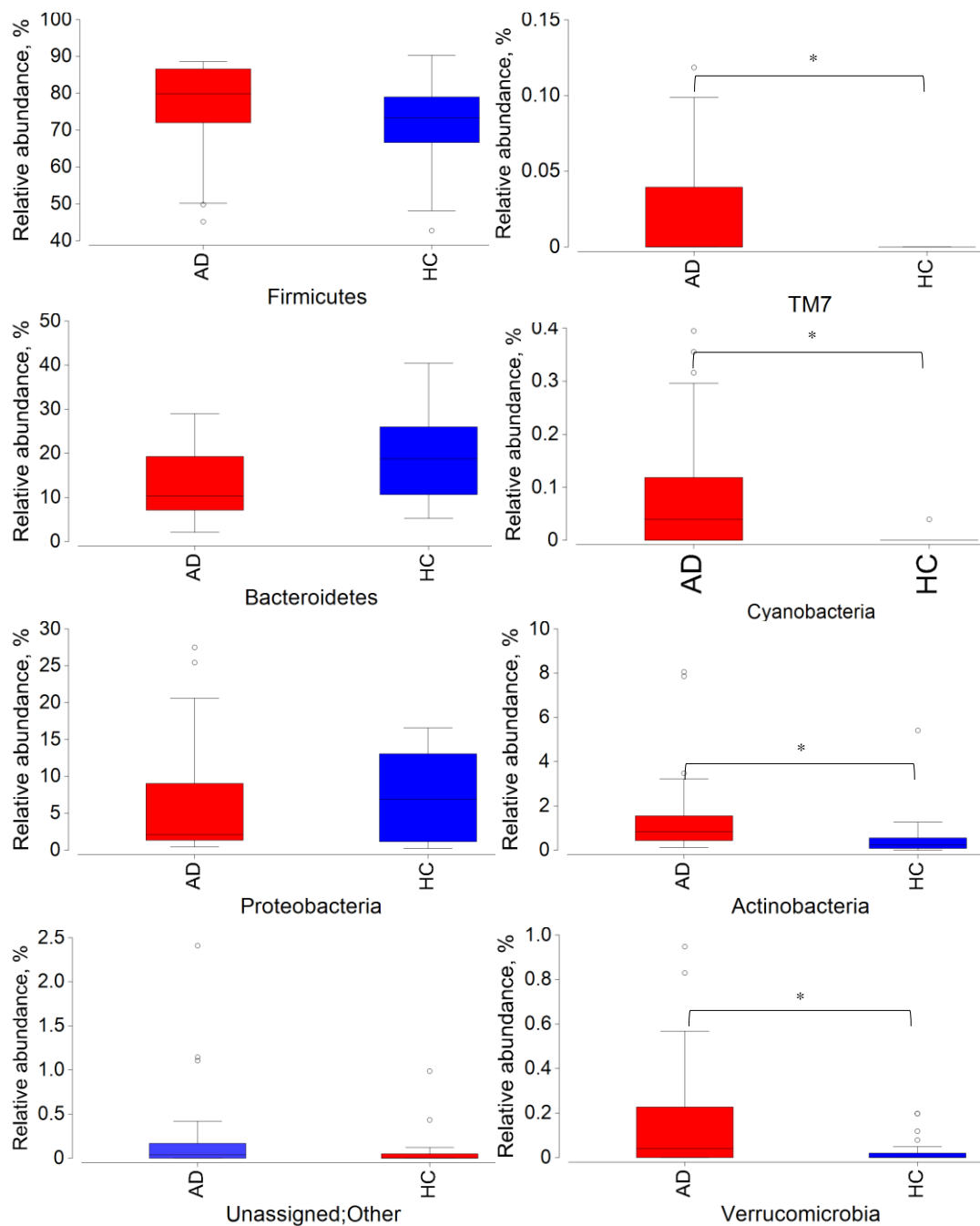


Fig 10 . Box plots indicate relative abundance at the phylum level of the two groups.

AD group represents with red boxes and HC group represents with blue boxes

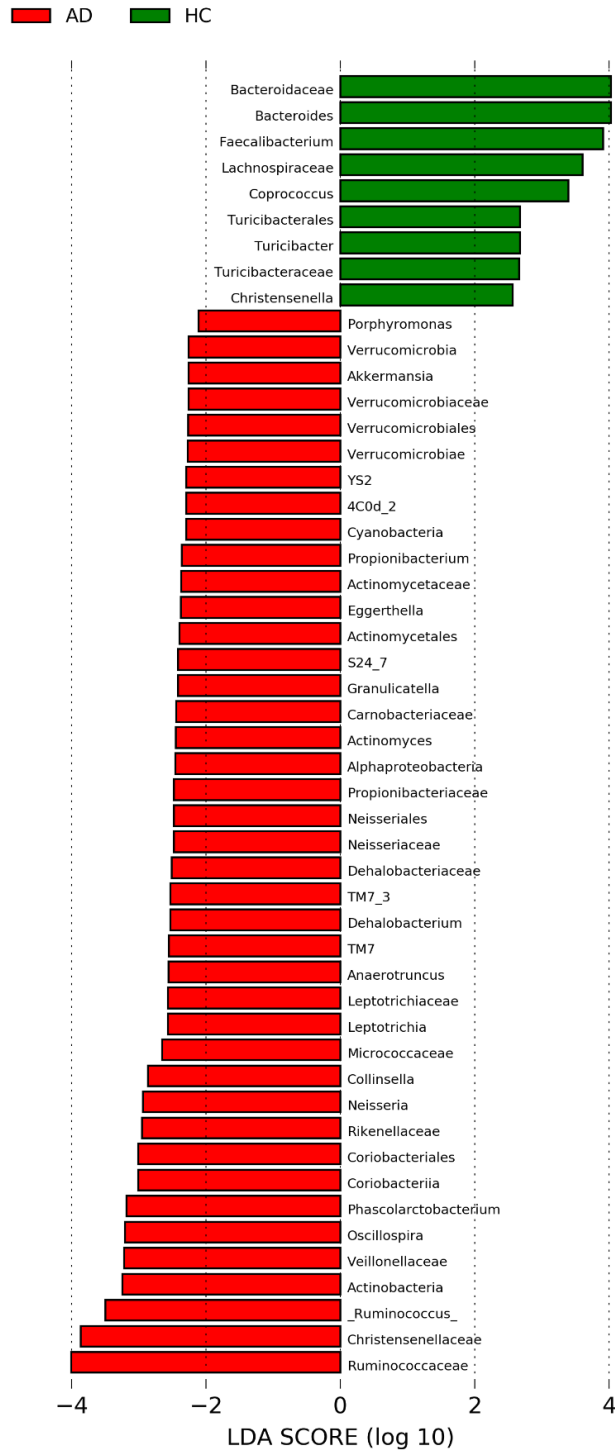


Fig 11. Bar plot from LefSe analysis indicating significant changes in taxonomies between AD and HC groups. The related bacteria names of each column are listed at the bottom of Y-axis, and the score number is shown on the X-axis. HC group-enriched taxa are indicated with a positive LDA score (green), and taxa enriched in AD have a negative score (red) ($p < 0.05$, LDA score 10).

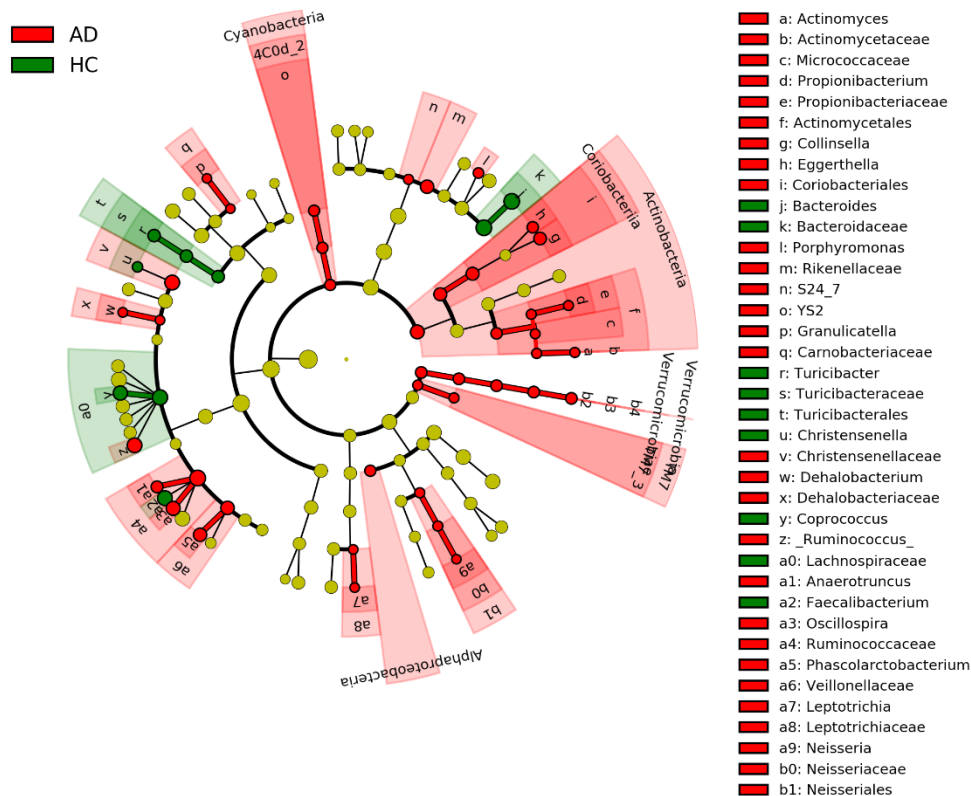
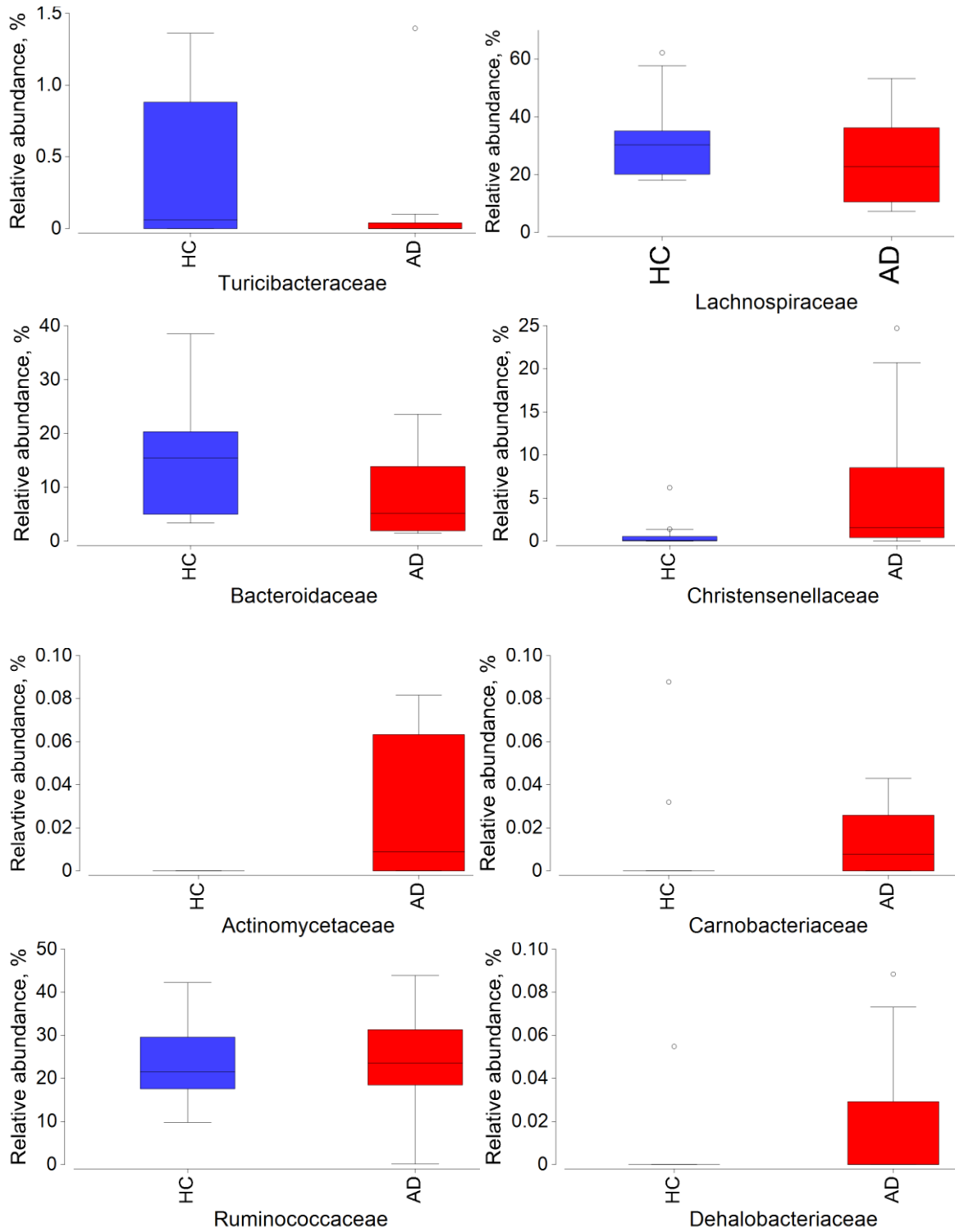


Fig 12. Cladogram plotted from LEfSe analysis showing the taxonomic levels represented by rings with phyla in the outermost the ring and genus in the innermost the ring. Each circle is a member within that level. Those taxa in each level are colored by the group for which it is more abundant, with the green color indicated HC group and red color indicated AD group ($p < 0.05$; LDA score 2).

The bar plot and cladogram showed the differences between the two groups in terms of distinct taxonomies but relative abundances of each different feature were not clearly indicated. In order to know how different their abundances were, box plots (Fig. 13) which figured out their relative abundances at the family level. There were 15 distinct families contributed to the differences in gut microbiota between the two groups. As shown in the Fig 13, the first three families were more prevalent in HC group than those in the diseased group, included *Bacteroidaceae*, *Turicibacteraceae*, and *Lachnospiraceae*. Families which were richer in AD group were 12, with *Verrucomicrobiaceae*, *Actinomycetaceae*, *Micrococcaceae*, *Propionibacteriaceae*, *Rikenellaceae*, *Carnobacteriaceae*, *Ruminococcaceae*, *Leptotrichiaceae*, *Neisseriaceae*, *Dehalobacteriaceae*, *Christensenellaceae*, and *Veillonellaceae*. Especially, *Actinomycetaceae*, *Carnobacteriaceae*, *Dehalobacteriaceae*, *Neisseriaceae*, *Leptotrichiaceae*, and *Propionibacteriaceae* seemed to disappear in the HC group. The three most abundant

families were *Bacteroidaceae*, *Lachnospiraceae*, and *Ruminococcaceae*, with relative abundances of 14.82% and 7.59%, 29.97% and 24.92%, and 23.48% and 24.69%, corresponded with HC and AD group, respectively.

At the genus level, the top ten most abundant genera which showed the significant differences between the two groups were displayed as histograms in detail for each genus (Fig 14), included *Faecalibacterium*, *Bacteroides*, *Ruminococcus*, *Eggerthella*, *Coprococcus*, *Anaerotruncus*, *Oscillospira*, *Phascolarctobacterium*, *Akkermansia*, and *Collinsella*. The genus *Faecalibacterium*, one of the important genus in the gut microbiota ecosystem, seemed to disappear in the AD group. While *Anaerotruncus*, *Phascolarctobacterium*, *Akkermansia*, *Eggerthella*, and *Collinsella* were more dominant in AD group.



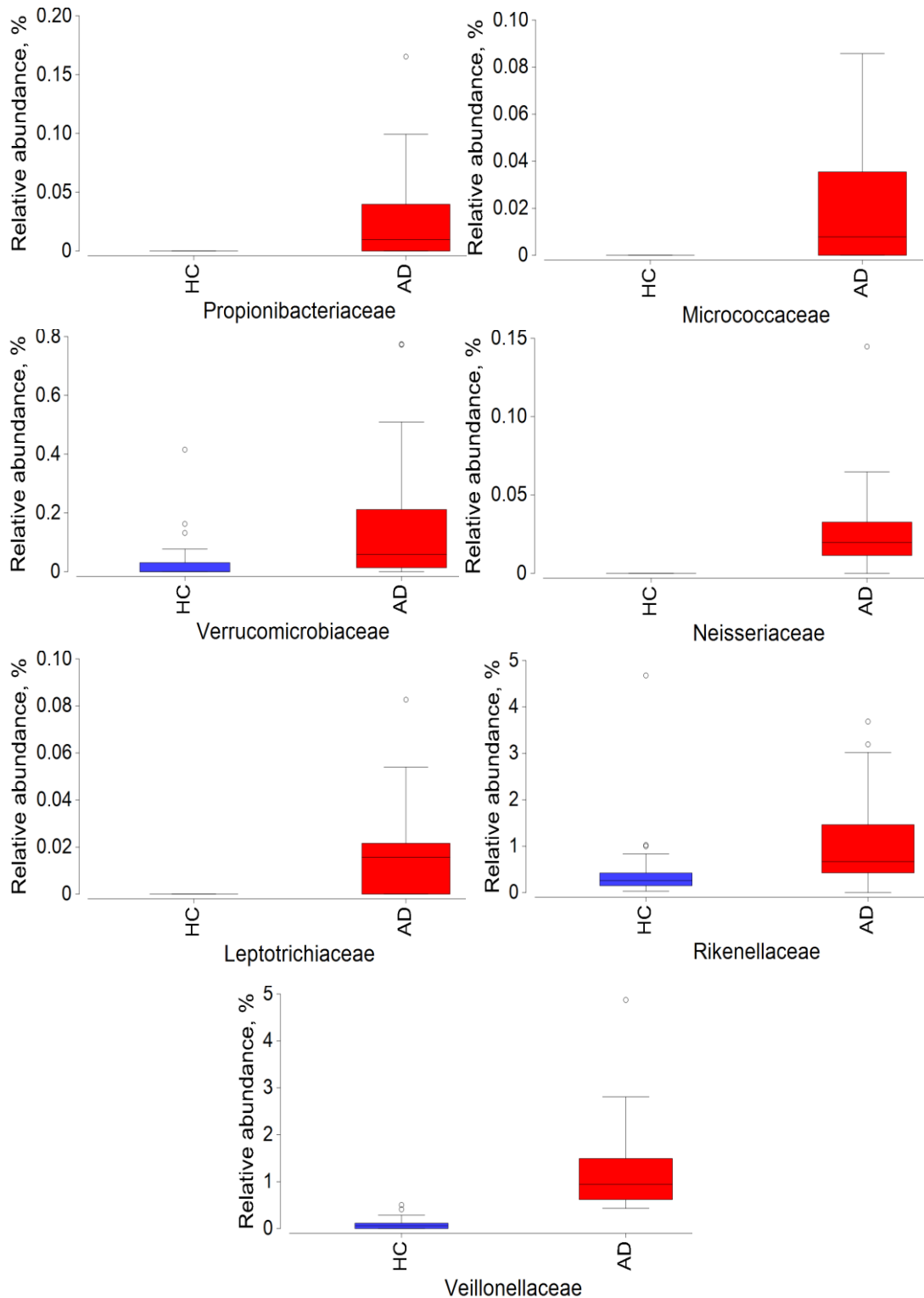


Fig 13. Box plots indicating the significant differences in relative abundance at the family level of the gut microbiota of AD compared to HC group. The upper and lower quartile with the median is displayed, whiskers are extended to 1.5 times the interquartile range and the circles show outliers.

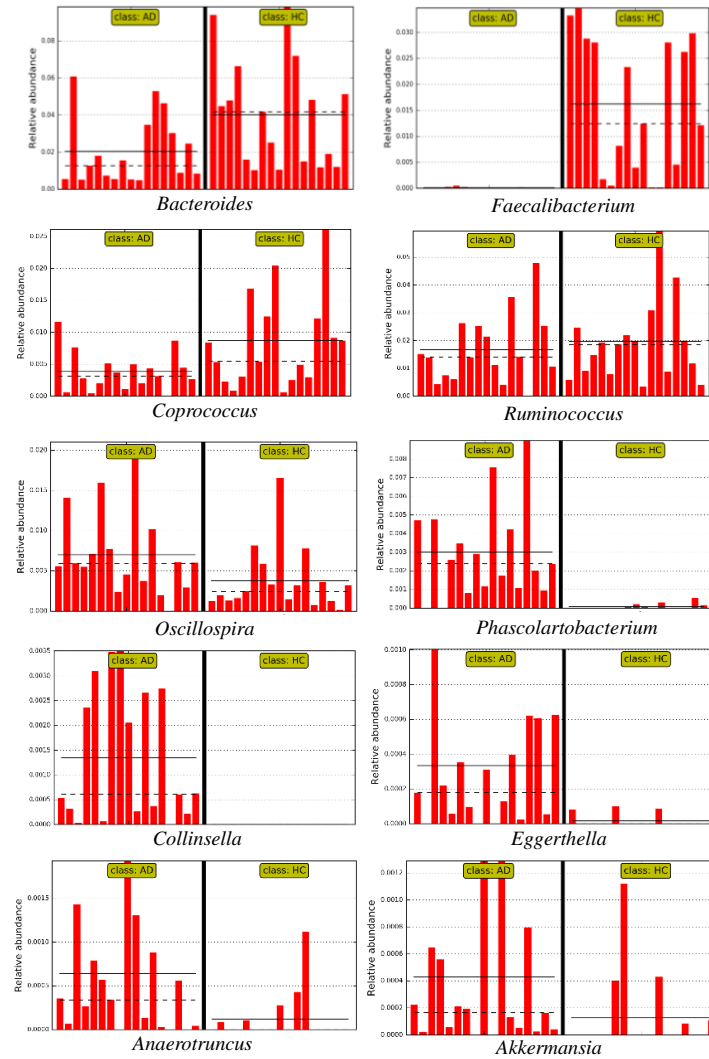


Fig. 14. Histograms showing genus that are more abundant in each group ranked by linear discriminant analysis (LDA) score 2. Values of all participants in each group are displayed. The top four genera were more abundant in the HC group while the bottom six genera were more abundant in the AD group. The mean and median relative abundance of these genera are indicated with solid and dashed lines, respectively.

- Diversity analysis

The diversity of gut microbiota of AD and HC groups were evaluated based on alpha diversity and beta diversity. Alpha diversity was evaluated to assess the species richness and evenness within gut microbiota community diversity of the two groups (Fig. 15). The Chao1 was calculated to estimate richness based on the observed number of species (Hughes *et al.*, 2001). Shannon index was used to assess the diversity by considering both species richness and evenness (Magurran, 2004). Faith's phylogenetic diversity (PD) was used to estimate their diversity based on the minimum total length of all the phylogenetic branches required

to span a given set of taxa on the phylogenetic tree (Faith, 1992; Faith and Baker, 2006). And observed OTUs counted the number of observed species in a given sample with non-phylogenetic richness.

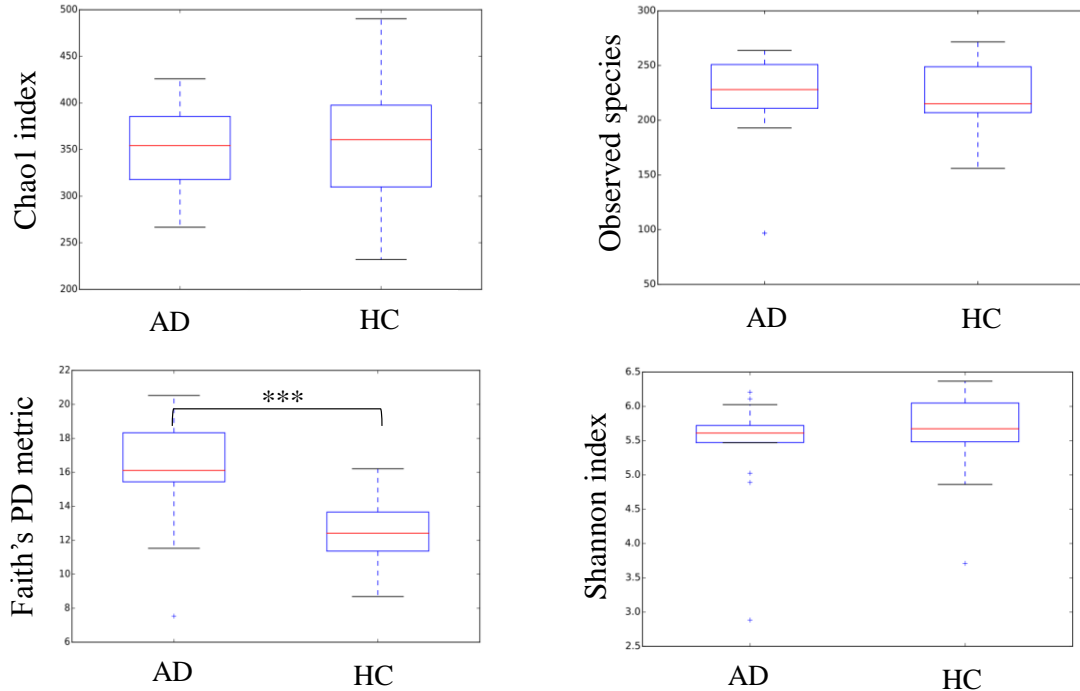


Fig 15. Box plots showing comparisons of alpha diversity of gut microbiota between Japanese AD and HC groups.

There were no significant differences in the number of observed OTU, Shannon index and diversity of the species estimated by Chao1. In HC and AD group, observed species were 216.89 ± 34.99 and 223.00 ± 38.37 , respectively; Shannon index were 5.58 ± 0.63 and 5.46 ± 0.72 , and Chao1 were 353.32 ± 71.02 and 350.84 ± 43.22 , respectively. However, interestingly, Faith's PD whole tree was significantly reduced in the HC group, reached 12.66 ± 2.1 in the HC group and 15.99 ± 2.29 in AD group ($p < 0.05$).

The gut microbiota community was not only measured based on the diversity within each group but also between the two groups to provide an overview of gut microbiota structure. Unweighted and weighted UniFrac Principle Coordinate Analysis (PCoA) and their UniFrac distance of the gut microbiota community in both groups were analyzed (Fig. 16). Unweighted UniFrac was calculated based only on sequence distances (phylogenetic tree) (does not include abundance information) and weighted UniFrac: branch lengths are weighted by relative abundances (includes both sequence and abundance information) (Lozupone and Knight, 2005).

On the unweighted plot the points were closer to each other than those on the weighted plot. The largest principle coordinates, PC1 and PC2, were 14.36% and 8.18% of total variation, respectively, in the unweighted plot, while they were 26.11% and 18.22%, respectively, in the weighted plot. The shifting of the gut composition of AD patients was indicated in bar plots of unweighted and weighted UniFrac distance analysis (Fig. 16). The UniFrac distances between AD and HC groups were significant different at $p < 0.001$, except for HC-AD and AD-AD distances in the weighted plot.

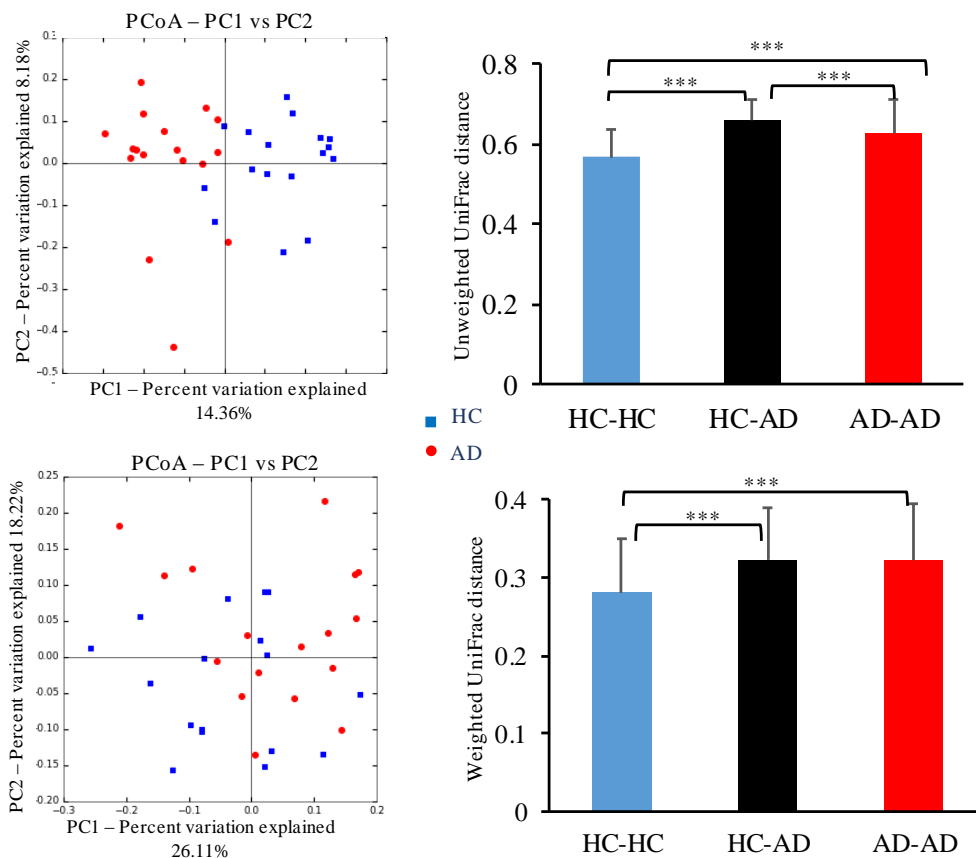


Fig. 16. Multidimensional scaling (MDS) plots of unweighted UniFrac and weighted UniFrac. Each dot represents a scaled measure of the composition of a given sample, color-coded by cohort with the blue dots code for HC samples and the red dots code for AD samples.

- Comparison of predicted metabolic pathways associated with the gut microbiome between the HC and AD groups

The gut microbiota plays a key function in the host's health due to its effect on their metabolic pathways. Between HC and AD group, the significant differences in metabolic

pathways generated from the gut microbiota community were shown in figure 17 at first, second, and third level which were classified according to the KEGG database. At the second level, the HC group was more enriched in 5 pathways than those in AD group, included carbohydrate metabolism, unclassified metabolism, amino acid metabolism, nervous system and endocrine system. However, the AD group was enriched in 10 pathways, listed as glycan biosynthesis and metabolism, metabolism of other amino acids, xenobiotics biodegradation and metabolism, neurodegenerative disease, digestive system, folding, sorting and degradation, genetic information processing, lipid metabolism, membrane transport, and cellular processes and signalling.

At the lower level, third level of metabolic pathways, 14 pathways included starch and sucrose metabolism, amino sugar and nucleotide sugar metabolism, phenylalanine, tyrosine and tryptophan biosynthesis, bacterial chemotaxis, cytoskeleton proteins, alanine, aspartate and glutamate metabolism, thiamine metabolism, carbohydrate metabolism, lipid metabolism, amino acid metabolism, epithelial cell signaling in *Helicobacter pylori* infection, linoleic acid metabolism, glutamatergic synapse, and insulin signaling pathway were higher in HC group than those in AD group. On the other hand, the intestinal bacteria of AD group were enriched with metabolic pathways involving taurine and hypotaurine metabolism, protein digestion and absorption, vitamin B6 metabolism, Alzheimer's disease, mineral absorption, protein export, lipoic acid metabolism, bacterial secretion system, lipid biosynthesis proteins, cell motility and secretion, tryptophan metabolism, protein folding and associated processing, membrane and intracellular structural molecules, oxidative phosphorylation, lipopolysaccharide biosynthesis, lipopolysaccharide biosynthesis proteins.

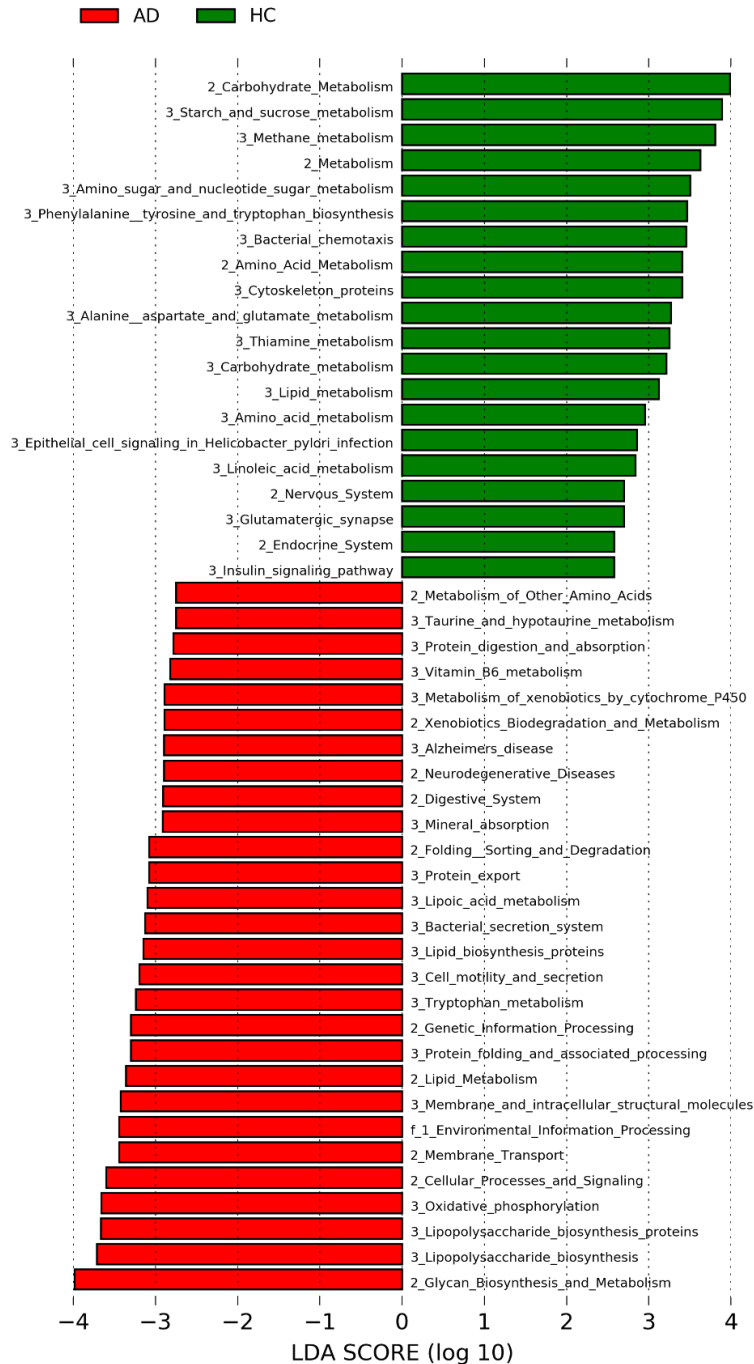


Fig 17. Differences in predicted KEGG functional pathways at first, second, and third levels between AD (red) and HC (green) participants. Pathway differences plotted as LDA scores (log 10). Bars which locate on the right of zero line represent bacterial functions enriched in the microbiome of AD participants, while bars which locate on the left of zero line represent bacterial functions enriched in the microbiome of HC participants.

b. Comparison of the gut microbiota of Japanese AD patients and American AD patients

- Taxonomic comparison

The gut microbiota of 17 Japanese AD and 25 American AD patients was evaluated. The total reads were 4,000,035 reads ($95,238.93 \pm 71,613.29$ reads/sample) which were grouped into 14,593 OTUs, comprised of 12 phyla, 26 classes, 30 orders, 79 families, and 180 genera. An overall gut bacterial of the American group and Japanese group at phylum level was displayed on a stacked bar plot (Fig. 18).

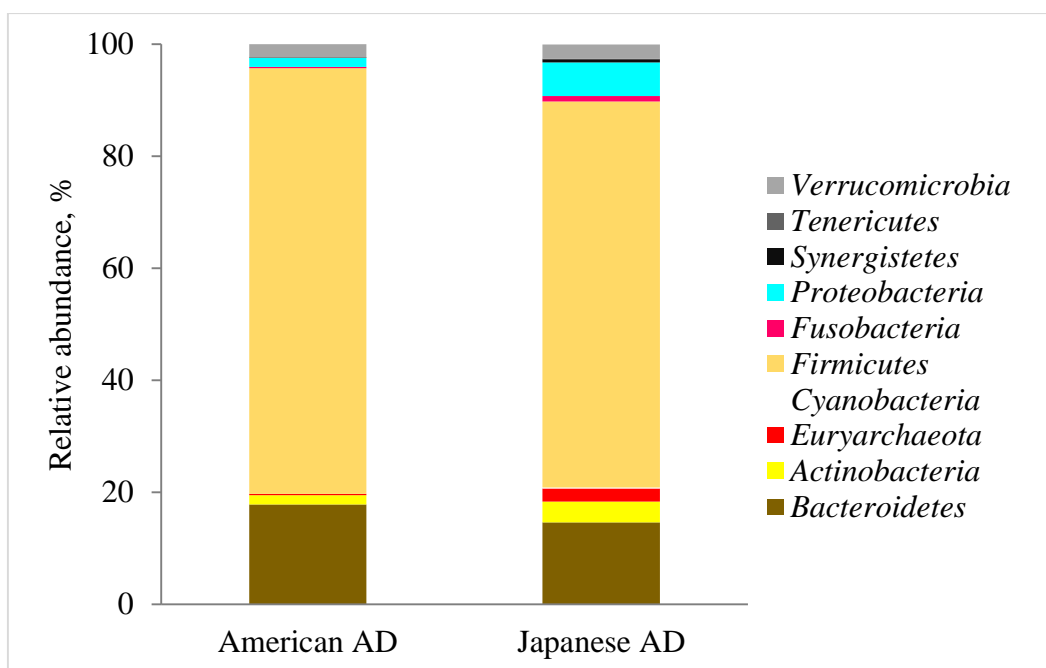


Fig 18. Gut bacterial compositions of American and Japanese groups at the phylum level

The phyla *Firmicutes* and *Bacteroidetes* were two major phyla in both groups, with the relative abundance of 75.97 ± 8.20 %, and 68.94 ± 11.70 % of *Firmicutes*, and 17.78 ± 7.93 %, and 14.60 ± 8.33 % of *Bacteroidetes* in American and Japanese AD groups, respectively. Lower contributors were *Actinobacteria*, *Verrucobacteria*, *Proteobacteria*, and *Cyanobacteria*. Only the two phyla *Proteobacteria* and *Archaea* made the differences in the gut microbiota of these two groups, they were richer in Japanese group than in American group. For *Proteobacteria*, the relative abundance of America group was 1.56 ± 3.69 % while it accounted for 6.04 ± 7.66 % in Japanese group. Relative abundance of the phylum *Euryarchaeota* were 0.23 ± 0.40 % and 2.39 ± 4.71 % in American and Japanese groups, respectively.

A bar plot (Fig. 19) and a cladogram (Fig. 20) were generated to compare the differences in taxonomy at many levels from phylum to genus between the two groups. The bar plot displayed the differences in bacterial taxonomies based on relative abundance

between the two groups while the cladogram indicated the differences based on the color and classification of their phylogeny. On the bar plot, bars lie on the left of zero indicated taxonomies that were more abundant in Japanese group than in American group and vice versa.

As indicated on the two figures, within *Proteobacteria*, the classes *Betaproteobacteria* and *Gammaproteobacteria*, the orders *Burkholderiales*, *Enterobacteriales*, families *Alcaligenaceae*, *Oxalobacteraceae* and *Enterobacteriaceae* and genus *Sutterella* were the factors which were less abundant in American than in Japanese group. For *Euryarchaeota* of kingdom *Archaea*, class *Methanobacteria*, order *Methanobacteriales*, family *Methanobacteriaceae* and genus *Methanobrevibacter* contributed to the imbalance, they were higher in Japanese group than those in American group.

Although the phylum *Firmicutes* did not make the differences between the two group, some its lower hierarchies made the differences. While class *Clostridia* was richer in American group, classes *Bacilli* and *Erysipelotrichi* was poorer in American group than those in Japanese group. Within the class *Clostridia*, families *Dehalobacteriaceae*, *Christensenellaceae*, *Clostridiaceae*, *Lachnospiraceae*, and *Ruminococcaceae*, and genus *Anaerotruncus*, *Faecalibacterium*, *Ruminococcus*, *Blautia*, *Lachnospira*, and *Coprococcus* created the imbalance. In the class *Bacilli*, order *Lactobacillales*, family *Streptococcaceae*, and genus *Streptococcus* brought the differences with higher abundant in Japanese group. And within the class *Erysipelotrichi*, order *Erysipelotrichales*, family *Erysipelotrichaceae*, and genus *Eubacterium* had a higher rate in Japanese group than those in American group. Furthermore, the phylum *Bacteroidetes* abundance was not different between the two groups but two their families *Porphyromonadaceae* and *Bacteroidaceae* made the differences, with higher *Porphyromonadaceae* and lower *Bacteroidaceae* abundances in Japan group than those in America group. Differences in relative abundances of families and genera which figured out by the cladogram were plotted in box plots (Fig. 21) and histograms (Fig. 22, 23) to have clearer and detailed dissimilarities between the two groups.

At the family level, notably, the family *Bacteroidaceae* in American AD patients were higher than those in Japanese AD patients, reached 13.95% and 8.89% in, respectively. The most abundant family, *Lachnospiraceae*, had 37.76% and 22.36% in American and Japanese group, respectively. The family *Oxalobacteraceae* seemed to disappear in Japanese AD

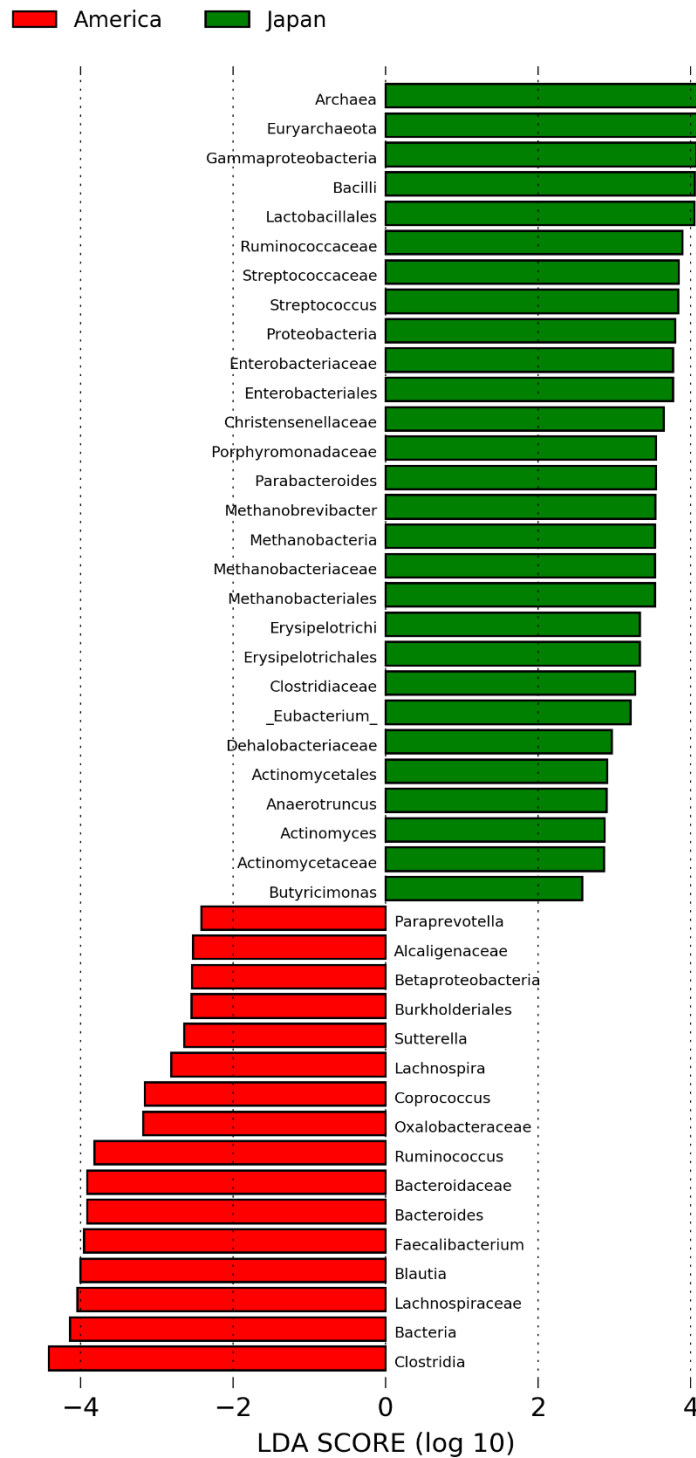


Fig 19. Bar plot from LEfSe analysis indicating significant changes in taxonomies between America and Japan groups. The related bacteria names of each column are listed at the bottom of the Y-axis, and the score number is shown on the X-axis. Japan group-enriched taxa are indicated with a positive LDA score (green), and taxa enriched in America group have a negative score (red) ($p < 0.05$, LDA score 10).

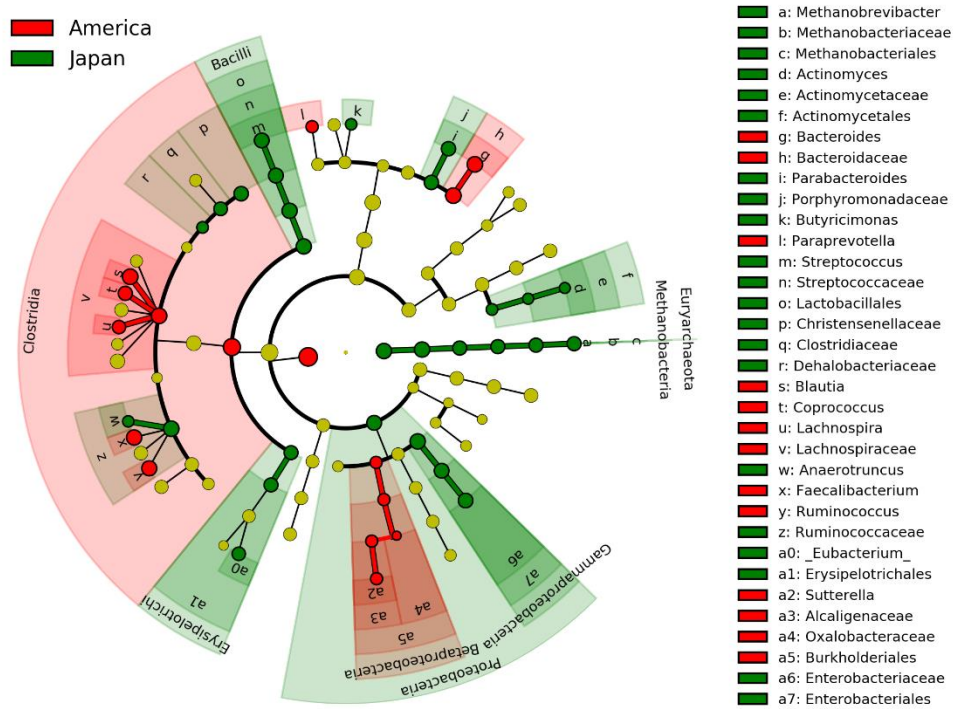


Fig. 20. Cladogram plotted from LEfSe analysis showing the taxonomic levels represented by rings with phyla in the outermost the ring and genus in the innermost the ring. Each circle is a member within that level. Those taxa in each level are colored by the groups for which it is more abundant, with the green color indicates Japan group and the red color indicates America group ($p < 0.05$; LDA score 2).

patients while accounted for 0.008% in American group. The *Methanobacteriaceae* family was richer in Japan group than that in America group.

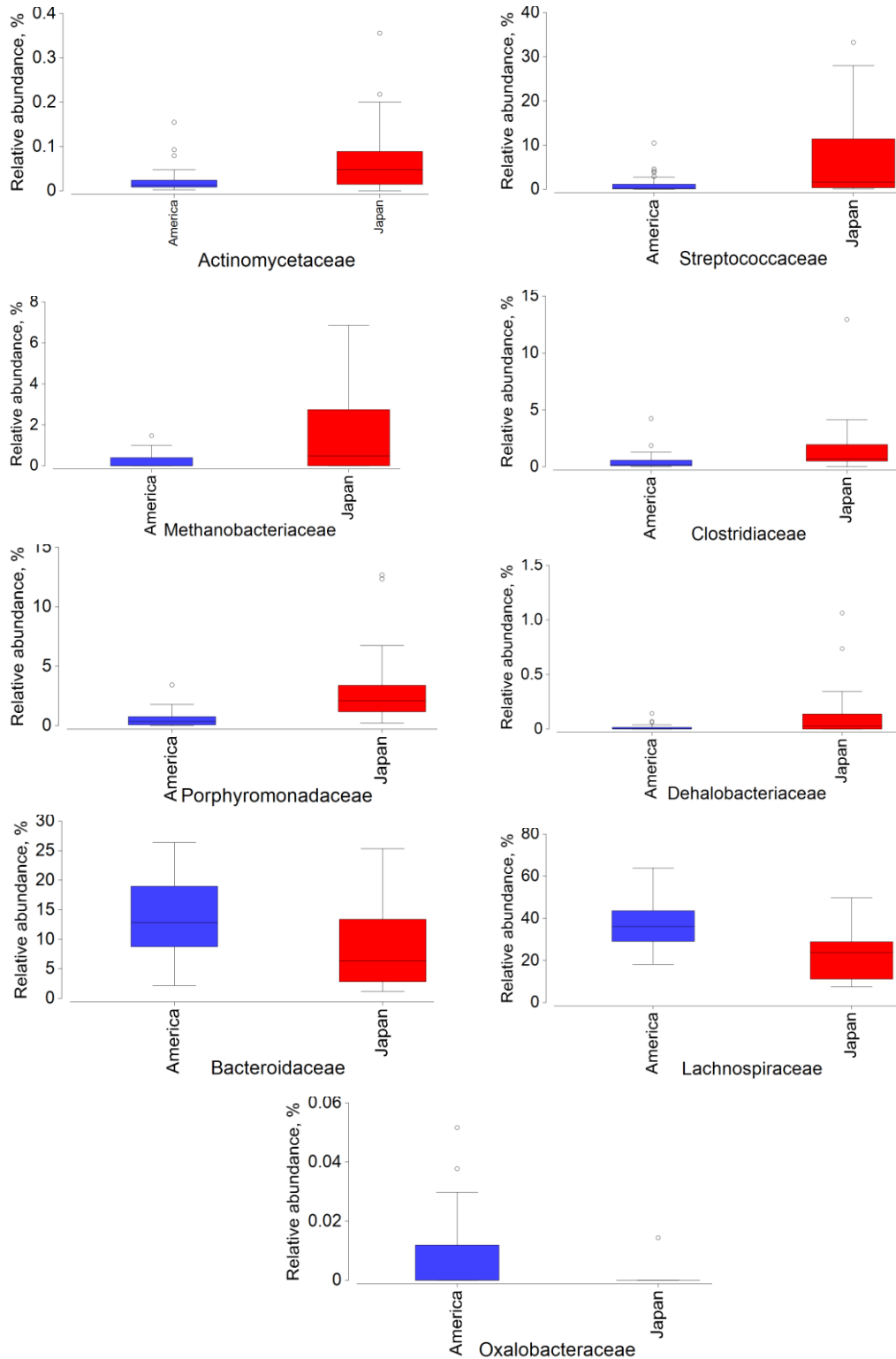


Fig 21. Box plots indicating the significant differences in relative abundance at the family level of gut microbiota of participants between the two countries are shown. The upper and lower quartile with the median are shown, whiskers are extended to 1.5 times the interquartile range, and the circles show outliers.

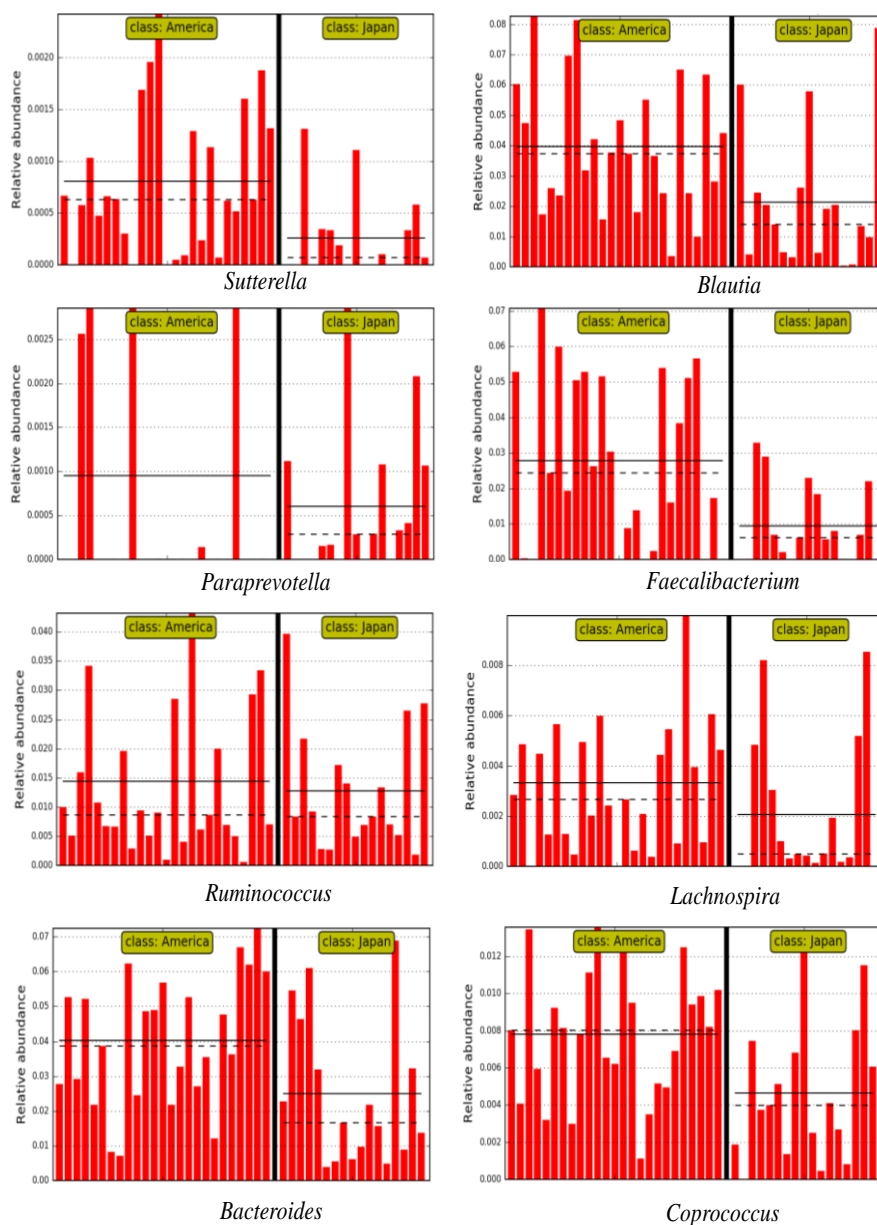


Fig. 22. Histograms showing genus that are more abundant in American group ranked by LDA score 2. Values of all participants in each group are displayed. The mean and median relative abundance of these genera are indicated with solid and dashed lines, respectively.

As indicated in Fig. 22, the genus *Sutterella*, *Blautia*, *Paraprevotella*, *Faecalibacterium*, *Ruminococcus*, *Lachnospira*, *Bacteroides* and *Coprococcus* had higher relative abundance in American group than those in Japanese group. The genus *Paraprevotella* did not evenly distribute amongst all participants in the American group. The lower relative abundance of *Faecalibacterium* in Japanese group was an interesting result since this genus also decreased in Japanese AD group in comparison with Japanese HC group.

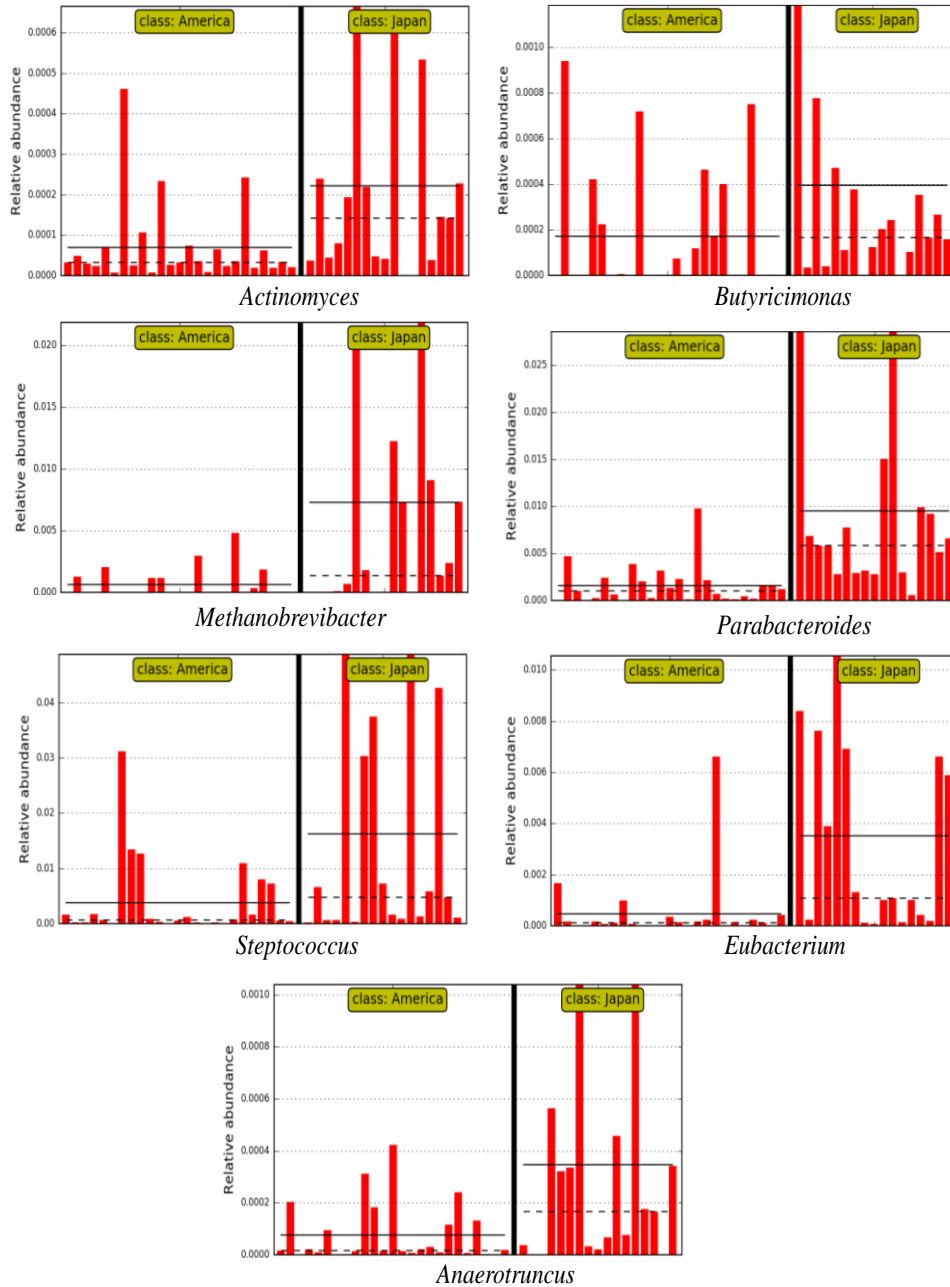


Fig. 23. Histograms showing genus that are more abundant in Japanese group ranked by LDA score 2. Values of all participants in each group are displayed. The mean and median relative abundance of these genera are indicated with solid and dashed lines, respectively.

Fig. 23 showed the falling relative abundance of *Actinomyces*, *Butyricimonas*, *Methanobrevibacter*, *Parabacteroides*, *Streptococcus*, *Eubacterium*, and *Anaerotruncus* in American group compared to those in Japanese group.

- Diversity analysis

The alpha diversity of the gut microbiota between Japanese AD and American AD patients were different in richness, included observed OTU and Chao1 index (Fig. 24). The observed OTU were 351.48 ± 71.11 and 449.90 ± 72.68 ($p < 0.001$) in Japanese and American groups, respectively. The Chao1 index reached 606.42 ± 160.43 and 1006.40 ± 217.52 ($p < 0.001$), corresponding to Japanese and American groups. However, there was a similarity in their diversity, consisted of Shannon index and Faith's phylogenetic diversity. Shannon index were 5.77 ± 0.70 in Japanese group and 5.88 ± 0.47 in American group ($p = 0.56$) and Faith's PD were 22.79 ± 4.38 and 22.28 ± 4.77 ($p = 0.73$), respectively.

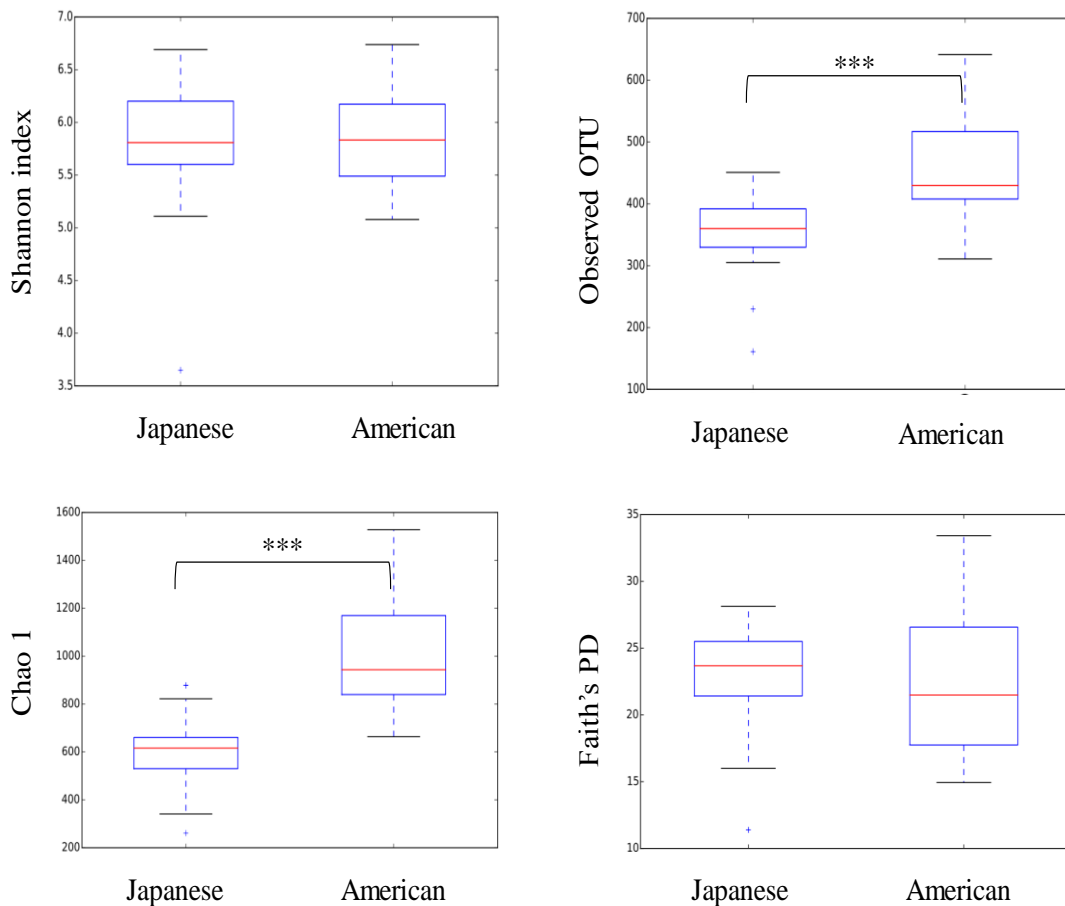


Fig. 24. Box plots showed comparisons of alpha diversity of gut microbiota between Japanese AD and American AD groups.

In terms of beta diversity, as indicated on PCoA plots (Fig 25), the principle components, PC1 and PC2, in unweighted UniFrac plot were 12.78% and 8.31% while they were 28.10% and 19.47% of total variation in weighted UniFrac plot, respectively. Both unweighted and weighted UniFrac analyses showed significant differences ($p < 0.001$) in the

overall gut microbiota structure between American and Japanese subjects (Fig. 25). The data also revealed significantly higher inter-individual variability in the gut microbiota of Japanese subjects compared to American subjects in weighted plot. However, the inter-individual variability of Japanese group was lower than those of American group as indicated in unweighted plot.

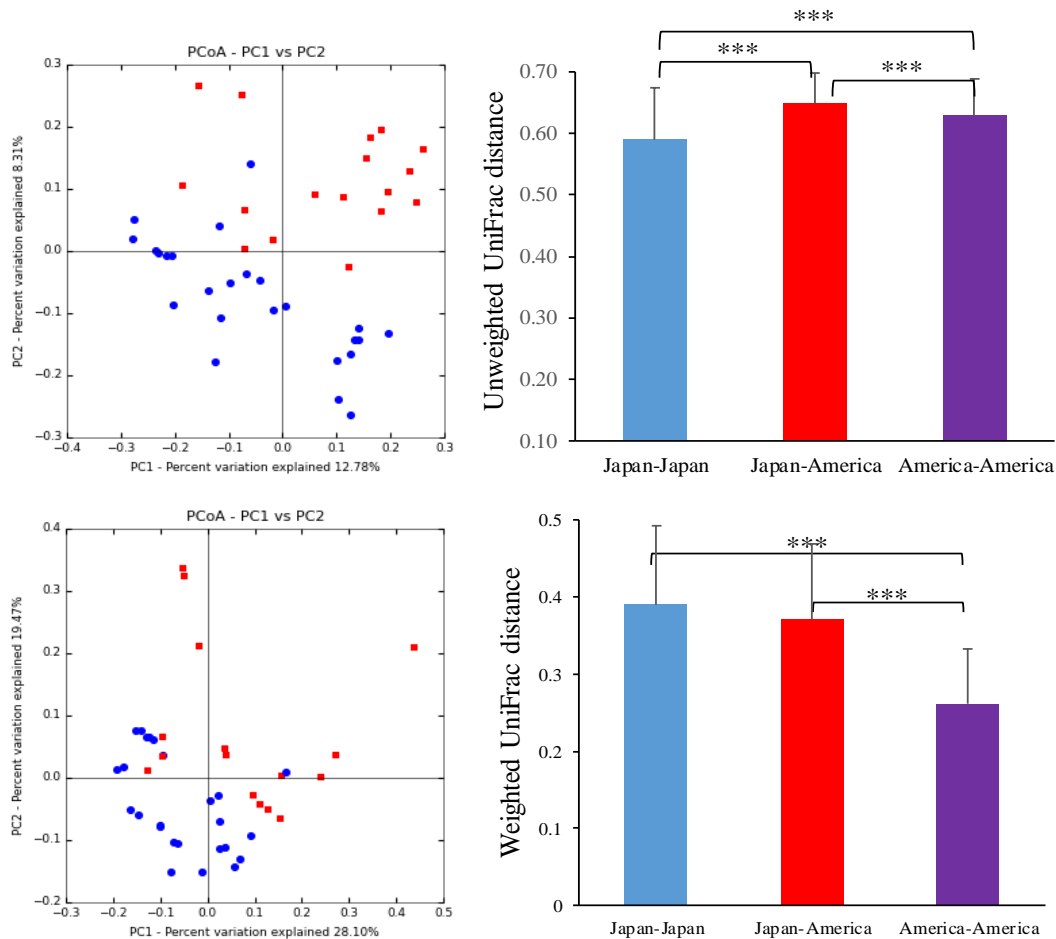


Fig. 25. MDS plots of unweighted UniFrac and weighted UniFrac. Each dot represents a scaled measure of the composition of a given sample, color-coded by cohort with the blue dots code for American samples and the red dots code for Japanese samples.

- Metabolic pathway analysis

Different composition and diversity of gut microbiota led to the different metabolic pathways which generated from the gut microbiome between American and Japanese group. The Japanese group was enriched pathways of lipopolysaccharide biosynthesis protein, butanoate metabolism, tryptophan metabolism, *Staphylococcus aureus* infection, geraniol degeneration, fatty acid metabolism, mineral absorption, biosynthesis of unsaturated fatty

acids, secretion system, apoptosis, and taurine and hypotaurine metabolism. However, the American group had richer pathways of insulin signaling pathway, glutamatergic synapse, linoleic acid metabolism, carbohydrate metabolism, biotin metabolism, cell division, epithelial cell signaling in *Helicobacter pylori* infection, protein export, lipid metabolism, thiamine metabolism, amino acid related enzymes, cytoskeleton proteins, alanine aspartate and glutamate metabolism, phenylalanine, tyrosine and tryptophan biosynthesis, and starch and sucrose metabolism.

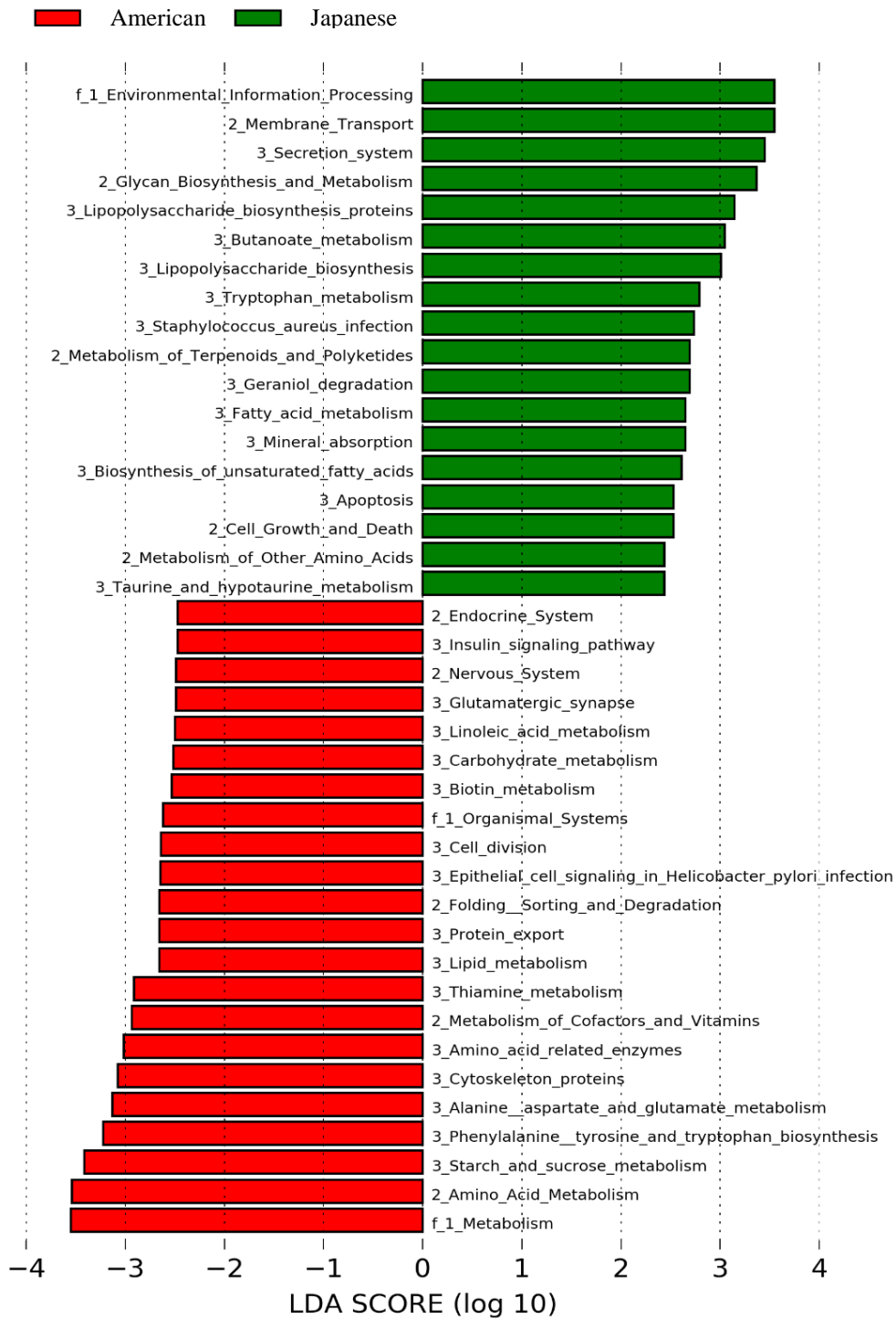


Fig. 26. Differences in predicted KEGG functional pathways at first, second, and third level between American (red) and Japanese (green) participants. Pathway differences plotted as LDA scores (log 10). Bars which locate on the right of zero line represent bacterial functions enriched in the microbiome of Japanese participants, while bars which locate on

the left of zero line represent bacterial functions enriched in the microbiome of American participants.

4. Discussion

In recent years, the bi-directional communication between the human gut microbiota and the central nervous system has been widely studied. Those studies demonstrated that microbial alteration may effect on normal brain functions, leading to anxiety, depression and cognitive deficits (Mancuso and Santangelo, 2018; Westfall *et al.*, 2017). In this study, we used DNA of fecal samples of 17 Japanese AD patients and 17 Japanese healthy people to compare their bacterial community as well as metabolic pathways generated from their microbiome.

The differences in taxonomies between the AD group and HC group was characterized and displayed on Fig. 11 and 12. Their relative abundances were shown in box plots and histograms Fig. 13, 14 and 15 at the phylum, family and genus levels, respectively. At the phylum level, the increases in the phyla *Cyanobacteria*, *Actinobacteria*, *Verrucomicrobia*, and *TM7* in AD group was recorded in comparison with HC group. Notably, a higher abundance of *Cyanobacteria* in AD group was an interesting result since this bacteria group is believed to be correlated with AD (Banack *et al.*, 2010). The *Cyanobacteria* bacteria can produce neurotoxins of β -N-methylamino-L-alanine (BMAA), anatoxin-a and saxitoxin, which are neurotoxin amino acids (Banack *et al.*, 2010; Hu *et al.*, 2016). These compounds may contribute to the onset and development of cognitive dysfunctions, a signal of AD invasion (Banack *et al.*, 2010; Hu *et al.*, 2016). BMAA can be inappropriately inserted into the polypeptide chains of brain proteins and then lead to protein misfolding, a hallmark characteristic of A β plaque in AD patients (Hu *et al.*, 2016; Mancuso and Santangelo, 2018; Mulligan and Chakrabartty, 2013). As indicated in Fig. 15, of predicted KEGG functional pathways, protein folding and associated processing in AD group was higher in HC group. This may explain for the correlation between the gut microbiota and their functional pathways in AD group. Furthermore, the increase of cyanobacterial toxin BMAA from gut microbiota may increase the deposition of A β and the risk of AD (Cox *et al.*, 2016; Hu *et al.*, 2016). The saxitoxin and anatoxin-a may further contribute to human neurological disease, especially during aging when the intestinal epithelial barrier of the gastrointestinal tract becomes more permeable (Bhattacharjee and Lukiw, 2013). Thus, besides potentially altering CNS neurochemistry and neurotransmission, the human gut microbiota does not

only secrete molecules that potentially modulate systemic and CNS amyloidosis, they also widely utilize their own amyloid peptides as structural materials, adhesion molecules, toxins, molecules that function in the protection against host defenses and auto-immunity (Bhattacharjee and Lukiw, 2013). However, another study which carried out to identify gut microbiota community of American AD patients did not report that the phylum *Cyanobacteria* was altered between AD and HC groups (Vogt *et al.*, 2017).

The increase in the *Actinobacteria* in gut microbiota of AD group was in good agreement with the result in depression patients. Depression is the most common psychiatric disorders in AD (Brockman *et al.*, 2011). The beta-diversity of the gut microbiota in major depressive disorder patients showed significant increase in *Actinobacteria* and decreased abundance of *Bacteroidetes* (Sharon *et al.*, 2016; Zheng *et al.*, 2016). In this study, the species richness indicated by Chao1 index and number of observed species and the diversity indicated by Shannon index were not significant different between AD and HC groups. An observation on another inflammatory disease of CNS, multiple sclerosis (MS), based on Japanese MS patients also showed high similarity of species richness of their gut microbiota with those of healthy controls (Miyake *et al.*, 2015). However, the UniFrac analysis of both studies, our study and MS study, revealed the significant differences in the overall gut microbiota structure between patients and healthy groups. The gut microbiota of patients with both MS and AD showed higher inter-individual variability than did that of healthy controls.

There were no significant differences in relative abundance of the two major phyla, *Firmicutes* and *Bacteroidetes* between HC and AD gut microbiota. However, the decreased abundance of *Firmicutes* and *Actinobacteria* and the increased abundance of *Bacteroidetes* and *Tenericutes* were found in the intestine of transgenic AD mice CONVR- APP/PS1 aged 8-months (Harach *et al.*, 2015; Mancuso and Santangelo, 2018). Another clinical trial study which performed on elderly subjects with dementia support evidence of the role of amyloid and related bacterial accumulation in the pathogenesis of cognitive damage. They indicated amyloid-related cognitive impairment is associated with a reduction in certain anti-inflammatory bacteria belonging to the phyla *Firmicutes* and *Bacteroidetes* compared to an increase of other pro-inflammatory bacteria of phylum *Proteobacteria* (Cattaneo *et al.*, 2017; Mancuso and Santangelo, 2018).

It can be predicted metabolic pathways of the gut microbiome based on their gut microbiota community. Several molecular mechanisms of neurodegeneration in AD linking neuronal toxicity to A β and tau protein have so far been hypothesized, including neuro-inflammation, oxidative stress, impaired cell stress response, mitochondrial dysfunction, lipid metabolism, apoptosis, disruption of Ca²⁺ homeostasis, reduced cytoskeletal integrity, enzymatic deregulation (phosphatases, kinases, proteases), epigenetic changes, and, most importantly, the failure of neurotransmitter pathways (Mancuso and Santangelo, 2018). Furthermore, brain glucose metabolism is impaired in AD since the type 2 diabetes mellitus (T2DM) is reported to increase the risk for dementia, including AD. The total and the phosphorylated components of the insulin signaling pathway were decreased in AD and T2DM brains (Liu *et al.*, 2011). In our study, the insulin signaling pathways was higher in HC group than AD group, which was in good consistent with Liu et al (2011) results.

Moreover, the Fig. 15 indicated that the pathway of lipopolysaccharide (LPS) biosynthesis proteins and lipopolysaccharide biosynthesis enriched in AD group's microbiome than HC group's microbiome. The LPS has been believed to be played a role in causing sporadic AD (Zhan *et al.*, 2018). Plasma levels of LPS in patients with AD were three times higher than healthy controls (Jiang *et al.*, 2017; Zhang *et al.*, 2009). This may contribute to AD development. Additionally, SCFA has been hypothesized that they may attenuate AD by serving as substrates for energy metabolism and providing an alternative energy source to rectify brain hypo-metabolism that contributes to neuronal dysfunctions in AD and other neurodegenerative conditions (Ho *et al.*, 2018). Decreased levels of SCFAs might facilitate microglial activation induced by increased CNS levels of LPS or bacterial amyloids, which may be involved in the development of AD (Jiang *et al.*, 2017). The genus *Faecalibacterium*, which possesses species *Faecalibacterium prausnitzii*, is known as a major producer of butyrate and other SCFAs in the human gut (Louis and Flint, 2009). The depletion of *Faecalibacterium* in AD group as showed in Fig. 15 may reflect the decrease in SCFAs in AD group. This result agreed with a study which investigated the alteration of fecal microbiota composition in patients with major depressive disorder. They indicated that level of *Bacteroidetes*, *Proteobacteria*, and *Actinobacteria* were strongly increased, whereas that of *Firmicutes* was significantly reduced in the diseased gut microbiota compared with the healthy group. At the genus level, they also found that the patient group had reduced levels of *Faecalibacterium* (Jiang *et al.*, 2015).

The human gut microbiota has their own specific composition and diversity, varying on geography and ethnicity (Gupta *et al.*, 2017). In comparison with other countries, the gut microbiota of Japanese is unique thanks to their particular dietary culture and habit. Their gut microbiome has a higher number of genes for aquatic plant-derived polysaccharide degrading enzymes than those of Americans (Hehemann *et al.*, 2010; Nishijima *et al.*, 2016). The comparison in the gut microbiota composition of Japanese and American was investigated based on healthy volunteer's fecal samples. However, in this study, we compared the gut microbiota of American and Japanese persons, who were diagnosed with AD.

In the results which showed the comparison of the gut microbiota between Japanese AD group and Japanese HC group stated above, the relative abundance of *Firmicutes* and *Bacteroidetes* phyla were not significant different. However, there were the decreased *Firmicutes*, increased *Bacteroidetes*, and decreased *Bifidobacterium* in the gut microbiota of American AD group in comparison with American healthy group (Vogt *et al.*, 2017). In contrast, the Japanese AD group had a higher rate of *Proteobacteria* compared with Japanese HC group, while this phylum was similar in American AD group and American HC group (Vogt *et al.*, 2017). Furthermore, the phylum *Actinobacteria* which was richer in American HC group than in American AD group was poorer in Japanese HC group than in Japanese AD group.

The alpha diversity and beta diversity of the gut microbiota of AD group and HC group of the two countries were evaluated. While the species richness of the gut microbiota in Japanese AD and HC was similar, the species richness of American AD group was reduced compared to American HC group. The American's results also showed a significant decreased in alpha diversity, characterized by the Shannon index and Faith's PD, in their AD group compared with HC group (Vogt *et al.*, 2017). However, our results indicated that the Shannon index was not different in gut microbiota of Japanese AD and Japanese HC but the Faith's PD was higher in Japanese AD group than in Japanese HC group. Similar to our results in terms of beta diversity, unweighted UniFrac and weighted UniFrac analysis of American study was compositional differences in the gut microbiota between AD and HC groups.

The taxonomic comparisons did not show the differences between the two major phyla, *Firmicutes* and *Bacteroidetes* between Japanese and American AD patients. However, the

phyla of *Proteobacteria* and *Archaea* made the differences in the gut microbiota of the two groups, they were richer in Japanese group than those in American group. The genus *Methanobrevibacter* contributed to the imbalance, they were higher in Japanese group than those in American group (2.51% vs 0.21%, $p < 0.05$, respectively). However, it was reported that the genus *Methanobrevibacter* was lower in Japanese healthy person than that in healthy people of other countries, including America (Nishijima *et al.*, 2016). Hence, this is the most important finding and may explain for the alteration of this community in the human gut microbiota from country to country regarding their health status. The alpha diversity of the gut microbiota between Japanese AD and American AD patients were different in richness, included observed OTU and Chao1 index but their bacterial diversities were not different, consisted of the Shannon index and Faith's phylogenetic diversity. However, the diversity of the gut microbiota of AD patients in American differed from that in Japanese AD patients, except for Japanese and American groups when considering both the presence and abundance of each OTU in each group, the weighted UniFrac comparison.

Furthermore, in the American group, PICRUSt analysis revealed broad functional changes in predicted metabolism, included bacterial cell motility, and signal transduction pathways in the gut microbiome of AD participants. However, the specific bacteria which are responsible for compositional and functional alterations in gut microbiota may differ between conditions, it has been proposed that these broad-scale changes in gut microbiota. Although the predicted metabolic pathways of the compared groups were different, it is unclear to have an insight that how the gut influences the development of neuropathology (Vogt *et al.*, 2017).

III. CHARACTERIZATION OF BUTYRATE-PRODUCING BACTERIA ISOLATED FROM FECES OF ALZHEIMER'S DISEASE PATIENTS

Abstract

The group of butyrate-producing bacteria within the human gut microbiome may be associated with positive effects on memory improvement, according to previous studies on dementia-associated diseases. Here, fecal samples of four elderly Japanese diagnosed with Alzheimer's disease (AD) were used to isolate butyrate-producing bacteria. 226 isolates were randomly picked, their 16S rRNA genes were sequenced, and assigned into sixty OTUs (operational taxonomic units) based on BLASTn results. Four isolates with less than 97% homology to known sequences were considered as unique OTUs of potentially butyrate-

producing bacteria. In addition, 12 potential butyrate-producing isolates were selected from the remaining 56 OTUs based on scan-searching against the PubMed and the ScienceDirect databases. Those belonged to the phylum *Bacteroidetes* and to the clostridial clusters I, IV, XI, XV, XIVa within the phylum *Firmicutes*. 15 out of the 16 isolates were indeed able to produce butyrate in culture as determined by high-performance liquid chromatography with UV detection. Furthermore, encoding genes for butyrate formation in these bacteria were identified by sequencing of degenerately primed PCR products and included the genes for butyrate kinase (*buk*), butyryl-CoA: acetate CoA-transferase (*but*), CoA-transferase-related, and propionate CoA-transferase. The results showed that eight isolates possessed *buk*, while five isolates possessed *but*. The CoA-transfer-related gene was identified as butyryl-CoA:4-hydroxybutyrate CoA transferase (*4-hbt*) in four strains. No strains contained the propionate CoA-transferase gene. The biochemical and butyrate-producing pathways analyses of butyrate producers presented in this study may help to characterize the butyrate-producing bacterial community in the gut of AD patients. Whole genome sequences of 13 butyrate-producing bacteria were sequenced and annotated.

1. Introduction

The trillions of microorganisms in the human gut play a key role in the host's life with many beneficial health effects. They may promote digestion of foods and absorption of nutrients, produce vitamins, protect the host from opportunistic pathogens, improve the immune system, and maintain the host's homeostasis of its immune system (Sommer and Backhed, 2013; Wallace *et al.*, 2011). Within the community of human gut microbiota, the group of butyrate-producing bacteria attracts particular attention because of the specific health-promoting effects they provide to their hosts (Vital *et al.*, 2014). Their major metabolic end-product, butyrate, is not only a preferred energy source for colonocytes but also a major contributor to the preservation of intestinal epithelial permeability and the protection of the host from carcinogenic, inflammatory, and oxidative factors (Hamer *et al.*, 2008). Furthermore, butyrate was shown to improve memory function in an AD mouse model (Govindarajan *et al.*, 2011).

The characteristics and phylogenetic diversity of butyrate-producing bacteria in the healthy human gut have been widely investigated (Barcenilla *et al.*, 2000; Hamer *et al.*, 2008; Louis and Flint, 2009; Pryde *et al.*, 2002; Vital *et al.*, 2014). Butyrate-producing bacteria are extremely difficult to cultivate due to their obligate anaerobic lifestyle and their requirement

for specific nutrients. They are mostly Gram-positive bacteria, belonging to the phylum of *Firmicutes* within clostridial clusters IV and XIVa (Barcenilla *et al.*, 2000; Louis and Flint, 2009; Pryde *et al.*, 2002; Rivièrè *et al.*, 2016). However, a metagenomic analysis indicated that a minor portion also included the phyla *Actinobacteria*, *Bacteroidetes*, *Fusobacteria*, *Proteobacteria*, *Spirochaetes*, and *Thermotogae* (Vital *et al.*, 2014).

The effect of butyrate-producing bacteria on the host-gut microbiota relationship has been investigated in previous studies (Bourassa *et al.*, 2016; Geirnaert *et al.*, 2017; Li *et al.*, 2017; Liu *et al.*, 2015; Vital *et al.*, 2017; Vital *et al.*, 2013). Some of these studies examined butyrate-producing bacteria as probiotic in regards to their effects on various diseases (Geirnaert *et al.*, 2017; Liu *et al.*, 2015). For examples, in patients with inflammatory bowel disease, a reduction in the population of butyrate-producing bacteria was reported (Geirnaert *et al.*, 2017; Ott *et al.*, 2004). In an *in vitro* system simulating the mucus- and lumen-associated microbiota, supplementation of either *Faecalibacterium prausnitzii* or *Butyricoccus pullicaecorum* 25-3^T and a mix of other six butyrate-producers, to the fecal microbiota of Crohn's disease patients, helped to increase butyrate production and improved epithelial barrier integrity (Geirnaert *et al.*, 2017). Furthermore, in mice suffering from vascular disease, which is the second most common dementia-associated disease after AD, the administration of live *Clostridium butyricum* to their diet helped to regulate gut microbiota by increasing their diversity. This was reported to increase butyrate in murine brains, which improved memory. Therefore, *C. butyricum* was considered as a probiotic and it may become an economical therapeutic option to protect against vascular disease (Liu *et al.*, 2015).

AD is a progressive neurodegenerative disorder of the central nervous system, characterized by an onset of dementia in the elderly population (aged above 65 years) (Mandell and Green, 2011). It was hypothesized that butyrate or butyrate-producing bacteria may have positive effects on memory improvement in mouse models of dementia-related diseases (Govindarajan *et al.*, 2011; Liu *et al.*, 2015). Thus, here we wanted to determine if butyrate-producing bacteria are at all present or completely absent in the gut microbiota of AD patients. The application of single or mixtures of butyrate producers in studies associated with dementia-related disease (mentioned above) emphasizes the importance of identifying butyrate-producing bacteria and to assess their rate of butyrate production.

In chapter II, the disappearance of genus *Faecalibacterium*, which is considered as main butyrate producer in human gut microbiota, in AD group, gave us a question that if other butyrate-producing bacteria exist in AD patient's gut. By using NGS, some genus which are at low abundance cannot detect. Therefore, in the work presented here, we isolated bacteria from the feces of four Japanese elders diagnosed with Alzheimer's disease. The 16S rRNA gene of each isolate was sequenced. Subsequently, we selected bacteria that might possess butyrate producing ability based on species-related information available in the literature. We then analyzed them in culture for the production of SCFAs, including butyrate, using high-performance liquid chromatography (HPLC). Furthermore, the presence of encoding genes for butyrate production in each strain was identified. These included butyrate kinase (*buk*), butyryl-CoA:acetate CoA-transferase (*but*), CoA-transferase-related, and propionate CoA-transferase. Our findings are the first to provide valuable insight into the existence of the butyrate-producing microbial community in the guts of AD patients.

2. Materials and Methods

a. Fecal sample

From the 17 samples of AD patients which was described in chapter II, four samples were randomly selected to isolate butyrate-producing bacteria.

b. Isolation of bacteria from fecal samples

Bacteria from fecal samples were recovered following previous methods with a minor modification (Morita *et al.*, 2007). All isolation processes were performed under anaerobic conditions. Therefore, PBS solutions, culture media, and other materials were kept in an anaerobic chamber up to 24 hours before use. The anaerobic condition was maintained in the work-station by using a tank of anaerobic mixed gas (5% carbon dioxide, 5% hydrogen, and 90% nitrogen) along with a tank of nitrogen gas. 0.4 ml of each fecal stock sample was recovered in 9.6 ml of PBS solution (Life Technologies, Japan) to generate a 10^2 dilution of the original fecal material. This solution was thoroughly vortexed and then subsequently diluted serially in 10-fold steps until a 10^8 -fold dilution was obtained. 0.1 ml of each dilution was spread onto blood liver (BL) agar medium (Eiken, Japan) supplemented with 5% defibrinated horse blood and yeast extract, casitone, fatty acids (YCFA) agar medium. All plates were incubated at 37°C for 3 – 7 days in the anaerobic chamber. YCFA medium contained (per 100 ml) 1.5 g agar, 1 g casitone, 0.25 g yeast extract, 0.4 g NaHCO₃, 0.1 g cysteine, 0.045 g K₂HPO₄, 0.045 g KH₂PO₄, 0.09 g NaCl, 0.009 g MgSO₄·7H₂O, 0.009 g

CaCl₂, 0.1 mg resazurin, 1 mg hemin, 1 µg biotin, 1 µg cobalamin, 3 µg p-aminobenzoic acid, 5 µg folic acid and 15 µg pyridoxamine. SCFAs were added to the medium at final concentrations of 33 mM acetate, 9 mM propionate, and 1 mM each of isobutyrate, isovalerate, and valerate. After sterilization by autoclaving, a sterile-filtered solution of vitamins and sugars was added to the medium, at a final concentration of 50 mg/l each of thiamine and riboflavin (Duncan *et al.*, 2002) and 2 g/l each of glucose, maltose and cellobiose (Browne *et al.*, 2016). Single colonies were picked randomly and re-streaked on the same media until pure colonies appeared as confirmed by morphology. Each pure isolate was used for colony PCR (Polymerase Chain Reaction) and cultivated in 5 ml of GAM broth (Gifu Anaerobic Media, Eiken, Japan) at 37°C under anaerobic conditions. The resulting cultures were used to create stocks which were stored at –80°C (Atarashi *et al.*, 2013).

c. Colony PCR, 16S rRNA gene amplicon sequencing, and sequence analysis

Each pure colony was picked up with a sterile toothpick and transferred into a PCR tube (0.2 ml) containing 5 µl of sterile distilled water. Next, a mixture consisting of 0.4 µl of each universal primer, 27Fmod and 1525R (5'-AGRGTGGATYMTGGCTCAG-3'; 5'-AAGGAGGTGWTCARCC-3', respectively, Eurofins, Tokyo, Japan), 10 µl of Emerald PCR Master Mix (Takara, Japan), and 4.2 µl of sterile distilled water was added to the PCR reaction tube. The amplification program was performed according to a previous study (Schulze-Schweifing *et al.*, 2014) with a small modification: initial denaturation at 98°C for 1 min, followed by 30 cycles of denaturation at 98°C for 10 s, annealing at 55°C for 20 s, elongation at 72°C for 2 min, and a final elongation at 72°C for 10 min using a thermocycler (Biometra, T1 Thermocycler, Germany). The amplified fragments were then cleaned up with ExoSAP-IT (Thermo Fisher Scientific, USA) according to the manufacturer's instructions. The purified amplicons were sequenced using a 3730xl DNA Analyzer with a BigDye Terminator v3.1 Cycle sequencing kit (Thermo Fisher Scientific, USA) by the Eurofins MWG lab in Tokyo, Japan. The resulting sequences of each isolate were analyzed against each other with BLASTn and the similarity of their 16S rRNA gene sequence (~850 bp) was determined by comparison against GenBank entries using Match/Mismatch scores of 1,-2 and a linear gap costs parameter (Altschu *et al.*, 1990). A 97% identity cut-off value was used to group species into operational taxonomic units (OTUs) while other isolates showing lower similarity values were each considered as individual OTUs (Li *et al.*, 2016a). Thereafter, each representative OTU was subjected to near-full-length 16S rRNA gene

sequencing to obtain virtually complete 16S rRNA sequences. Isolate names mentioned hereafter indicate that they are representative isolates of their OTU. Contigs of each OTU (~1400 bp) were created using GeneStudio software (<http://genestudio.com/>), which were then BLASTn compared against two databases of 16S ribosomal RNA sequences and RefSeq Genome (organism: Bacteria (taxid:2)) in the GenBank database (<https://blast.ncbi.nlm.nih.gov>), the SILVA database (<https://www.arb-silva.de/>) (Pruesse *et al.*, 2012), and the EzTaxon database (<https://www.ezbiocloud.net/resources/16s> download) (Yoon *et al.*, 2017), to identify the underlying species.

d. Screening of butyrate-producing bacteria

Based on the 16S rRNA gene sequencing results, all identified species were analyzed for their butyrate-producing ability by scan-searching against the PubMed and the ScienceDirect databases (Hamer *et al.*, 2008). Keywords used for the scanning were the species name of each representative OTU, butyrate, and short-chain fatty acid. To be inclusive, all isolates with less than 97% sequence homology to known species were separately considered as potential butyrate producers. Subsequently, the suspected butyrate-producing candidates were assessed for their butyrate-producing ability by HPLC with ultraviolet (UV) absorbance detection.

e. Quantification of short-chain fatty acids

Concentrations and identities of select SCFAs were determined by HPLC-UV. They included formic acid, acetic acid, lactic acid, propionic acid, butyric acid, and valeric acid (Eeckhaut *et al.*, 2011). Isolates were re-cultivated in GAM broth for 48 hours except for three strains that required four days to grow (as indicated in Table 1) at 37°C under anaerobic conditions. The optical density (OD) of each strain was measured at a wavelength of 620 nm using a microplate reader (Bio-Rad, Japan) and the OD₆₂₀ value of the un-inoculated medium was subtracted. Next, the culture was centrifuged at 1400 × g, at 4°C, for 20 min. The cell pellet was used for DNA extraction and the supernatant was collected for SCFA quantification. The pH of the supernatant was measured with a pH meter (F-52, Horiba, Japan) and then adjusted to pH 2.0 using 6N HCl. In the next step, the acidified supernatant was centrifuged under the same conditions as described above and passed through a 0.2 μm filter. SCFAs were extracted from the protein-containing cell-free supernatant with ethyl acetate (Sigma-Aldrich) as described (García-Villalba *et al.*, 2012), with a minor modification: 2 ml of the supernatant were mixed with 4 ml of ethyl acetate and left to stand

undisturbed for 15 min, after which the upper organic layer was transferred into a new tube. This extraction step was repeated three times. Afterwards, the pooled organic solution was evaporated to dryness in a centrifugal evaporator (Sakuma, Japan). Finally, 1 ml of HPLC grade water was added and the extract was subjected to HPLC analysis. Standards were formic acid, butyric acid (Wako, Japan), acetic acid, propionic acid (Nacalai Tesque, Japan), lactic acid, and valeric acid (Sigma Aldrich). A calibration curve for each standard was generated and used to quantify the concentration of each of the corresponding compounds in the samples.

The HPLC-UV system consisted of a system controller (SCL-10A, Shimadzu), a degassing device (ERC-3115 α , ERC Inc), an HPLC pump (LC-10AD, Shimadzu), a column oven (CTO-10AC, Shimadzu) and a detector (SPD-20A, Shimadzu). SCFAs in 100 μ l of each sample extract was separated at 30°C on a YMC Pack ODS-AM column, 4.6 mm inner diameter \times 250 mm length, with 5 μ m particles, 120 Å pore size. The mobile phase A contained 5% (v/v) acetonitrile (Nacalai Tesque, Japan) and 0.05% (v/v) trifluoroacetic acid (Wako, Japan) in HPLC grade water, and phase B contained 90% (v/v) acetonitrile and 0.05% (v/v) trifluoroacetic acid in HPLC grade water. The flow rate was 1 ml/min. The solvent gradient after injection was 5 min at 0% B, to 100% B at 40 min, and kept at 100% B until 45 min. Finally, the column was equilibrated back to 0% B by 50 min. The detector wavelength was set to 220 nm. HPLC chromatograms were analyzed with the Chromato-PRO software version 3.0 (Runtime Instrument, Japan). Each strain was tested twice and in duplicate HPLC analyses.

f. Phylogenetic tree analyses based on sequences of the 16S rRNA gene

A phylogenetic tree was constructed to evaluate the relationship of isolates in this study with confirmed butyrate-producing reference strains. Reference sequences of Type strains were downloaded from the EzTaxon database (Yoon *et al.*, 2017). All sequences were aligned and equalized with MEGA7 (Kumar *et al.*, 2016) using the neighbor-joining method (Saitou and Nei, 1987) with a bootstrap test (1000 times) (Felsenstein, 1985), and pairwise gap deletion (Eeckhaut *et al.*, 2011; Nei and Kumar, 2000). *Escherichia coli* NCTC9001^T (LN831047) was used as an outgroup.

g. Bacterial DNA extraction for butyrogenic gene detection

The pellets of single butyrate-producing bacteria were rinsed twice with TE buffer (pH 8) (1 M Tris-HCl, 0.5 M EDTA, Invitrogen), suspended in TE buffer and incubated at 37°C

for 1 h with 15 mg/ml lysozyme (Sigma-Aldrich). All of next steps were similar to DNA extraction procedure which was described in Chapter II. The genomic DNA was used for butyrogenic gene detection and whole genome sequencing.

h. Identification of genes encoding for butyrate production in bacteria

The presence of four functional genes involved in butyrate biosynthesis in suspected isolates was analyzed by using four pairs of degenerate primers. They included *buk*, *but*, CoA-transferase-related, and propionate CoA-transferase genes (Eeckhaut *et al.*, 2011). Purified genomic DNA of all butyrate-producing bacteria was used as a PCR template. Primers PTBfor2 and BUKrev1 (5'-GTATAGATTACTIRYIATHAAYCCNGG-3'; 5'-CAAGCTCRTCIACIACIACN-GGRTCNAC-3') were designed to amplify the butyrate kinase operon in clostridia through the ramped annealing approach with the following conditions: initial denaturation (2 min at 94°C), 35 cycles of denaturation (30 s at 94°C), annealing (20 s at 55°C, 5 s at 50°C, 5 s at 45°C, 5 s at 40°C, 15 s at 35°C), and elongation (1.5 min at 72°C), with a final extension step (10 min at 72°C). (Louis *et al.*, 2004). The *but* gene was amplified with BCoATscrF and BCoATscrR degenerate primers (5'-GCIGAICATTTACITGGAAAYWSITGGCAYATG-3', 5'-CCTGCCTTTGCAATRTCIACRAANGC-3'). The amplification cycle used was 1 cycle of 95°C for 3 min; 40 cycles of 53°C, and 72°C for 30 s; 1 cycle each of 95°C and 55°C for 1 min (Louis and Flint, 2007). Primers CoATDF1 and CoATDR2 (5'-AAGGATCTCGGIRTICAYWSIGARATG-3'; 5'-GAGGTCGTCICKRAAITYIG-GRTGNGC-3') were used to amplify a broad range of CoA-transferase-related sequences (Charrier *et al.*, 2006). Primers PCTfor1 and PCTrev2 (5'-GTAGGATTARRIACITWYRTIGAYCC-3'; 5'-TCCACCACCATCRTARSARTCRAAYTG-3') were designed to detect the propionate CoA-transferase gene from *Clostridium propionicum* (Charrier *et al.*, 2006). Primers CoATDF1/CoATDR2 and primers PCTfor1/PCTrev2, the following PCR conditions were used: initial denaturation (2 min at 94°C), then 35 cycles of denaturation (30 s at 94°C), annealing (20 s at 55°C, 5 s at 50°C, 5 s at 45°C, 5 s at 40°C), elongation (1 min at 72°C), and a final extension (10 min at 72°C). PCR amplicons in bands of expected sizes were purified using MagExtractor-PCR & Gel Clean-Up kit (Toyobo, Japan). The genes were sequenced with the same method as described above for sequencing of 16S rRNA genes. Contigs were created using GeneStudio and the exported sequences were translated into deduced amino acids sequences using the ExPASy translate tool (<https://web.expasy.org/translate/>) (Gasteiger *et al.*, 2003). These deduced

amino acids were blasted against the GenBank database using BLASTP with a Reference Proteins database (Altschu *et al.*, 1990). Amino acid sequences from isolates in this study and of corresponding reference genes were used to create phylogenetic trees using the same methods and parameters as those used for reconstructing for 16S rRNA gene-based phylogenetic tree (Felsenstein, 1985; Kumar *et al.*, 2016; Nei and Kumar, 2000; Zuckerkandl and Pauling, 1965).

i. Whole genome sequencing of butyrate-producing bacteria

The purified genomic DNA of butyrate strains which were identified as butyrate-producing bacteria were sequenced their whole genome by using Illumina Miseq platform. The DNA concentration of each strain was adjusted to 0.2 ng/μl with Qubit™ dsDNA HS Assay Kit (ThermoFisher Scientific) by using QuBit Fluorometer (ThermoFisher Scientific). Then, the pool library of DNA was then prepared as instruction manual of Nextera XT DNA library prep kit (Illumina) (https://support.illumina.com/content/dam/illumina-support/documents/documentation/chemistry_documentation/samplepreps_nextera/nextera-xt/nextera-xt-library-prep-reference-guide-15031942-03.pdf) and was sequenced with MiSeq sequencer at BioBank (Okayama University, Japan).

The resulting sequences were trimmed with quality score of 0.05 and a maximum number of ambiguous nucleotides 2. Next, the output sequences were removed their adapters. Then, they were de-multiplexed by removing the barcodes and the linker sequences since there were total 96 samples were sequenced in one sequencing run. The sequence reads were then assembled using CLC Genomics Workbench version 9.0.1. (http://resources.qiagenbioinformatics.com/manuals/clcgenomicsworkbench/current/User_Manual.pdf). The assembled sequences were analyzed with <https://dfast.nig.ac.jp/> and the genome annotations were achieved. Genome information comprised of total length, % GC, number of CDS (CoDing Sequences), number of rRNAs, number of tRNAs was recorded. Furthermore, the presence or absence of encoding genes for butyrate production in each strain was also clarified from their whole genome sequences by using BLAST and/or their genome annotations.

j. Nucleotide sequence accession numbers

All sequences were deposited into the GenBank database, excepted for whole genome sequences. Accession numbers of the 16S rRNA gene sequences (MH282437–MH282438, MH282441–MH282445, MH282449, and MH282451–MH282457) matching with each

isolate are shown in Fig. 27. And the accession numbers of functional gene sequences (MH390321–MH390337) corresponding to these isolates are described in Fig. 28A, 28B, and 28C.

3. Results

a. Isolation, identification, and validation of isolates of butyrate-producing bacteria

From a total of 226 colonies, randomly picked from both media, we identified four isolates as distinct OTUs and grouped 222 isolates into 56 OTUs (Supplementary Table S2). The near-full-length 16S rRNA gene sequences of these combined 60 representative OTUs were again compared to existing sequence databases, including the 16S ribosomal RNA sequence, the RefSeq Genome, the EzTaxon, and the SILVA databases (Supplementary Table S3).

In the high identity group, each isolate was found to have identical species name in the four reference databases, except for eight isolates 30A20, 35Y30, 35Y33, 36Y11, 6Y13, 30Y20, 30Y9, and 35A7, which did not. Isolate 30A20 matched with a *Bacteroides* sp.-related strain in the RefSeq Genome database but it was identified as *Bacteroides nordii*-related strain in the three remaining databases. Similarly, isolate 35Y30 and 35Y33 were identified as a *Clostridium* sp. and as a *Clostridiales* bacterium in the RefSeq Genome database, respectively. However, isolates 35Y30 and isolate 35Y33 were identified as *Clostridium tertium*-related and *Flavonifractor plautii*-related strains (formerly *Clostridium orbiscindens* (Carlier *et al.*, 2010)), respectively, based on the other three databases. Isolate 36Y11 was identified as a *Blautia wexlerae*-related strain in the EzTaxon and the SILVA databases. However, it matched with the entry *Blautia luti*-related strain in the 16S ribosomal RNA sequence database, and the entry *Blautia* sp.-related strain in the RefSeq Genome database. Other two isolates 6Y13 and 30Y20 were determined as *Escherichia fergusonii*-related strain and *Tyzzrella nexilis*-related strain (formerly *Clostridium nexile* (Holdeman and Moore, 1974; Yutin and Galperin, 2013)), respectively, in the 16S ribosomal RNA sequence and the EzTaxon databases. However, they were identified as an *Escherichia coli*-related strain and a *Tyzzrella* sp.-related strain in the two remaining databases, respectively. Finally, two isolates 30Y9 and 35A7 were identified as a *Terrisporobacter mayombei*-related strain and a *Terrisporobacter petrolearius*-related strain, respectively, in the 16S ribosomal RNA sequence and the EzTaxon databases. But they were identified as a *Terrisporobacter* sp.-related strain and an uncultured bacterium, respectively, in the SILVA

database. Interestingly, both of them matched with *Terrisporobacter othiniensis*-related strains in comparison with entries in the RefSeq Genome database.

Out of the four isolates in the low identity group, three isolates (isolates 30Y2, 35Y37, and 36Y5) were identified based on the 16S ribosomal RNA sequences, the RefSeq Genome, and the EzTaxon databases while the one remaining (isolate 30A1) was identified with the SILVA database (Supplementary Table S3). The first isolate 30Y2 was identified as an *Oscillibacter valericigenes*-related strain with 95.74%–95.79% identity against the 16S ribosomal RNA sequence and the EzTaxon databases but it was classified as an *Oscillibacter* sp.-related strain with more than 98% identity in the two remaining databases. The second isolate 35Y37 was classified as an *Intestinimonas butyriciproducens*-related strain with 95.04%–95.19% identity in the 16S ribosomal RNA sequences and EzTaxon databases. However, its species name matched an *Intestinimonas massiliensis*-related strain with more than 99% identity in the two other databases. The third isolate 36Y5 matched to a *Sutterella stercoricanis*-related strain with identity lower than 95% identity in the 16S ribosomal RNA sequence and EzTaxon databases. However, it was identified as an uncultured bacterium (94.78% identity) and a *Dakarella massiliensis*-related strain (99.71% identity) by matching with entries deposited in the SILVA and the RefSeq Genome database, respectively. The final isolate 30A1 matched to a *Butyricimonas faecihominis*-related strain in the 16S ribosomal RNA sequence and EzTaxon databases, with more than 99% identity. It was also identified as a *Butyricimonas faecihominis*-related strain but with only 95.50% identity in the SILVA database. However, it matched to *Butyricimonas* sp. An62 in the RefSeq Genome database with 97.89% identity. The identification analyses of each strain played an important role because they helped to determine encoding genes for butyrate synthesis in the corresponding bacteria.

It was assumed that the four low identity isolates could produce butyrate. Based on various literature references (see Table 1), 12 OTUs were selected as putative butyrate-producers out of the 56 representative OTUs of high identity isolates. In total, these 16 frozen stocks were then recovered and cultured for quantification of short-chain fatty acid production and gene identification.

b. Quantification of short-chain fatty acids

Considered as the first study to isolate butyrate-producing bacteria in the human gut, Barcenilla and co-authors chose a cut-off value of 2 mM butyrate produced by bacteria in

the culture at 24 h after inoculation under anaerobic conditions in M2GSC broth (Barcenilla *et al.*, 2000). They suggested that this value could be used to clearly distinguish butyrate produced by the bacteria from the original butyrate concentration of the broth (Barcenilla *et al.*, 2000). However, the initial concentrations of each SCFA in un-inoculated M2GSC broth was not shown in their study. Therefore, in our study, by subtracting the butyrate concentration of each inoculated culture from the initial butyrate concentration of the GAM broth, every strain tested here that measurably increased the original butyrate concentration was considered as a true butyrate producer.

The SCFAs data analysis showed that 15 out of the 16 cultivable strains could produce butyrate. The concentration of butyrate varied from 0.25 ± 0.05 mM to 19.22 ± 5.36 mM (Table 3). The *Sutterella stercoricanis*-like isolate 36Y5 did not produce butyrate. Two isolates of the family *Odoribacteraceae* within the phylum *Bacteroidetes* (isolates 30A1 and 30A7) exhibited a high ability to produce butyrate. OD values did not correlate with a strain's level of butyrate production. Some strains did not grow well in the GAM broth but their final butyrate concentration in the culture was higher than that of other better-growing bacteria and vice versa. Furthermore, the increase or decrease in the broth's pH after incubation of the cultures were also not associated with the final concentration of butyrate and other SCFAs. None of the tested butyrate-producing strains were found to produce propionate. Almost all bacterial strains consumed acetate in the medium for their growth, except for the *Anaerostipes caccae*-like isolate 6A29, which released acetate into the culture.

The 16S rRNA gene sequences of all cultivable butyrate-producing isolates and of other known butyrate-producing bacteria were used to construct a phylogenetic tree (Fig. 27). All isolates were distributed into two phyla, which included clostridial clusters I, IV, XI, XIVa and XV of the phylum *Firmicutes* and families *Odoribacteraceae* and *Bacteroidaceae* of the phylum *Bacteroidetes*. Isolates that belonged to the clostridial clusters I and IV were more abundant than isolates of other clusters.

Table 3. Relationships and short-chain fatty acids quantification of cultivable putative butyrate-producing bacterial isolates from AD patients

Isolate	Species identified (16S rRNA gene % homology, accession number)	OD ₆₂₀	pH	Short-chain fatty acids concentration, mM					References
				Formic	Lactic	Acetic	Butyric	Valeric	
	Blank (GAM broth)		7.10±0.04	4.20±0.90	16.17±0.49	0.72±0	1.45±0.14	17.43±1.05	
35Y8B	<i>Clostridium baratii</i> ATCC27638 ^T (99.86%, X68174)	0.83±0.27	6.1±0.58	2.89±2.97	5.22±1.26	ND	0.78±0.29	2.28±0.12	(Rainey, 2009)
30Y4	<i>Clostridium paraputrificum</i> DSM 2630 ^T (99.57%, X73445)	0.025±0.02	6.23±0.02	ND	7.36±4.28	ND	1.57±0.46	4.35±0.74	(Rainey, 2009)
36A18	<i>Clostridium perfringens</i> ATCC 13124 (99.78%, CP000246)	0.575±0.03	6.81±0.00	ND	17.95±3.85	ND	0.41±0.73	4.58±0.42	(Li <i>et al.</i> , 2016a)
35Y30	<i>Clostridium tertium</i> DSM 2485 ^T (99.93%, Y18174)	0.29±0.04	5.96±0.09	0.20±0.01	19.14±4.08	ND	1.22±0.48	1.42±0.08	(Rainey, 2009)
35Y33	<i>Flavonifractor plautii</i> ATCC 29863 ^T (99.65%, JH417629)	0.02±0.01	6.83±0.01	ND	2.79±0.95	ND	1.86±0.04	14.21±3.64	(Li <i>et al.</i> , 2016a)
35Y26	<i>Intestinimonas butyriciproducens</i> SRB-521-5-I ^T (99.93%, KC311367)	0.07±0.01	6.86±0.05	1.05±0.99	11.7±0.00	ND	0.54±0.55	1.58±1.21	(Bui <i>et al.</i> , 2016)
30Y2	<i>Oscillibacter valericigenes</i> NBRC 101213^{T*} (95.79%, AP012044)	0.03±0.01	7.14±0.01	1.65±0.07	14.3±2.01	ND	0.95±0.23	0.41±0.52	< 97%
35Y37	<i>Intestinimonas butyriciproducens</i> SRB-521-5-I^T (95.04%, KC311367)	0.06±0.02	7.20±0.02	0.06±0.56	15.83±2.48	ND	1.93±0.10	1.26±1.53	< 97%
35A14	<i>Paeniclostridium sordellii</i> ATCC 9714 ^T (98.63%, AB075771)	0.09±0.03	6.4±0.40	ND	10.85±6.70	ND	0.25±0.55	ND	(Rainey, 2009)
6A16	<i>Anaerostipes caccae</i> DSM 14662 ^T (100%, ABAX03000031)	0.13±0.05	6.93±0.02	6.31±1.47	ND	3.91±3.75	2.51±0.39	0.95±1.38	(Schwiertz <i>et al.</i> , 2002)

Isolate	Species identified (16S rRNA gene % homology, accession number)	OD ₆₂₀	pH	Short-chain fatty acids concentration, mM					References
				Formic	Lactic	Acetic	Butyric	Valeric	
30A19	<i>Eubacterium limosum</i> ATCC 8486 ^{T*} (100%, M59120)	0.03±0.02	7.13±0.07	2.14±1.16	2.72±0.60	ND	1.06±0.48	1.31±0.13	(Rainey, 2009)
35Y21B	<i>Anaerofustis stercorihominis</i> DSM 17244 ^{T*} (99.72, ABIL02000006)	0.03±0.02	7.11±0.01	0.03±0.11	17.22±2.77	ND	0.63±0.16	2.49±1.55	(Li <i>et al.</i> , 2016a)
30A7	<i>Odoribacter splanchnicus</i> DSM 20712 ^T (99.57%, CP002544)	0.22±0.18	7.35±0.15	ND	27.02±2.80	ND	19.22±5.36	ND	(Li <i>et al.</i> , 2016a)
30A1	<i>Butyricimonas faecihominis</i> 180-3 ^T (99.72%, AB916501)	0.39±0.25	5.86±0.13	0.93±0.18	10.49±5.88	ND	14.4±3.71	ND	(Sakamoto <i>et al.</i> , 2014)
6A29	<i>Bacteroides caccae</i> ATCC 43185 ^T (99.93%, AAVM02000012)	0.40±0.49	5.76±0.00	0.42±0.05	19.89±0.13	ND	1.2±0.64	1.85±1.27	(Sakurazawa and Ohkusa, 2005)
36Y5	<i>Sutterella stercoricanis</i> CCUG 47620^T (92.34%, AJ566849)	0.03±0.00	7.38±0.00	ND	ND	ND	ND	3.16±1.61	< 97%

Note: - Species name and identity of all isolates were identified based on the EzTaxon database.

- Isolates presented are representative of their OTUs, with more than 97% homology with the 16S rRNA gene sequence of their closest valid named neighbors.

- Isolates with less than 97% homology with the 16S rRNA gene sequence of their closest valid named neighbors are in bold.

- The concentration of each short-chain fatty acid (SCFA) was shown after subtracting the concentration of SCFA in the culture from the concentration of SCFA in GAM media.

- *: These isolates were cultivated in GAM broth for 96 hours at 37°C under anaerobic conditions before use.

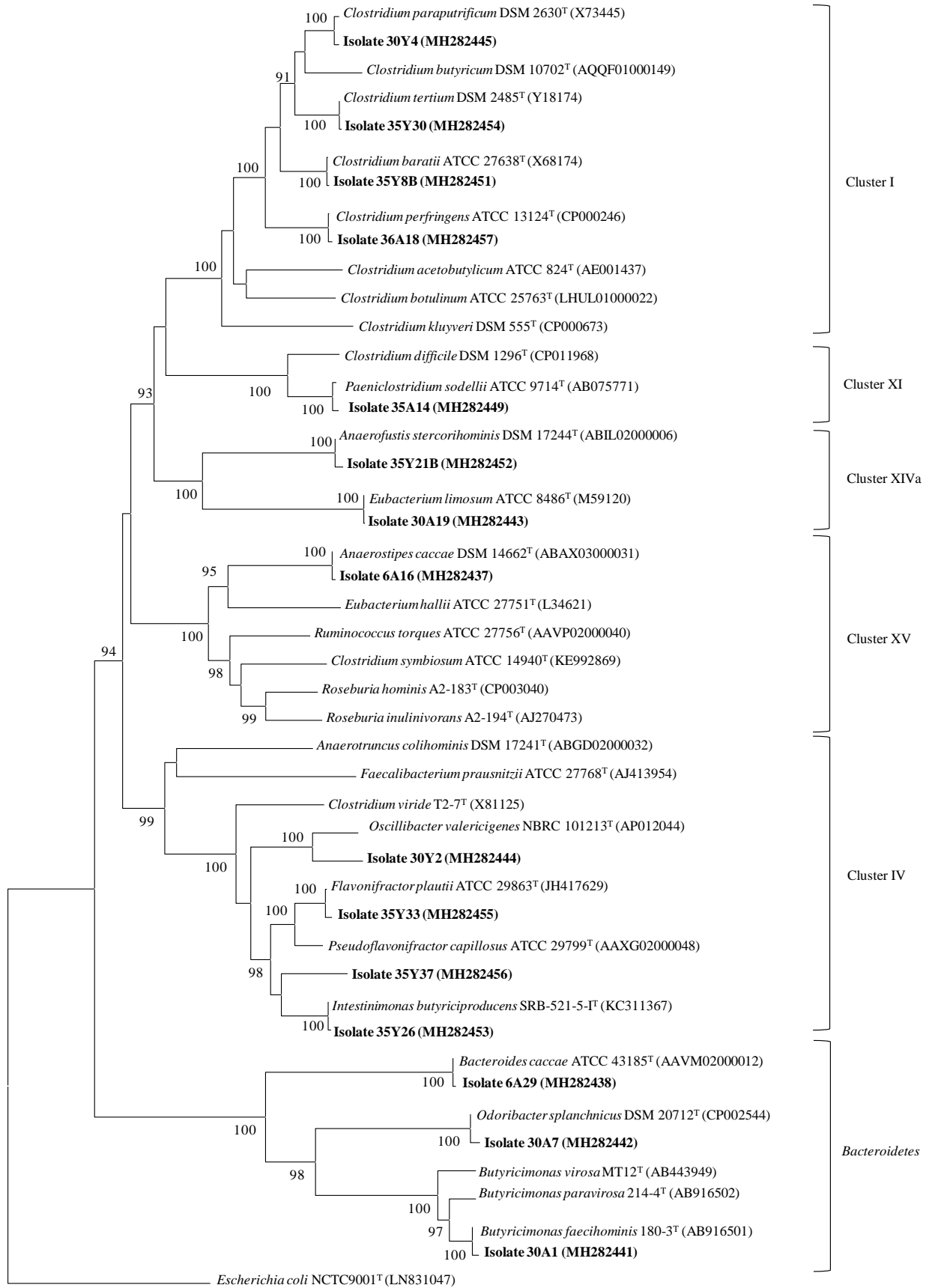
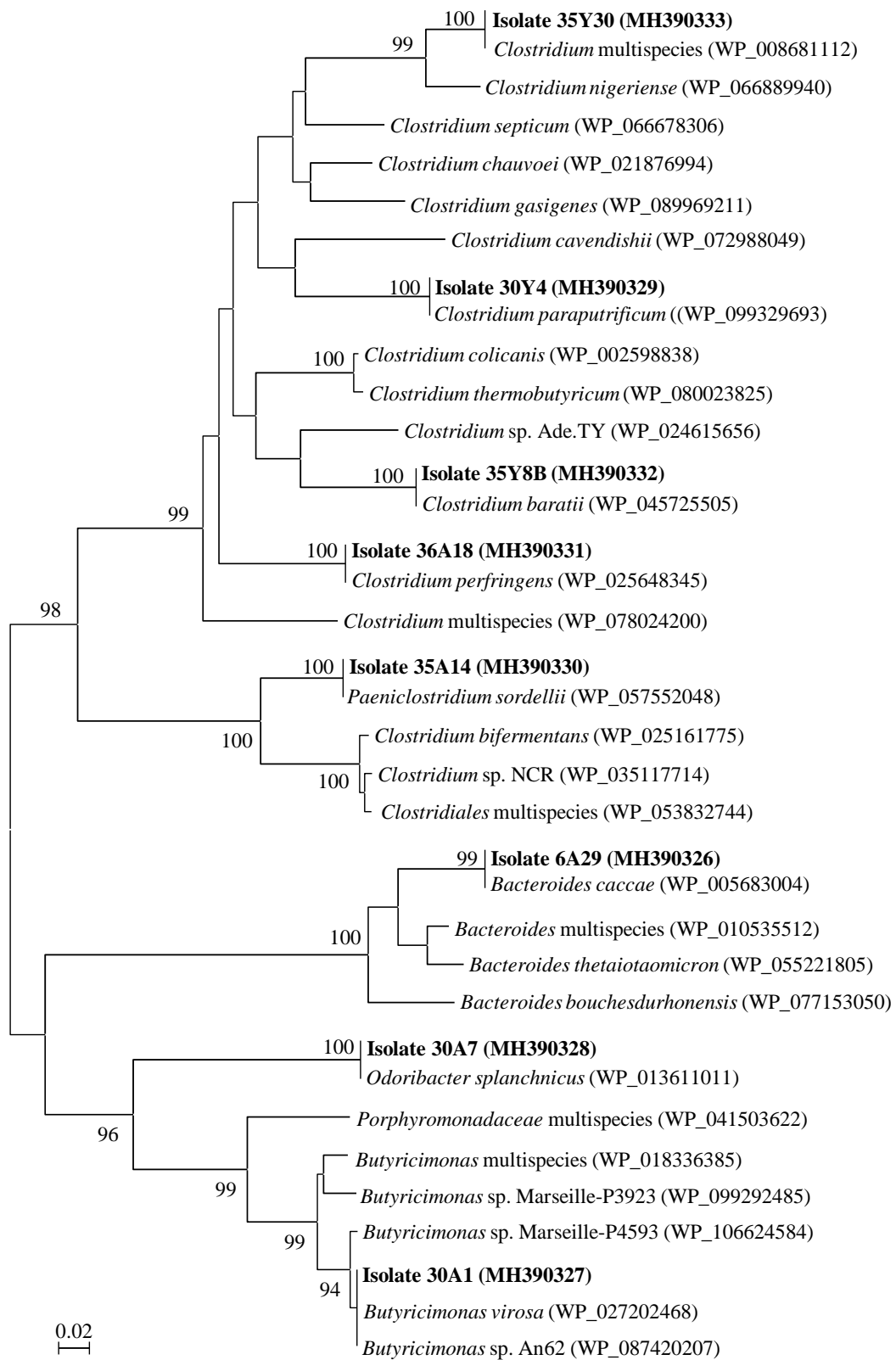


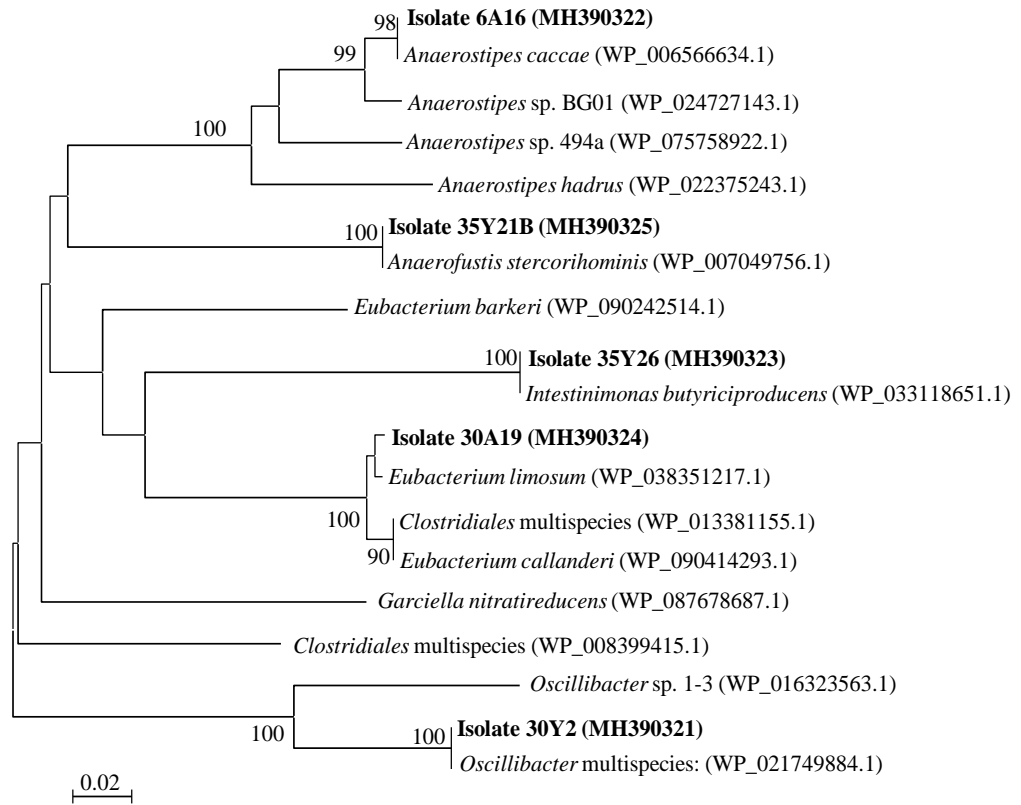
Fig 27. 16S rRNA gene sequence-based phylogenetic tree of butyrate-producing isolates (in bold) and of known reference. Roman numerals indicate clostridial clusters. Accession numbers of Type strains are from the EzTaxon database (in parentheses). Bootstrap values are shown at the nodes of the tree (values under 90% were removed). 16S rRNA gene sequences of *Escherichia coli* NCTC9001^T (LN831047) was used as an outgroup at the root of the tree. Scale bar: 0.02 substitutions per nucleotide position.

c. Identification of genes encoding for butyrate production in bacteria

Different encoding genes for butyrate production were identified in each isolate by using four sets of degenerate primers (Supplementary Table S4). By using PTBfor2 and BUKrev1 primers, the *buk* gene was detected in 8 isolates (Fig. 28A), with an expected size of ~380 bp. They separated into two main branches of the phylogenetic tree, which was generated from their deduced amino acid sequences and their references. One branch was populated by *Bacteroidetes* isolates 30A1, 30A7, and 6A29, while another one contained clostridial cluster I isolates 36A18, 30Y4, 35Y30 and 35Y8B, and the XI isolate 35A14 of the phylum *Firmicutes*. The tree was highly consistent with the 16S rRNA gene-based phylogenetic tree, except for isolates 30A1 and 35Y30. As described by their protein phylogenetic tree, the Buk protein of isolate 30A1 and 35Y30 indicated that they were related to *Butyricimonas* sp. An62 and *Butyricimonas virosa*, and multiple species of *Clostridia*, respectively, while not being closely related to *Butyricimonas faecihominis* and *Clostridium tertium* as identified by their 16S rRNA gene sequences.



28B



28C

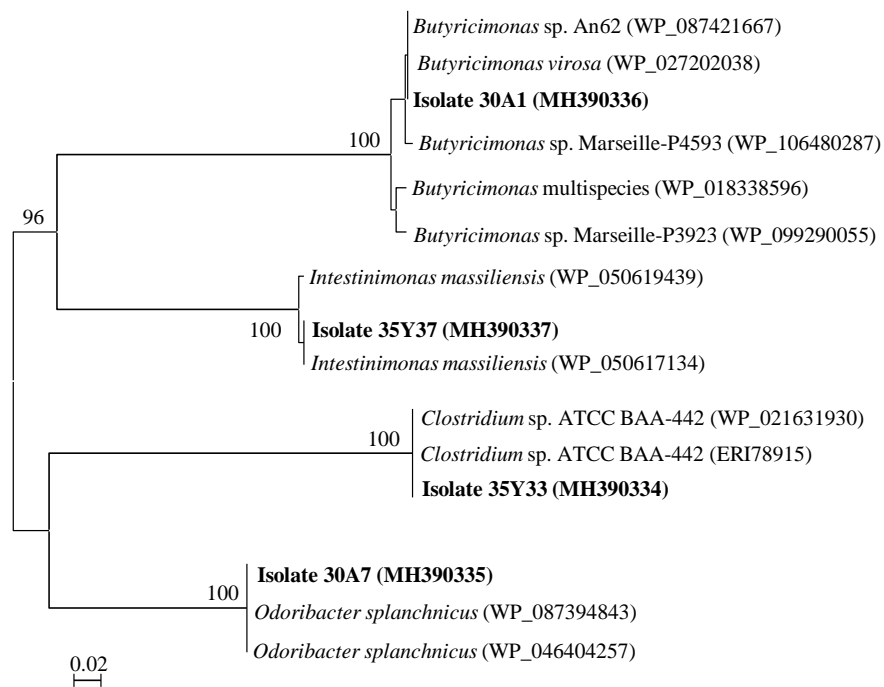


Fig 28. Phylogenetic tree based on deduced proteins of isolates from this study and of reference strains. Buk proteins (28A), But proteins (28B), and 4-Hbt proteins (28C). Accession numbers are given in parentheses. Bootstrap values are indicated at the nodes of the tree (values under 90% were removed). Scale bar: 0.02 substitutions per nucleotide position.

After considering their valid species name assignment, we concluded that isolate 30A1 was actually a *B. faecihominis*-related strain and isolate 35Y30 was a *C. tertium*-related strain. However, the *but* gene segment had an expected size of ~510 bp and was detected in five isolates of the phylum *Firmicutes* by using the BCoATscrF and BCoATscrR primer pairs. They were distributed across clostridial clusters IV (isolates 30Y2 and 35Y26), XIVa (isolates 35Y21B and 30A19), and XV (isolate 29A16). The phylogeny was consistent between the 16S rRNA gene-based phylogenetic tree and the deduced But protein phylogenetic tree (Fig. 28B), with the exception of isolate 30Y2. The protein-based phylogeny of isolate 30Y2 indicated that it was related identification analyses as that of isolates 30A1 and 35Y30, we propose that isolate 30Y2 to *Oscillibacter* sp., not to *Oscillibacter valericigenes*. However, based on similar was an *O. valericigenes*-related strain.

The degenerate primer set of CoATDF1 and CoATDR2, which was used for detection of a broad range of CoA transferase-related sequences, was able to amplify butyryl-CoA:4-hydroxybutyrate CoA-transferase gene (*4-Hbt*) in 2 isolates of the clostridial cluster IV (isolates 35Y37 and 35Y33) and in 2 isolates of the family *Odoribacteraceae*, phylum *Bacteroidetes* (isolates 30A1 and 30A7). Only the phylogeny of the *4-hbt* gene sequences of isolate 30A7 was in good agreement with the 16S rRNA gene-based phylogeny. Three out of four isolates did not correlate well between their *4-hbt* gene-based phylogeny and their 16S rRNA gene-based phylogeny, including isolates 30A1, 35Y33 and 35Y37. Isolate 35Y37 showed that it was closely related to *Intestinimonas massiliensis* in the protein phylogeny. This observation was consistent with entries of its 16S rRNA gene sequence in the SILVA and RefSeq Genome databases. However, the 16S rRNA gene sequence of isolate 35Y37 corresponded to an *Intestinimonas butyriciproducens*-related strain in the 16S ribosomal RNA sequence and EzTaxon databases as noted in the sections above. Therefore, with the support of protein evidence and the two former databases, isolate 35Y37 was confirmed as an *I. massiliensis*-related strain. Isolate 30A1, for which both the *buk* gene and

the *4-hbt* gene were detected, showed consistent butyrate-gene-based phylogenetic trees, demonstrating that it was closely related to *Butyricimonas* sp. An62 and *Butyricimonas virosa*. Finally, the *4-hbt* gene of isolate 35Y33 named *Flavonifractor plautii* was closely related to *Clostridium* sp. as described in Fig. 28C.

The 16S rRNA sequence of isolate 35Y33 corresponded with the entry titled *F. plautii*-related strain in the three databases namely, the SILVA, 16S rRNA sequence and EzTaxon databases whereas it was linked to an entry entitled “unclassified *Clostridiales* bacterium” in the RefSeq Genome database. Therefore, we concluded that isolate 35Y33 was *Flavonifractor plautii*-related strain. Finally, propionate CoA-transferase was not amplified in any isolates in this study when using the PCTfor1 and PCTrev2 primers.

d. Whole genome sequencing of butyrate-producing bacteria

Draft genome information of 13 butyrate-producing strains comprised of total length, % GC, number of CDS (CoDing Sequences), number of rRNAs, number of tRNAs were presented in Table 4.

Table 4. Genome information of 13 butyrate-producing bacteria

Isolate	Species name identified by 16S rRNA gene	Total sequence length	GC content, %	16S rRNA gene identity	Number of sequences	Number of CDSs	Number of rRNAs	Number of tRNAs
6A29	<i>Bacteroides caccae</i>	4,610,258	43.0	99.93	842	3093	3	37
30A7	<i>Odoribacter splanchnicus</i>	4,456,689	43.9	99.57	670	3375	3	36
35Y33	<i>Flavonifractor plautii</i>	4,433,523	59.3	99.65	442	4227	3	78
30A1	<i>Butyricimonas faecihominis</i>	4,411,320	43.3	99.72	748	3121	1	36
30A19	<i>Eubacterium limosum</i>	4,121,541	47.5	100.00	315	3753	3	36
30Y2	<i>Oscillibacter valericigenes</i>	3,584,044	60.0	95.79	229	3541	3	62
35Y37	<i>Intestinimonas massiliensis</i>	3,502,884	59.6	95.04	185	3377	4	65
6A16	<i>Anaerostipes caccae</i>	3,333,625	44.3	100.00	218	3246	2	40
30Y4	<i>Clostridium paraputrificum</i>	2,671,571	30.7	99.57	878	1958	4	16
35Y8B	<i>Clostridium baratii</i>	2,407,206	28.9	99.86	562	1899	5	40
35Y21B	<i>Anaerofustis stercorihominis</i>	2,285,697	33.9	99.72	173	2195	3	35
35Y30	<i>Clostridium tertium</i>	1,823,064	29.8	99.93	907	1008	1	6
35A14	<i>Paeniclostridium sordellii</i>	1,802,519	28.6	98.01	577	1336	2	29

The genus *Bacteroides* is one of the major lineages of bacteria and arose early during the evolutionary process. The species *Bacteroides caccae* anaerobic, bile-resistant, non-spore-forming and Gram-negative rods genus. They can ferment carbohydrate to produce volatile fatty acids that can be used by the host as an energy source (Wexler, 2007). The genome of *Bacteroides caccae* isolated from feces of AD patients has a total sequence length of 4,610,258 bp, containing the G+C content of 43.0%, 3,093 predicted protein-coding genes, and 842 contigs. The complete genome of *Bacteroides caccae* ATCC43185^T has total length of 4,570,800 bp with the GC content of 41.9% and protein count of 3550. It can be seen that the isolated *Bacteroides caccae* has longer length of base pair than *Bacteroides caccae* ATCC43185^T but it has 457 protein coding genes less than the type strain, *Bacteroides caccae* ATCC 43185^T. In these proteins, we found that they included *buk* gene in their genome. It agreed with the results of HPLC and *buk* gene sequences which amplified with degenerate primers as stated above.

Strains of *Odoribacter splanchnicus* are an anaerobic, Gram-negative, and non-motility bacterium. It comprises 4,456,689 bp of total length, with the G+C content of 43.9%. It has 670 contigs and contains 3,375 predicted coding proteins. The genome of the type strain of *Odoribacter splanchnicus*, strain 1651/6T (= DSM 20712 = ATCC 29572 = JCM 15291) consists of a 4,392,288 bp, with a G+C content of 43.4% and 3,672 protein-coding genes (Göker *et al.*, 2011). As identified of functional butyrate gene using degenerate primers, the isolated strain contains two butyrate genes, the *buk* and *4-Hbt*. However, its annotation indicated the presence of the *buk* gene in the genome and the absence of the *4-hbt* gene. This annotation was in good consistency with annotation of strain DSM 20712 that this type strain contains only the *buk* gene without the *4-hbt* gene. However, our PCR product's sequences indicated that the fragment of the *4-hbt* gene which purified from isolate 30A7 matched with *4-hbt* gene of *Odoribacter splanchnicus* strain NCTC 10825 (SNV37528). Therefore, we supposed that our isolate *Odoribacter splanchnicus* 30A7 possesses both genes, *buk* and *4-Hbt*, for its butyrate-producing pathways.

The *Flavonifractor plautii* (formerly *Clostridium orbiscindens* or *Eubacterium plautii*) are asaccharolytic and produce acetate and butyrate species. This is an obligate anaerobe, motile, peritrichous, Gram-variable, and forms spores. It is capable of cleaving the flavonoid C-ring (Carlier *et al.*, 2010). *Flavonifractor plautii*-related strain 35Y33 isolated from AD patient's feces contains 4,433,523 bp of genome total length, 59.3% of the G+C content, and

4,227 protein-coding genes. In comparison with *F. plautii*-related strain 35Y33, the complete genome of *Flavonifractor plautii* YL31 has a shorter total length, containing 3,818,478 bp. It also has a lower number of protein-coding genes, 3,592 vs 4,227 protein-coding genes. However, *F. plautii* YL31 contains a higher G+C content, possesses up to 60.6% G+C content (Uchimura *et al.*, 2016). A number of rRNAs and tRNAs of *Flavonifractor plautii* 35Y33 and *F. plautii* YL31 are 3 and 78, and 2 and 55, respectively. The *4-hbt* gene was annotated in the genome of *F. plautii* 35Y33 as well as by using the CoATDF1 and CoATDR2 degenerate primers. However, the genome of *F. plautii* YL31 does not show the *4-hbt* gene (NZ_CP015406.2), it contains 4-hydroxybutyrate--acetyl-CoA CoA transferase gene.

The genus *Butyricimonas* comprise of four known species (*B. faecihominis*, *B. synergistica*, *B. paravirosa* and *B. virosa*), found by Sakamoto in 2009 (Sakamoto *et al.*, 2014). They are anaerobic, Gram-negative, motility, and non-spore forming bacteria. The draft genome of *Butyricimonas faecihominis* 30A1 consists of 4,411,320 bp of total length, possessing 43.3% of the G+C content and 3121 protein-coding sequences. A number of rRNAs and tRNAs of this organism are one and 36, respectively. The genome of species *B. faecihominis* and *B. paravirosa* have not been annotated according to searching results of the GenBank database. The genome of *B. virosa* DSM 23226^T (NZ_JAEW01000000) has 4,715,876 bp long, 42.3% G+C content and 3,753 protein-coding genes. The *B. synergistica* DSM 23225^T (NZ_ARBK01000000) consists of 4,770,778 bp in its genome, including 3,748 protein-coding genes, 43.8% of G+C content, three rRNAs, and 54 tRNAs. The genome length of *B. faecihominis* 30A1 has a shorter length and a smaller number of protein-coding genes than those in both *B. virosa* DSM 23226^T and *B. synergistica* DSM 23225^T. These two strains contain the *buk* gene in their genome (WP_027202468 and OKZ19775). Although the *buk* gene was not found in the genome of *B. faecihominis* 30A1 according to genome annotation, it was identified by using the PTBfor2 and BUKrev1 degenerate primers. The *4-hbt* gene was not detected in *B. virosa* DSM 23226^T and *B. synergistica* DSM 23225^T according to their genome annotation on GenBank database but it is included in the genome of *B. faecihominis* 30A1 according to our annotation and butyrate gene identification using degenerate primers. In combination with other species genome annotation and our results, we conclude that *B. faecihominis* 30A1 contains both the *buk* gene and *4-hbt* gene.

The genus *Eubacterium* is uniform or pleomorphic nonspore-forming, Gram-positive rods, non-motile or motile, and obligate anaerobic microbe. They usually produce mixtures of organic acids from carbohydrates or peptone, often including large amounts of butyric, acetic, or formic acids (Rainey, 2009). The genome of *Eubacterium limosum* strain 30A19 has 4,121,542 bp in length, 47.5% of G+C content, 315 number of sequences, 3,753 protein-coding genes, and the number of rRNAs and tRNAs are 3 and 36, respectively, as our annotation. This bacterium's genome is similar to the complete genome of *Eubacterium limosum* SA11, which isolated from the rumen of a New Zealand sheep. It contains 4,150,332 bp with 47.43% of G+C content and 3,805 protein-coding genes (Kelly *et al.*, 2016). However, the draft genome sequence of *E. limosum* ATCC 8486 has a longer length than 30A19 and SA11 strains, containing 4,370,113 bases with 47.2% G+C content, 4,309 predicted open reading frames, 51 tRNA genes, and 11 rRNA genes (Song and Cho, 2015). The *E. limosum* strain 30A19 possess the *but* gene which was also included in the strain *E. limosum* SA11 (Kelly *et al.*, 2016). The *4-hbt* gene was also included in *E. limosum* strain 30A19 as its genome annotation but it was not detected by using the degenerate primer as stated above. And the *4-hbt* gene also exists in the strain *E. limosum* SA11. Thus, we supposed that the strain *E. limosum* 30A19 contains both *4-hbt* and *but* genes.

The *Oscillibacter* genus is a strictly anaerobic, mesophilic, neutrophilic, Gram-negative staining, non-sporulating and motile by peritrichous flagella. It represents a distinct phylogenetic lineage in clostridial cluster IV which has the low-G+C-content, Gram-positive bacteria branch based on 16S rRNA gene sequence analysis. The type species is *Oscillibacter valericigenes* and the type strain is Sjm18-20T (=NBRC 101213^T = DSM 18026^T) (Iino *et al.*, 2007). The genome of strain *O. valericigenes* 30Y2 in this study possesses 3,584,044 bp with 60.0% of the G+C content. It has 229 contigs, 3,541 protein-coding genes, three rRNAs, and 62 tRNAs. The complete genome sequence of *O. valericigenes* Sjm18-20^T has a longer size than our strain, having 4,470,622 bp in size, 53.2% of the G+C content, 4,723 protein-coding genes and three rRNAs (Katano *et al.*, 2012). The *but* gene was found in both *O. valericigenes* 30Y2 and *O. valericigenes* Sjm18-20^T. The *4-hbt* gene was not detected by degenerate primers in this study but it was indicated in the genome annotation. The *O. valericigenes* Sjm18-20^T also contains the *4-hbt* gene in its genome. Therefore, we concluded that the isolated strain *O. valericigenes* 30Y2 contains both the *but* and the *4-hbt* genes.

The isolate *Intestinimonas massiliensis* 35Y37 contains 3,502,884 bp in length, with 59.6% of the G+C contents, and 3,377 protein-coding genes. As annotated, it has 185 contigs, four rRNAs and 65 tRNAs. The strain was a low identity strain as noted above, < 97% identity against the 16S rRNA gene sequence database in GenBank. The genome of type strain *I. massiliensis* GD2^T (NZ_CWJP01000000), which was isolated from the stool of a healthy 28-year-old French donor, has 3,103,031 bp and a smaller size compared with isolate *I. massiliensis* 35Y37. The type strain has 60.7% of the G+C contents, 2,935 protein-coding genes, 56 tRNAs and two rRNAs (Durand *et al.*, 2017). This bacterium *Intestinimonas massiliensis* is a nonmotile, Gram-negative, non-spore-forming activity, catalase and oxidase were also negatives (Durand *et al.*, 2017). The *but* and the *4-hbt* genes were found in the type strain (WP_050617526 and WP_050619439, respectively). However, only the *4-hbt* gene was found the isolate *I. massiliensis* 35Y37 by using its genome annotation and PCR method with degenerate primers as described above.

Anaerostipes caccae is a non-motile, non-spore-forming rods species, Gram-positive but older cultures (>16 h) may stain Gram-negative, strictly anaerobic and catalase and oxidase negative. Butyrate, acetate and lactate are the major products of glucose metabolism (Schwiertz *et al.*, 2002). The *A. caccae* strain 6A16 isolated in this study contains 3,333,625 bp, including 44.3% of the G+C content, 3,246 protein-coding genes, 2 rRNAs, and 40 tRNAs. The complete genome of the type strain of *Anaerostipes caccae* DSM 14662^T has a larger size, consisting of 3,605,636 bp, 3,363 protein-coding genes, and 44.35% of the G+C content (Schwiertz *et al.*, 2002). The *Anaerostipes caccae* 6A16 contains the *but* gene, as annotated by its genome annotation and the PCR results. This is in good agreement with the genome annotation of the type strain, which also possesses the *but* gene for its butyrate biosynthesis.

The species *Clostridium paraputrificum* are Gram-stain-positive but rapidly become Gram-stain-negative (Rainey, 2009). The isolate *C. paraputrificum* 30Y4 has 2,671,571 bp in length of its genome, containing 30.7% of the G+C content, and 1,958 protein-coding genes. However, the whole genome sequences of a *C. paraputrificum* AGR2156 (NZ_AUJC01000000) shows a larger size of its genome, with 3,556,514 bp of total length, 3,363 protein-coding genes, and 29.75% of the G+C content. Our isolate *C. paraputrificum* 30Y4 contains the *buk* gene as identified by the degenerate primers and its genome annotation. It is consistent with the genome annotation of the *C. paraputrificum* AGR2156,

which indicated that only the *buk* gene takes part in butyrate production in its metabolic pathways.

The *Clostridium baratii* is a botulinum neurotoxin-producing species (Smith *et al.*, 2015). The cells in PYG broth are Gram-stain-positive, often granulose positive, and non-motile, straight rods (Rainey, 2009). The isolated *C. baratii* 35Y8B strain has 2,407,206 bp of total length, including 28.9% of the G+C content and 1,899 protein-encoding genes. The annotation showed it contains 562 contigs, five rRNAs, and 40 tRNAs. The complete genome of *C. baratii* str. Sullivan has a longer size in the genome than of the isolated strain, obtaining up to 3,153,266 bp and 3,082 protein-coding genes (NZ_CP006905). The G+C content is similar to our strain, with 28.0%. The *C. baratii* species only contains the *buk* gene for its butyrate formation, confirming by our genome annotation as well as GenBank database of *C. baratii* str. Sullivan. Our PCR results also brought the same conclusion for the butyrate-producing pathways of this species (Fig. 28A).

Our isolate *Anaerofustis stercorihominis* 35Y21B and a type strain *A. stercorihominis* DSM 17244^T (NZ_ABIL02000000) have similar total sequence length, the G+C content, and the number of protein-coding genes in their genome. They have 2,285,697 bp vs 2,284,603 bp, 33.9% and 33.3% of the G+C content, and 2,195 and 2,195 protein-coding genes, corresponding to strain 35Y21B and DSM 17244, respectively. Both of them consist of 2 rRNAs and 35 and 44 tRNAs, respectively. They both produce butyrate thanks to the *but* gene in their genome, which was also identified by using the degenerate primer in the strain 35Y21B.

The *Clostridium tertium* is a Gram-stain-positive, motile, non-exotoxin-producing, aerotolerant species that is considered an uncommon pathogen in humans (Shah *et al.*, 2016). The isolate *C. tertium* 35Y30 contains total sequence length of 1,823,064 bp, possessing 29.8% of the G+C content and 1008 protein-coding genes. However, the genome of *Clostridium tertium* (NZ_OBJV01000000) has approximate two times longer than strain 35Y30, consisting of 3,970,186 bp, 3,583 protein-coding genes and 27.8% of the G+C content in its genome. Butyrate-producing pathway of this strain demonstrated by the presence of the *buk* gene in their genome as well as its PCR result (Fig. 28A).

Paeniclostridium sordellii (formerly *Bacillus oedematis*, *Bacillus sordellii*, (Hall and Scott, 1927; Kim *et al.*, 2017)). *P. sordellii* is an anaerobic, Gram-stain-positive, spore-forming rod bacterium with flagella. Some strains of this species have been associated with

severe infections of humans and animals. Our isolate *P. sordellii* 35A14 contains 1,802,519 bp in its genome, comprising of 1,336 protein-coding genes and 28.6% of the G+C content. The total sequence length of this strain is smaller than other *P. sordellii* strain, strain CBA7122 (NZ_BDJI01000000). The genome of CBA7122 strain contains up to 3,550,411 bp, with 3,266 protein-coding genes and 27.3% of the G+C content. The presence of the *buk* gene in their genome helps it to synthesize butyrate, which was also confirmed by HPLC and PCR results.

4. Discussion

a. Identification of butyrate-producing bacteria

Based on 16S rRNA gene sequences, the identification of butyrate-producing bacteria isolated from the human fecal samples indicated that they are mainly comprised of Gram-positive *Firmicutes* bacteria (Louis and Flint, 2009). They are related to the class Clostridia, including clostridial clusters I, III, IV, XI, XIVa, XV, and XVI (Louis *et al.*, 2007) according to the classification by Collins and co-authors (Collins *et al.*, 1994). In our study, a remarkable variety amongst the small group of distinct butyrate-producing bacteria was noted. The phylogeny indicated that the isolated bacteria appeared in most of the clostridial clusters, except for clusters III and XVI. Clostridial cluster IV and XIVa are considered as major butyrate producers in the human gut (Louis and Flint, 2009; Pryde *et al.*, 2002). Here, isolates of cluster IV were *F. plautii*-like isolates (isolate 35Y33), *I. massiliensis*-like isolates (isolates 35Y37), *I. butyriciproducens*-like isolates (isolate 35Y26), and *O. valericigenes*-like isolates (isolate 30Y2). These bacteria synthesize butyrate via the protein-fed pathway (Vital *et al.*, 2017). The successful isolation of these strains demonstrated that although the dominant butyrate-producing bacteria of the human gut utilize carbohydrates as a major energy source, the butyrate-producing bacteria that consume proteins can also be isolated. Moreover, three OTUs related to Gram-negative *Bacteroidetes* bacteria were cultured and identified. Our finding provides evidence that cultivable butyrate producers in the human gut do not only belong to the *Firmicutes* phylum but that they also exist in another phylum such as *Bacteroidetes*. Consistently, similar findings were reported in a study which investigated cultivable butyrate-producing bacteria in the gut contents and feces of pigs by successful identification of some butyrate producers that belonged to the phyla of *Fusobacteria* and *Bacteroidetes* (Eckhaut *et al.*, 2011).

The weak consistency between 16S rRNA gene-based phylogeny and functional gene-based phylogeny of some strains is likely due to insufficient gene annotations.

b. Genes encoding for butyrate production in bacteria

Butyrate is produced in the human gut from carbohydrates or proteins via four different synthesis pathways, including the acetyl-CoA pathway (Ac pathway), the glutarate, the lysine, and the 4-aminobutyrate/succinate pathways (Vital *et al.*, 2014). While the Ac pathway, which uses carbohydrates as its major fuel, plays a predominant and important role in butyrate metabolism, other pathways fed by proteins were considered as minor contributors (Louis *et al.*, 2004; Vital *et al.*, 2014). In the Ac pathway, butyrate can be produced from butyryl-CoA via the catalysis of either terminal enzymes Buk or But (Louis *et al.*, 2004; Vital *et al.*, 2014). The *buk* and *but* genes are also considered as terminal genes for the glutarate pathway due to the absence of the co-substrate for butyryl-CoA transferase beyond this pathway (Fig 29) (Vital *et al.*, 2014).

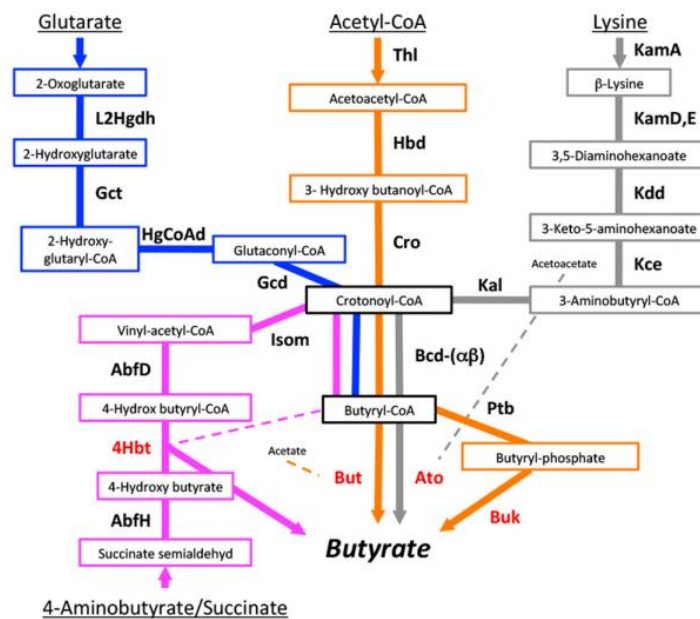


Fig 29. Four different pathways for butyrate synthesis and corresponding genes (protein names) are shown. Major substrates are displayed. Terminal genes are highlighted in red. L2Hgdh, 2-hydroxyglutarate dehydrogenase; Gct, glutaconate CoA transferase (α,β subunits); HgCoAd, 2-hydroxy-glutaryl CoA dehydrogenase (α, β, γ subunits); Gcd, glutaconyl-CoA decarboxylase (α, β subunits); Thl, thiolase; hbd, -hydroxybutyryl-CoA dehydrogenase; Cro, crotonase; Bcd, butyryl-CoA dehydrogenase (including electron transfer protein α, β subunits); KamA, lysine-2,3-aminomutase; KamD,E, -lysine- 5,6-

aminomutase (α , β subunits); Kdd, 3,5-diaminohexanoate dehydrogenase; Kce, 3-keto-5-aminohexanoate cleavage enzyme; Kal, 3-aminobutyrylCoA ammonia lyase; AbfH, 4-hydroxybutyrate dehydrogenase; AbfD, 4-hydroxybutyryl-CoA dehydratase; Isom, vinylacetyl-CoA 3,2-isomerase (same protein as AbfD); 4Hbt, butyryl-CoA:4-hydroxybutyrate CoA transferase; But, butyryl-CoA:acetate CoA transferase; Ato, butyryl-CoA:acetoacetate CoA transferase (α , β subunits); Ptb, phosphate butyryltransferase; Buk, butyrate kinase. Cosubstrates for individual butyryl-CoA transferases are shown (Vital *et al.*, 2014).

Butyrate producers with the *buk* gene were characterized by lower abundance than other butyrate producers that contained the *but* gene. The *buk* gene was found only in few members of the clostridial clusters IV and XIVa (Eeckhaut *et al.*, 2011; Louis *et al.*, 2004). For example, only one out of 16 butyrate-producing bacteria isolated from the caecum of chickens (Eeckhaut *et al.*, 2011) and four out of 38 butyrate producers isolated from the healthy human gut (Louis *et al.*, 2004) carried this gene. However, in this study, isolates 30Y4, 36A18, 35Y8B and 35Y30 belonging to clostridial cluster I, as well as isolates 35A14 of cluster XI, possessed this gene. More interestingly, *Bacteroidetes* bacteria (isolates 6A29, 30A7, and 30A1) also showed the ability to produce butyrate in this way. Although *but* gene-carrying butyrate-producing bacteria were more abundant than *buk* gene carriers, as described in the previous studies (Eeckhaut *et al.*, 2011; Louis *et al.*, 2004), the number of isolates in this study possessing the *but* gene was not high (5 out of 15 isolates).

Bacteria often carry multiple types of CoA-transferases in their genomes (Louis and Flint, 2017) and some bacteria in the human large intestine use it for butyrate production (Charrier *et al.*, 2006). In the previous studies in which the genes encoding butyrate formation in bacteria were detected, *but* gene amplicons were obtained using the CoATDF1 and CoATDR2 degenerate primers (Charrier *et al.*, 2006; Eeckhaut *et al.*, 2011). However, none of the strains possessing *but* gene in this study could be amplified with the CoATDF1 and CoATDR2 primers. This indicated that BcoATscrF and BcoATscrF degenerate primers which were used to identify the *but* gene had higher specificity to their target than the CoATDF1 and CoATDR2 degenerate primers (Eeckhaut *et al.*, 2011). However, identification of the expected sizes amplicons with CoATDF1 and CoATDR2 degenerate primers revealed the presence of the *4-hbt* gene. Butyrate-producing bacteria that possessed the *4-hbt* gene in this study were two isolates of clostridial IV, *I. massiliensis*-like and *C.*

tertium-like strains, and two isolates of the family *Odoribacteraceae*, *B. faecihominis*-like and *O. splanchnicus*-like strains. Consistent with our observations, it was previously shown that the *Butyricimonas* and *Odoribacter* genera were able to produce butyrate via a 4-aminobutyrate pathway with the participation of the *4-hbt* gene as a terminal gene (Vital *et al.*, 2017).

The usage of degenerate primers PCTfor1 and PCTrev2 did not lead to any specific amplicons of the propionate CoA-transferase gene in the tested butyrate-producing bacteria. In the previous study on butyrate-producing bacteria isolated from chicken caecum, the propionate CoA-transferase gene could be amplified with these primers in some strains (Eeckhaut *et al.*, 2011). Their results indicated that bacteria carrying a propionate CoA-transferase gene took part in the butyrate synthesis process. There may be another reason for the involvement of propionate CoA-transferase in butyrate formation since this gene is located directly downstream of the butyrate central pathway genes in the butyrate-producing bacteria cluster XVI (Eeckhaut *et al.*, 2011). Members of clostridial cluster XVI were not isolated in this study. On the other hand, the absence of propionate CoA-transferase gene in all tested strains was supported by the evidence that no strains were able to produce propionate as their final metabolites.

In the 15 tested strains, either a strain carried the *buk* gene or the *but* gene but none of the strains possessed both genes. No isolates of the *Bacteroidetes* phylum carried the *but* gene but all of them possessed the *buk* gene. Interestingly, two strains carrying the *buk* gene also possessed the *4-hbt* gene, including isolates 30A1 and 30A7 of the phylum *Bacteroidetes*. This finding emphasized the flexibility in energy source usage by these strains when producing butyrate, and may hint towards a central role for the energy management of butyrate synthesis (Vital *et al.*, 2017).

Amongst the four pathways for butyrate synthesis, the glutarate-based and 4-aminobutyrate pathways were recorded as the least prevalent pathways (Vital *et al.*, 2017). The 4-aminobutyrate (γ -aminobutyrate, GABA) is a product of glutamate degradation in a number of gut bacteria under acid stress conditions. GABA is an inhibitory neurotransmitter and plays an important role in regulating our mood, cognition, and behavior (Feehily and Karatzas, 2013). An imbalance between the excitatory glutamate and GABA in the nervous system may contribute to neuronal disorders, leading to Alzheimer's disease, Huntington's disease, and schizophrenia (Li *et al.*, 2016b). The production or consumption of GABA by

gut microbes may lead to changes in mood and behavior (Louis and Flint, 2017). In the brain of AD patients, the GABA level was lower than in healthy elderly people (Li *et al.*, 2016b). In the human gut microbiota, GABA is converted to 4-hydroxybutyrate, a substrate of the *4-hbt* gene, by the enzymes 4-aminobutyrate aminotransferase and 4-hydroxybutyrate dehydrogenase, which is an important step in the 4-aminobutyrate pathways of butyrate metabolism (Vital *et al.*, 2014). Therefore, the existence of butyrate producers carrying the *4-hbt* gene in the gut of AD patients may provide leads for further study on this bacterial group in AD patients.

In this study, many butyrate-producing bacteria were identified and characterized for their butyrate-producing ability, SCFA production, and genotype. To our knowledge, this is the first study to use a brain-related disease sample to isolate butyrate-producing bacteria in the human gut. Interestingly, butyrate-producing bacteria are not totally absent in the gut of elderly Japanese patients diagnosed with Alzheimer's disease. For a deeper understanding of the role of butyrate-producing bacteria in these particular patients, a study related to their butyrate synthesis pathways should be carried out in the future.

IV. SUMMARY

AD is an age-associated disease which accounts for 60–80% of all dementia. According to the amyloid cascade hypothesis of AD pathogenesis, the deposition in the brain of an extracellular protein fragment called β -amyloid plaques and an intracellular abnormal form of protein tau were considered as two hallmarks of AD. Recently, there has been increasing evidence indicates the etiology of diseases associated with the CNS has a relationship with gut microbiota, creating a complex gut-brain-axis. The bidirectional communication between the gut microbiota and the CNS plays a key role in physiological as well as mental health, influencing the immune system, gastrointestinal tract and CNS functions. Alteration of gut microbiota may lead to brain disorders and neurological diseases. Additionally, the group of butyrate-producing bacteria within the human gut microbiota is associated with positive effects on memory improvement.

This study aimed to investigate the alteration in the gut microbiota of AD patients by next-generation sequencing approach. Additionally, investigation of the cultivable butyrate-producing bacteria in AD patient's gut microbiota by the cultural approach was carried out. The gut microbiota of 17 Japanese who were diagnosed with AD (AD group) was compared with that of 17 Japanese HC group in terms of their bacterial taxonomies, diversities and

predicted metabolic pathways. Furthermore, the gut microbiota of the Japanese AD group was also analyzed to compare with those of American AD group to have the insight of the gut microbial diversity of AD patients from two different geographical locations. Next, butyrate-producing bacteria which were isolated from AD patient's feces were characterized depending on their phylogenetic diversity, butyrate production ability, the determination of genes encoding for butyrate synthesis and their whole genome sequence annotations.

The first study was the comparison of the gut microbiota of 17 Japanese AD group with that of 17 Japanese HC. The hypervariable regions V3–V4 of 16S rRNA gene of bacterial genome which were purified from all fecal samples of Japanese were sequenced with primers Tru357F and Tru806R using MiSeq platform (Illumina). The resulting sequences were analyzed with QIIME 1.9.1 and the outputs were used to assess the bacterial compositions, diversities, and metabolic pathways. Total sequences of 181,580 reads were assigned to 2,583 OTUs (operational taxonomic units), consisted of 12 phyla, 22 classes, 33 orders, 70 families and 147 genera. The phyla of *Actinobacteria*, *Verrucomicrobia*, *Cyanobacteria*, and *TM7* contributed to the differences in phylum level between the two groups with $p < 0.05\%$. Notably, a higher abundance of *Cyanobacteria* in AD group was an interesting result since this group of bacteria is believed to be correlated with AD due to their production of (Banack *et al.*, 2010) neurotoxins, such as β -N-methylamino-L-alanine, anatoxin-a and saxitoxin. These compounds may contribute to the onset and development of cognitive dysfunctions, a signal of AD invasion. The Faith's phylogenetic diversity was significantly reduced in the HC group, reached 12.66 ± 2.1 in the HC group and 15.99 ± 2.29 in AD group ($p < 0.05$). The weighted and unweighted UniFrac distances between AD and HC groups were significant differences at $p < 0.001$. Predicted metabolic pathways of these gut microbiota indicated that the AD group was enriched in 10 pathways as compared to the HC group, especially AD pathway of the neurodegenerative disease pathway. The gut microbiota of 17 Japanese AD and 25 American AD group was also evaluated. The hypervariable regions V4 of 16S rRNA gene of the purified DNA of AD group were sequenced. The total reads were 4,000,035 reads which were grouped into 14,593 OTUs, comprised 12 phyla, 26 classes, 30 orders, 79 families, and 180 genera. The phylum *Proteobacteria* was specifically enriched in Japanese group than the American group. Hence, this is the most important finding and may explain the alteration of this community in the human gut microbiota according to the variation in geographical location and health status. The microbial richness, characterized by observed OTU and Chao1 index, of American

group was higher than those of Japanese group. The beta diversity of the gut microbiota of AD group in American differed from that in Japanese AD group.

The disappearance of *Faecalibacterium*, which is considered as main butyrate producer in human gut microbiota, in AD group gave us a question that if other butyrate-producing bacteria exist in AD patient's gut. By using NGS, some genus which are at low abundance cannot detect. Therefore, the second study aimed to isolate butyrate-producing bacteria from Japanese AD group. 226 isolates were randomly picked from four AD patient's fecal samples, their 16S rRNA genes were sequenced, and assigned into 60 OTUs based on BLASTn results. Four isolates with less than 97% homology to known sequences were considered as unique OTUs of potentially butyrate-producing bacteria. In addition, 12 potential butyrate-producing isolates were selected from the remaining 56 OTUs based on scan-searching against the public databases. Those belonged to the phylum *Bacteroidetes* and to the clostridial clusters I, IV, XI, XV, XIVa within the phylum *Firmicutes*. Fifteen out of the 16 isolates were indeed able to produce butyrate in culture as determined by high-performance liquid chromatography (Shimadzu) with UV detection. Furthermore, encoding genes for butyrate formation in these bacteria were identified by sequencing of degenerately primed PCR products and included the genes for butyrate kinase (*buk*), butyryl-CoA: acetate CoA-transferase (*but*), CoA-transferase-related, and propionate CoA-transferase. The results showed that eight isolates possessed *buk*, while five isolates possessed *but*. The CoA-transfer-related gene was identified as butyryl-CoA:4-hydroxybutyrate CoA transferase (*4-hbt*) in four strains. The biochemical and butyrate-producing pathways analyses of butyrate producers presented in this study may help to characterize the butyrate-producing bacterial community in the gut of AD group. Interestingly, butyrate-producing bacteria are not totally absent in the gut of elderly Japanese patients diagnosed with AD. Whole genome sequences of the butyrate-producing bacteria were sequenced and annotated for their features, included genes encoding for butyrate production. The presence of cultivable butyrate-producing bacteria in AD group suggested the further study of this community in AD group due to their positive effect.

ACKNOWLEDGEMENTS

Firstly, I would like to express my deepest gratefulness to my supervisor, Prof. Hidetoshi Morita for his valuable guidance, advice, encouragement, support and scientific approach towards the completion of this study. I am greatly thankful to my co-supervisors, Prof. Naoki Nishino and Prof. Kenji Inagaki for their helpful suggestion, advice and guidance. I really appreciate everything you have done for me. I have been trained to become a scientist under your supervision.

The special thanks to Assoc. Prof. Kensuke Arakawa, my labmates, neighbor labmates, and all of my Vietnamese and foreign friends for extending their help, encouragement, assistance, suggestion, friendship and always beside me whenever I needed.

My thank also goes to all staffs and students at the Graduate School of Environmental and Life Science, Okayama University for their assistance and support throughout the period of this work. Besides, the encouragement and supports came from my colleagues, who are working at Faculty of Food Technology and Engineering, College of Agriculture and Forestry, Hue University, helped me to complete my doctoral program. I appreciate their consideration so much.

I wish to express my deep sense of gratitude to my husband, daughter, parents, brothers, and sisters for their love, encouragement and support me during this study. Without their encouragement, I could not complete my dream of a doctoral degree.

Finally, this work would not be completed without the support of Project 911 of the Ministry of Education and Training of Vietnam and Japan Student Services Organization for their financial support throughout my study.

THANK YOU VERY MUCH.

Nguyen Thi Thuy Tien

REFERENCES

- Altschu, F.S., Gish, W., Miller, W., Myers, E.W., and Lipman, D.J. 1990. Basic local alignment search tool. *J. Mol. Biol.* **215**, 403–410.
- Association, A.s. 2018. Alzheimer's Disease Facts and Figures. *Alzheimers Dement* **2018** **13**, 325-373.
- Atarashi, K., Tanoue, T., Oshima, K., Suda, W., Nagano, Y., Nishikawa, H., Fukuda, S., Saito, T., Narushima, S., Hase, K., *et al.* 2013. T_{reg} induction by a rationally selected mixture of Clostridia strains from the human microbiota. *Nature* **500**, 232–236.
- Banack, S.A., Caller, T.A., and Stommel, E.W. 2010. The Cyanobacteria derived toxin beta-N-methylamino-L-alanine and amyotrophic lateral sclerosis. *Toxins* **2**, 2837-2850.
- Barcenilla, A., Pryde, S.E., Martin, J.C., Duncan, S.H., Stewart, C.S., Henderson, C., and Flint, H.J. 2000. Phylogenetic relationships of butyrate-producing bacteria from the human gut. *Appl. Environ. Microbiol.* **66**, 1654–1661.
- Bertram, L. 2007. The genetics of Alzheimer's disease. In Sisodia, S.S., and Tanzi, R.E. (eds.), Alzheimer's disease: Advances in genetics, molecular and cellular biology. Springer.
- Bhattacharjee, S., and Lukiw, W.J. 2013. Alzheimer's disease and the microbiome. *Frontiers in cellular neuroscience* **7**, 153.
- Bolte, E.R. 1998. Autism and clostridium tetani. *Medical Hypotheses* **51**, 133-144.
- Bourassa, M.W., Alim, I., Bultman, S.J., and Ratan, R.R. 2016. Butyrate, neuroepigenetics and the gut microbiome: Can a high fiber diet improve brain health? *Neurosci. Lett.* **625**, 56–63.
- Bravo, J.A., Forsythe, P., Chew, M.V., Escaravage, E., Savignac, H.M., Dinan, T.G., Bienenstock, J., and Cryan, J.F. 2011. Ingestion of *Lactobacillus* strain regulates emotional behavior and central GABA receptor expression in a mouse via the vagus nerve. *Proceedings of the National Academy of Sciences* **108**, 16050-16055.
- Brockman, S., Jayawardena, B., and Starkstein, S. 2011. The diagnosis of depression in Alzheimer's disease: review of the current literature. *Neuropsychiatry* **1**, 377-384.
- Browne, H.P., Forster, S.C., Anonye, B.O., Kumar, N., Neville, B.A., Stares, M.D., Goulding, D., and Lawley, T.D. 2016. Culturing of 'unculturable' human microbiota reveals novel taxa and extensive sporulation. *Nature* **533**, 543–546.

- Bu, X.L., Yao, X.Q., Jiao, S.S., Zeng, F., Liu, Y.H., Xiang, Y., Liang, C.R., Wang, Q.H., Wang, X., Cao, H.Y., et al.** 2015. A study on the association between infectious burden and Alzheimer's disease. *European journal of neurology* **22**, 1519-1525.
- Caporaso, J.G., Kuczynski, J., Stombaugh, J., Bittinger, K., Bushman, F.D., Costello, E.K., Fierer, N., Peña, A.G., Goodrich, J.K., Gordon, J.I., et al.** 2010. QIIME allows analysis of high-throughput community sequencing data. *Nat. Methods* **7**, 335-336.
- Carlier, J.P., Bedora-Faure, M., K'Ouas, G., Alauzet, C., and Mory, F.** 2010. Proposal to unify *Clostridium orbiscindens* Winter et al. 1991 and *Eubacterium plautii* (Seguin 1928) Hofstad and Aasjord 1982, with description of *Flavonifractor plautii* gen. nov., comb. nov., and reassignment of *Bacteroides capillosus* to *Pseudoflavonifractor capillosus* gen. nov., comb. nov. *Int. J. Syst. Evol. Microbiol.* **60**, 585–590.
- Cattaneo, A., Cattane, N., Galluzzi, S., Provasi, S., Lopizzo, N., Festari, C., Ferrari, C., Guerra, U.P., Paghera, B., Muscio, C., et al.** 2017. Association of brain amyloidosis with pro-inflammatory gut bacterial taxa and peripheral inflammation markers in cognitively impaired elderly. *Neurobiol. Aging* **49**, 60-68.
- Charrier, C., Duncan, G.J., Reid, M.D., Rucklidge, G.J., Henderson, D., Young, P., Russell, V.J., Aminov, R.I., Flint, H.J., and Louis, P.** 2006. A novel class of CoA-transferase involved in short-chain fatty acid metabolism in butyrate-producing human colonic bacteria. *Microbiology* **152**, 179–185.
- Clemente, J.C., Ursell, L.K., Parfrey, L.W., and Knight, R.** 2012. The impact of the gut microbiota on human health: An integrative view. *Cell* **148**, 1258 - 1270.
- Collins, M.D., Lawson, P.A., Willems, A., Cordoba, J.J., Fernandez-Garayzabal, J., Garcia, P., Cai, J., Hippe, H., and Farrow, J.A.** 1994. The phylogeny of the genus *Clostridium*: proposal of five new genera and eleven new species combinations. *Int. J. Syst. Bacteriol.* **44**, 812–826.
- Cox, P.A., Davis, D.A., Mash, D.C., Metcalf, J.S., and Banack, S.A.** 2016. Dietary exposure to an environmental toxin triggers neurofibrillary tangles and amyloid deposits in the brain. *Proceedings. Biological sciences* **283**.
- Cryan, J.F., and Dinan, T.G.** 2012. Mind-altering microorganisms: the impact of the gut microbiota on brain and behaviour. *Nat. Rev. Neurosci.* **13**, 701-712.

- De Angelis, M., Francavilla, R., Piccolo, M., De Giacomo, A., and Gobbetti, M.** 2015. Autism spectrum disorders and intestinal microbiota. *Gut microbes* **6**, 207–213.
- Duncan, S.H., Louis, P., Thomson, J.M., and Flint, H.J.** 2009. The role of pH in determining the species composition of the human colonic microbiota. *Environ. Microbiol.* **11**, 2112-2122.
- Duncan, S.H., Stewart, C.S., Hold, G.L., and Flint, H.J.** 2002. Growth requirements and fermentation products of *Fusobacterium prausnitzii*, and a proposal to reclassify it as *Faecalibacterium prausnitzii* gen. nov., comb. nov. *Int. J. Syst. Evol. Microbiol.* **52**, 2141–2146.
- Durand, G., Afouda, P., Raoult, D., and Dubourg, G.** 2017. “Intestinimonas massiliensis” sp. nov, a new bacterium isolated from human gut. *New Microbes and New Infections* **15**, 1-2.
- Edgar, R.C.** 2010. Search and clustering orders of magnitude faster than BLAST. *Bioinformatics* **26**, 2460-2461.
- Eeckhaut, V., Van Immerseel, F., Croubels, S., De Baere, S., Haesebrouck, F., Ducatelle, R., Louis, P., and Vandamme, P.** 2011. Butyrate production in phylogenetically diverse *Firmicutes* isolated from the chicken caecum. *Microbial biotechnology* **4**, 503–512.
- Emery, D.C., Shoemark, D.K., Batstone, T.E., Waterfall, C.M., Coghill, J.A., Cerajewska, T.L., Davies, M., West, N.X., and Allen, S.J.** 2017. 16S rRNA next generation sequencing analysis shows bacteria in Alzheimer’s post-mortem brain. *Front. Aging Neurosci* **9**.
- Faith, D.P.** 1992. Conservation evaluation and phylogenetic diversity. *Biol. Conserv.* **61**, 1-10.
- Faith, D.P., and Baker, A.M.** 2006. Phylogenetic diversity (PD) and biodiversity conservation: some bioinformatics challenges. *Evolutionary Bioinformatics Online* **2**, 121-128.
- Feehily, C., and Karatzas, K.A.** 2013. Role of glutamate metabolism in bacterial responses towards acid and other stresses. *J. Appl. Microbiol.* **114**, 11–24.
- Felsenstein, J.** 1985. Confidence limits on phylogenies: An approach using the bootstrap. *Evolution* **39**, 783–791.

- Flint, H.J., Scott, K.P., Louis, P., and Duncan, S.H.** 2012. The role of the gut microbiota in nutrition and health. *Nature Reviews Gastroenterology & Hepatology* **9**, 577.
- Folstein, M.F., Folstein, S.E., and McHugh, P.R.** 1975. Mini-mental state: A practical method grading the cognitive state of patients for the clinician. *J Psychiatr Research* **12**, 189–198.
- Forsythe, P., Kunze, W.A., and Bienenstock, J.** 2012. On communication between gut microbes and the brain. *Current opinion in gastroenterology* **28**, 557-562.
- García-Villalba, R., Giménez-Bastida, J.A., García-Conesa, M.T., Tomás-Barberán, F.A., Espín, J.C., and Larrosa, M.** 2012. Alternative method for gas chromatography-mass spectrometry analysis of short-chain fatty acids in faecal samples. *Journal of separation science* **35**, 1906–1913.
- Gasteiger, E., Gattiker, A., Hoogland, C., Ivanyi, I., Appel, R.D., and Bairoch, A.** 2003. ExpASY: the proteomics server for in-depth protein knowledge and analysis. *Nucleic Acids Res.* **31**, 3784–3788.
- Geirnaert, A., Calatayud, M., Grootaert, C., Laukens, D., Devriese, S., Smagghe, G., De Vos, M., Boon, N., and Van de Wiele, T.** 2017. Butyrate-producing bacteria supplemented *in vitro* to Crohn's disease patient microbiota increased butyrate production and enhanced intestinal epithelial barrier integrity. *Scientific reports* **7**, 11450.
- Göker, M., Gronow, S., Zeytun, A., Nolan, M., Lucas, S., Lapidus, A., Hammon, N., Deshpande, S., Cheng, J.F., Pitluck, S., et al.** 2011. Complete genome sequence of *Odoribacter splanchnicus* type strain (1651/6(T)). *Standards in Genomic Sciences* **4**, 200-209.
- Govindarajan, N., Agis-Balboa, R.C., Walter, J., Sananbenesi, F., and Fischer, A.** 2011. Sodium butyrate improves memory function in an Alzheimer's disease mouse model when administered at an advanced stage of disease progression. *J. Alzheimers. Dis.* **26**, 187–197.
- Gruninger, T.R., LeBoeuf, B., Liu, Y., and Garcia, L.R.** 2007. Molecular signaling involved in regulating feeding and other motivated behaviors. *Mol. Neurobiol.* **35**, 1–20.
- Gupta, V.K., Paul, S., and Dutta, C.** 2017. Geography, Ethnicity or Subsistence-Specific Variations in Human Microbiome Composition and Diversity. *Front Microbiol* **8**.

- Hall, I.C., and Scott, J.P.** 1927. *Bacillus sordellii*, a cause of malignant edema in man. *The Journal of Infectious Diseases* **41**, 329-355.
- Hamer, H.M., Jonkers, D., Venema, K., Vanhoutvin, S., Troost, F.J., and Brummer, R.J.** 2008. The role of butyrate on colonic function. *Alimentary pharmacology & therapeutics* **27**, 104–119.
- Harach, T., Marungruang, N., Duthilleul, N., Cheatham, V., McCoy, K.D., Neher, J.J., Jucker, M., Fak, F., Lasser, T., and Bolmont, T.** 2015. Reduction of Alzheimer's Disease Beta-amyloid Pathology in the Absence of Gut Microbiota. *Cornell University Library arXiv:1509.02273*.
- Hardy, J., and Selkoe, D.J.** 2002. The amyloid hypothesis of Alzheimer's disease: Progress and problems on the road to therapeutics. *Science's compass* **297**.
- Hehemann, J.-H., Correc, G., Barbeyron, T., Helbert, W., Czjzek, M., and Michel, G.** 2010. Transfer of carbohydrate-active enzymes from marine bacteria to Japanese gut microbiota. *Nature* **464**, 908.
- Ho, L., Ono, K., Tsuji, M., Mazzola, P., Singh, R., and Pasinetti, G.M.** 2018. Protective roles of intestinal microbiota derived short chain fatty acids in Alzheimer's disease-type beta-amyloid neuropathological mechanisms. *Expert review of neurotherapeutics* **18**, 83-90.
- Holdeman, L.V., and Moore, W.E.C.** 1974. New genus, *Coprococcus*, twelve new species, and emended descriptions of four previously described species of bacteria from human feces. *Int. J. Syst. Bacteriol.* **24**, 260–277.
- Hollister, E.B., Gao, C., and Versalovic, J.** 2014. Compositional and functional features of the gastrointestinal microbiome and their effects on human health. *Gastroenterology* **146**, 1449-1458.
- Hu, X., Wang, T., and Jin, F.** 2016. Alzheimer's disease and gut microbiota. *Science China. Life sciences* **59**, 1006-1023.
- Hughes, J.B., Hellmann, J.J., Ricketts, T.H., and Bohannon, B.J.M.** 2001. Counting the uncountable: Statistical approaches to estimating microbial diversity. *Appl. Environ. Microbiol.* **67**, 4399-4406.
- Iino, T., Mori, K., Tanaka, K., Suzuki, K., and Harayama, S.** 2007. *Oscillibacter valericigenes* gen. nov., sp. nov., a valerate-producing anaerobic bacterium isolated from

- the alimentary canal of a Japanese corbicula clam. *Int. J. Syst. Evol. Microbiol.* **57**, 1840-1845.
- Illumina.** 2013. 16S metagenomic sequencing library preparation.
- Jiang, C., Li, G., Huang, P., Liu, Z., and Zhao, B.** 2017. The gut microbiota and Alzheimer's disease. *Journal of Alzheimer's disease : JAD* **58**, 1-15.
- Jiang, H., Ling, Z., Zhang, Y., Mao, H., Ma, Z., Yin, Y., Wang, W., Tang, W., Tan, Z., Shi, J., et al.** 2015. Altered fecal microbiota composition in patients with major depressive disorder. *Brain Behav Immun* **48**, 186-194.
- Jones, B.V., Begley, M., Hill, C., Gahan, C.G., and Marchesi, J.R.** 2008. Functional and comparative metagenomic analysis of bile salt hydrolase activity in the human gut microbiome. *Proceedings of the National Academy of Sciences of the United States of America* **105**, 13580-13585.
- Kametani, F., and Hasegawa, M.** 2018. Reconsideration of amyloid hypothesis and tauhypothesis in Alzheimer's disease. *Frontiers in neuroscience* **12**, 25.
- Kanehisa, M., and Goto, S.** 2000. KEGG: Kyoto Encyclopedia of Genes and Genomes. *Nucleic Acids Res.* **28**, 27-30.
- Kang, D.W., Park, J.G., Ilhan, Z.E., Wallstrom, G., Labaer, J., Adams, J.B., and Krajmalnik-Brown, R.** 2013. Reduced incidence of Prevotella and other fermenters in intestinal microflora of autistic children. *PloS one* **8**, e68322.
- Karran, E., Mercken, M., and De Strooper, B.** 2011. The amyloid cascade hypothesis for Alzheimer's disease: an appraisal for the development of therapeutics. *Nat. Rev. Drug Discov.* **10**, 698-712.
- Katano, Y., Fujinami, S., Kawakoshi, A., Nakazawa, H., Oji, S., Iino, T., Oguchi, A., Ankai, A., Fukui, S., Terui, Y., et al.** 2012. Complete genome sequence of *Oscillibacter valericigenes* Sjm18-20(T) (=NBRC 101213(T)). *Standards in Genomic Sciences* **6**, 406-414.
- Kelly, W.J., Henderson, G., Pacheco, D.M., Li, D., Reilly, K., Naylor, G.E., Janssen, P.H., Attwood, G.T., Altermann, E., and Leahy, S.C.** 2016. The complete genome sequence of *Eubacterium limosum* SA11, a metabolically versatile rumen acetogen. *Standards in Genomic Sciences* **11**.

- Kim, J.Y., Kim, Y.B., Song, H.S., Chung, W.-H., Lee, C., Ahn, S.W., Lee, S.H., Jung, M.Y., Kim, T.-W., Nam, Y.-D., et al.** 2017. Genomic analysis of a pathogenic bacterium, *Paeniclostridium sordellii* CBA7122 containing the highest number of rRNA operons, isolated from a human stool sample. *Frontiers in Pharmacology* **8**.
- Klindworth, A., Pruesse, E., Schweer, T., Peplies, J., Quast, C., Horn, M., and Glockner, F.O.** 2013. Evaluation of general 16S ribosomal RNA gene PCR primers for classical and next-generation sequencing-based diversity studies. *Nucleic Acids Res.* **41**, e1.
- Knopman, D.S.** Methods in Molecular Medicine. In Hooper, N.M. (ed.), Alzheimer's Disease: Methods and Protocols Humana Press Inc., Totowa, NJ, Vol. 32.
- Kozich, J.J., Westcott, S. L., Baxter, N. T., Highlander, S. K., Schloss, P. D.** 2013. Development of a dual-index sequencing strategy and curation pipeline for analyzing amplicon sequence data on the miseq illumina sequencing platform. *Appl. Environ. Microbiol.* **79**, 5112–5120.
- Kumar, S., Stecher, G., and Tamura, K.** 2016. MEGA7: Molecular Evolutionary Genetics Analysis Version 7.0 for Bigger Datasets. *Mol. Biol. Evol.* **33**, 1870–1874.
- Langille, M.G.I., Zaneveld, J., Caporaso, J.G., McDonald, D., Knights, D., Reyes, J.A., Clemente, J.C., Burkepile, D.E., Vega Thurber, R.L., Knight, R., et al.** 2013. Predictive functional profiling of microbial communities using 16S rRNA marker gene sequences. *Nat. Biotechnol.* **31**, 814.
- Lathrop, S.K., Bloom, S.M., Rao, S.M., Nutsch, K., Lio, C.W., Santacruz, N., Peterson, D.A., Stappenbeck, T.S., and Hsieh, C.S.** 2011. Peripheral education of the immune system by colonic commensal microbiota. *Nature* **478**, 250-254.
- Lee, Y.K., and Mazmanian, S.K.** 2010. Has the microbiota played a critical role in the evolution of the adaptive immune system? *Science* **330**, 1768-1773.
- Li, X., Højberg, O., Canibe, N., and Jensen, B.B.** 2016a. Phylogenetic diversity of cultivable butyrate-producing bacteria from pig gut content and feces. *J. Anim. Sci.* **94**, 377–381.
- Li, Y., Sun, H., Chen, Z., Xu, H., Bu, G., and Zheng, H.** 2016b. Implications of GABAergic neurotransmission in Alzheimer's Disease. *Frontiers in aging neuroscience* **8**, 31.

- Li, Z., Yi, C., Katiraei, S., Kooijman, S., Zhou, E., Chung, K.C., Gao, Y., Heuvel, J.K., Meijer, O.C., Berbée, J.F.P., et al.** 2017. Butyrate reduces appetite and activates brown adipose tissue via the gut-brain neural circuit. *Gut microbiota* **0**, 1–11.
- Liu, J., Sun, J., Wang, F., Yu, X., Ling, Z., Li, H., Zhang, H., Jin, J., Chen, W., Pang, M., et al.** 2015. Neuroprotective effects of *Clostridium butyricum* against vascular dementia in mice via metabolic butyrate. *BioMed research international* **2015**, 412946.
- Liu, Y., Liu, F., Grundke-Iqbal, I., Iqbal, K., and Gong, C.X.** 2011. Deficient brain insulin signalling pathway in Alzheimer's disease and diabetes. *J. Pathol.* **225**, 54-62.
- López, O.L., and DeKosky, S.T.** 2008. Clinical symptoms in Alzheimer's disease. **89**, 207-216.
- Louis, P., Duncan, S.H., McCrae, S.I., Millar, J., Jackson, M.S., and Flint, H.J.** 2004. Restricted distribution of the butyrate kinase pathway among butyrate-producing bacteria from the human colon. *J. Bacteriol.* **186**, 2099–2106.
- Louis, P., and Flint, H.J.** 2007. Development of a semiquantitative degenerate real-time pcr-based assay for estimation of numbers of butyryl-coenzyme A (CoA) CoA transferase genes in complex bacterial samples. *Appl. Environ. Microbiol.* **73**, 2009–2012.
- Louis, P., and Flint, H.J.** 2009. Diversity, metabolism and microbial ecology of butyrate-producing bacteria from the human large intestine. *FEMS Microbiol. Lett.* **294**, 1–8.
- Louis, P., and Flint, H.J.** 2017. Formation of propionate and butyrate by the human colonic microbiota. *Environ. Microbiol.* **19**, 29–41.
- Louis, P., Scott, K.P., Duncan, S.H., and Flint, H.J.** 2007. Understanding the effects of diet on bacterial metabolism in the large intestine. *J. Appl. Microbiol.* **102**, 1197–1208.
- Lozupone, C., and Knight, R.** 2005. UniFrac: a new phylogenetic method for comparing microbial communities. *Appl. Environ. Microbiol.* **71**, 8228-8235.
- Magurran, A.E.** 2004. Measuring biological diversity. Blackwell Science.
- Mancuso, C., and Santangelo, R.** 2018. Alzheimer's disease and gut microbiota modifications: The long way between preclinical studies and clinical evidence. *Pharmacol. Res.* **129**, 329-336.
- Mandell, A.M., and Green, C.R.** 2011. Alzheimer's disease. In Budson, A.E., and Kowall, N.W. (eds.), The handbook of Alzheimer's disease and other dementias, 1st ed. Wiley-Blackwell, United Kingdom.

- Miklossy, J.** 2011. Emerging roles of pathogens in Alzheimer disease. *Expert Rev. Mol. Med* **13**, e30.
- Miklossy, J., and McGeer, L.P.** 2016. Common mechanisms involved in Alzheimer's disease and type 2 diabetes: a key role of chronic bacterial infection and inflammation. *Aging* **8**.
- Miyake, S., Kim, S., Suda, W., Oshima, K., Nakamura, M., Matsuoka, T., Chihara, N., Tomita, A., Sato, W., Kim, S.W., et al.** 2015. Dysbiosis in the gut microbiota of patients with multiple sclerosis, with a striking depletion of species belonging to Clostridia XIVa and IV clusters. *PloS one* **10**, e0137429.
- Morita, H., Kuwahara, T., Ohshima, K., Sasamoto, H., Itoh, K., Hattori, M., Hayashi, T., and Takami, H.** 2007. An improved DNA isolation method for metagenomic analysis of the microbial flora of the human intestine. *Microbes Environ.* **22**, 214–222.
- Mulligan, V.K., and Chakrabarty, A.** 2013. Protein misfolding in the late-onset neurodegenerative diseases: common themes and the unique case of amyotrophic lateral sclerosis. *Proteins* **81**, 1285-1303.
- Nei, M., and Kumar, S.** 2000. Molecular evolution and phylogenetics. Oxford University Press, New York.
- Nieuwdorp, M., Gilijamse, P.W., Pai, N., and Kaplan, L.M.** 2014. Role of the microbiome in energy regulation and metabolism. *Gastroenterology* 2014 **146**, 1525–1533.
- Nishijima, S., Suda, W., Oshima, K., Kim, S.W., Hirose, Y., Morita, H., and Hattori, M.** 2016. The gut microbiome of healthy Japanese and its microbial and functional uniqueness. *DNA Res.* **23**, 125–133.
- Niu, H., Álvarez-Álvarez, I., Guillén-Grima, F., and Aguinaga-Ontoso, I.** 2017. Prevalence and incidence of Alzheimer's disease in Europe: A meta-analysis. *Neurología (English Edition)* **32**, 523-532.
- O'Hara, A.M., and Shanahan, F.** 2006. The gut flora as a forgotten organ. *EMBO reports* **7**, 688-693.
- Odamaki, T., Kato, K., Sugahara, H., Hashikura, N., Takahashi, S., Xiao, J.Z., Abe, F., and Osawa, R.** 2016. Age-related changes in gut microbiota composition from newborn to centenarian: a cross-sectional study. *BMC Microbiol.* **16**, 90.

- Ott, S.J., Musfeldt, M., Wenderoth, D.F., Hampe, J., Brant, O., Folsch, U.R., Timmis, K.N., and Schreiber, S.** 2004. Reduction in diversity of the colonic mucosa associated bacterial microflora in patients with active inflammatory bowel disease. *Gut* **53**, 685–693.
- Pruesse, E., Peplies, J., and Glockner, F.O.** 2012. SINA: accurate high-throughput multiple sequence alignment of ribosomal RNA genes. *Bioinformatics* **28**, 1823–1829.
- Pryde, S.E., Duncan, S.H., Hold, G.L., Stewart, C.S., and Flint, H.J.** 2002. The microbiology of butyrate formation in the human colon. *FEMS Microbiol. Lett.* **217**, 133–139.
- Rainey, F.A.** 2009. Class II. Clostridia class. nov. In De Vos, P., Garrity, G.M., Jones, D., Krieg, N.R., Ludwig, W., Rainey, F.A., Schleifer, K., and Whitman, W.B. (eds.), *Bergey's manual of systematic bacteriology*, 2nd ed. Springer, Spring Street, New York, NY, USA.
- Rivière, A., Selak, M., Lantin, D., Leroy, F., and De Vuyst, L.** 2016. Bifidobacteria and butyrate-producing colon bacteria: Importance and strategies for their stimulation in the human gut. *Frontiers in microbiology* **7**, 979.
- Round, J.L., Lee, S.M., Li, J., Tran, G., Jabri, B., Chatila, T.A., and Mazmanian, S.K.** 2011. The Toll-like receptor 2 pathway establishes colonization by a commensal of the human microbiota. *Science* **332**, 974-977.
- Saitou, N., and Nei, M.** 1987. The neighbor-joining method: A new method for reconstructing phylogenetic trees. *Mol. Biol. Evol.* **4**, 406–425.
- Sakamoto, M., Tanaka, Y., Benno, Y., and Ohkuma, M.** 2014. *Butyricimonas faecihominis* sp. nov. and *Butyricimonas paravirosa* sp. nov., isolated from human faeces, and emended description of the genus *Butyricimonas*. *Int. J. Syst. Evol. Microbiol.* **64**, 2992–2997.
- Samuel, B.S., Shaito, A., Motoike, T., Rey, F.E., Backhed, F., Manchester, J.K., Hammer, R.E., Williams, S.C., Crowley, J., Yanagisawa, M., et al.** 2008. Effects of the gut microbiota on host adiposity are modulated by the short-chain fatty-acid binding G protein-coupled receptor, Gpr41. *Proceedings of the National Academy of Sciences of the United States of America* **105**, 16767-16772.
- Scheperjans, F., Aho, V., Pereira, P.A., Koskinen, K., Paulin, L., Pekkonen, E., Haapaniemi, E., Kaakkola, S., Eerola-Rautio, J., Pohja, M., et al.** 2015. Gut

- microbiota are related to Parkinson's disease and clinical phenotype. *Movement disorders : official journal of the Movement Disorder Society* **30**, 350-358.
- Schulze-Schweifing, K., Banerjee, A., and Wade, W.G.** 2014. Comparison of bacterial culture and 16S rRNA community profiling by clonal analysis and pyrosequencing for the characterization of the dentine caries-associated microbiome. *Frontiers in cellular and infection microbiology* **4**, 164.
- Schwartz, A., Hold, G.L., Duncan, S.H., Gruhl, B., Collins, M.D., Lawson, P.A., Flint, H.J., and Blaut, M.** 2002. *Anaerostipes caccae* gen. nov., sp. nov., a new saccharolytic, acetate-utilising, butyrate-producing bacterium from human faeces. *Syst. Appl. Microbiol.* **25**, 46-51.
- Segata, N., Izard, J., Waldron, L., Gevers, D., Miropolsky, L., Garrett, W.S., and Huttenhower, C.** 2011. Metagenomic biomarker discovery and explanation. *Genome biology* **12**, R60.
- Selkoe, D.J., and Hardy, J.** 2016. The amyloid hypothesis of Alzheimer's disease at 25 years. *EMBO molecular medicine* **8**, 595-608.
- Shah, S., Hankenson, J., Pabbathi, S., Greene, J., and Nanjappa, S.** 2016. Clostridium tertium in neutropenic patients: case series at a cancer institute. *International Journal of Infectious Diseases* **51**, 44-46.
- Sharon, G., Sampson, T.R., Geschwind, D.H., and Mazmanian, S.K.** 2016. The central nervous system and the gut microbiome. *Cell* **167**, 915-932.
- Smith, T.J., Hill, K.K., Xie, G., Foley, B.T., Williamson, C.H.D., Foster, J.T., Johnson, S.L., Chertkov, O., Teshima, H., Gibbons, H.S., et al.** 2015. Genomic sequences of six botulinum neurotoxin-producing strains representing three clostridial species illustrate the mobility and diversity of botulinum neurotoxin genes. *Infection, genetics and evolution : journal of molecular epidemiology and evolutionary genetics in infectious diseases* **30**, 102-113.
- Sommer, F., and Backhed, F.** 2013. The gut microbiota-masters of host development and physiology. *Nat. Rev. Microbiol.* **11**, 227-238.
- Song, Y., and Cho, B.K.** 2015. Draft genome sequence of chemolithoautotrophic acetogenic butanol-producing *Eubacterium limosum* ATCC 8486. *Genome Announcements* **3**.

- Thakur, A.K., Shakya, A., Husain, G.M., Emerald, M., and Kumar, V.** 2014. Gut-Microbiota and mental health: Current and future perspectives. *J Pharmacol Clin Toxicol* **2(1):1016**.
- Uchimura, Y., Wyss, M., Brugiroux, S., Limenitakis, J.P., Stecher, B., McCoy, K.D., and Macpherson, A.J.** 2016. Complete genome sequences of 12 species of stable defined moderately diverse mouse microbiota. *Genome Announcements* **4**.
- Vital, M., Howe, A.C., and Tiedje, J.M.** 2014. Revealing the bacterial butyrate synthesis pathways by analyzing (meta)genomic data. *MBio* **5**, e00889.
- Vital, M., Karch, A., and Pieper, D.H.** 2017. Colonic butyrate-producing communities in humans: An overview using omics data. *mSystems* **2**, e00130-00117.
- Vital, M., Penton, C.R., Wang, Q., Young, V.B., Antonopoulos, D.A., Sogin, M.L., Morrison, H.G., Raffals, L., Chang, E.B., Huffnagle, G.B., et al.** 2013. A gene-targeted approach to investigate the intestinal butyrate-producing bacterial community. *Microbiome* **1**, 8.
- Vogt, N.M., Kerby, R.L., Dill-McFarland, K.A., Harding, S.J., Merluzzi, A.P., Johnson, S.C., Carlsson, C.M., Asthana, S., Zetterberg, H., Blennow, K., et al.** 2017. Gut microbiome alterations in Alzheimer's disease. *Scientific reports* **7**, 13537.
- Wallace, T.C., Guarner, F., Madsen, K., Cabana, M.D., Gibson, G., Hentges, E., and Sanders, M.E.** 2011. Human gut microbiota and its relationship to health and disease. *Nutr. Rev.* **69**, 392–403.
- Wang, B., Yao, M., Lv, L., Ling, Z., and Li, L.** 2017. The human microbiota in health and disease. *Engineering* **3**, 71-82.
- Westfall, S., Lomis, N., Kahouli, I., Dia, S.Y., Singh, S.P., and Prakash, S.** 2017. Microbiome, probiotics and neurodegenerative diseases: deciphering the gut brain axis. *Cell. Mol. Life Sci.* **74**, 3769-3787.
- Wexler, H.M.** 2007. Bacteroides: the good, the gad, and the nitty-gritty. *Clin. Microbiol. Rev.* **20**, 593-621.
- Yoon, S.H., Ha, S.M., Kwon, S., Lim, J., Kim, Y., Seo, H., and Chun, J.** 2017. Introducing EzBioCloud: a taxonomically united database of 16S rRNA gene sequences and whole-genome assemblies. *Int. J. Syst. Evol. Microbiol.* **67**, 1613–1617.

- Yutin, N., and Galperin, M.Y.** 2013. A genomic update on clostridial phylogeny: Gram-negative spore formers and other misplaced clostridia. *Environ. Microbiol.* **15**, 2631–2641.
- Zhan, X., Stamova, B., and Sharp, F.R.** 2018. Lipopolysaccharide associates with amyloid plaques, neurons and oligodendrocytes in Alzheimer’s Disease brain: A Review. *Frontiers in aging neuroscience* **10**.
- Zhang, R., Miller, R.G., Gascon, R., Champion, S., Katz, J., Lancero, M., Narvaez, A., Honrada, R., Ruvalcaba, D., and McGrath, M.S.** 2009. Circulating endotoxin and systemic immune activation in sporadic amyotrophic lateral sclerosis (sALS). *J. Neuroimmunol.* **206**, 121-124.
- Zheng, P., Zeng, B., Zhou, C., Liu, M., Fang, Z., Xu, X., Zeng, L., Chen, J., Fan, S., Du, X., et al.** 2016. Gut microbiome remodeling induces depressive-like behaviors through a pathway mediated by the host’s metabolism. *Mol. Psychiatry* **21**, 786.
- Zuckermandl, E., and Pauling, L.** 1965. Evolutionary divergence and convergence in proteins. In Bryson, V., and Vogel, H.J. (eds.), *Evolving genes and proteins*. Academic Press, New York, p. 97–166.

CONTENTS

I. GENERAL INTRODUCTION	0
1. Overview of Alzheimer’s disease	1
2. Overview of human gut microbiota	8
3. The bidirectional communication between the gut microbiota and the central nervous system	12
4. Motivation, objectives and hypotheses	14
II. CHARACTERIZATION OF GUT MICROBIOTA OF JAPANESE ALZHEIMER’S DISEASE PATIENTS	16
Abstract	16
1. Introduction	17
2. Materials and Methods	18
3. Results	22
4. Discussion	46
III. CHARACTERIZATION OF BUTYRATE-PRODUCING BACTERIA ISOLATED FROM FECES OF ALZHEIMER’S DISEASE PATIENTS	50
Abstract	50
1. Introduction	51
2. Materials and Methods	53
3. Results	59
4. Discussion	75
IV. SUMMARY	79
ACKNOWLEDGEMENTS	82
REFERENCES	83
	96

